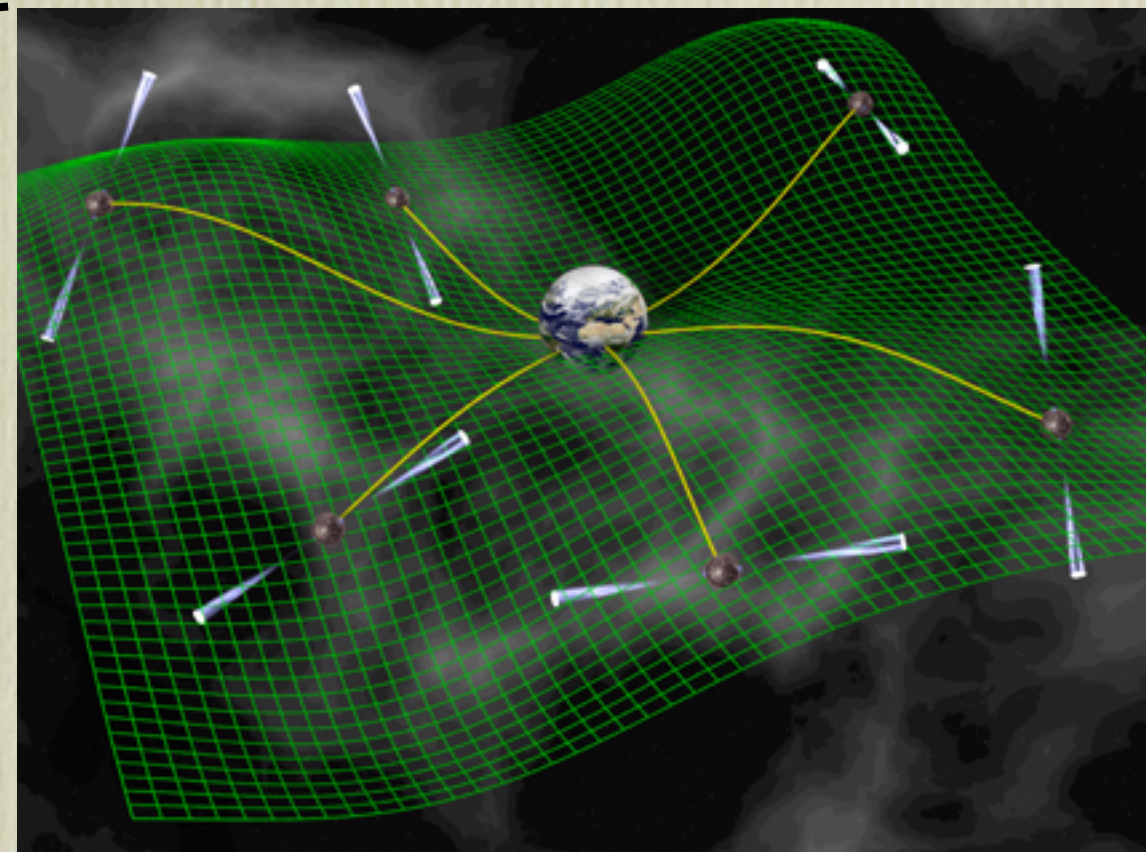
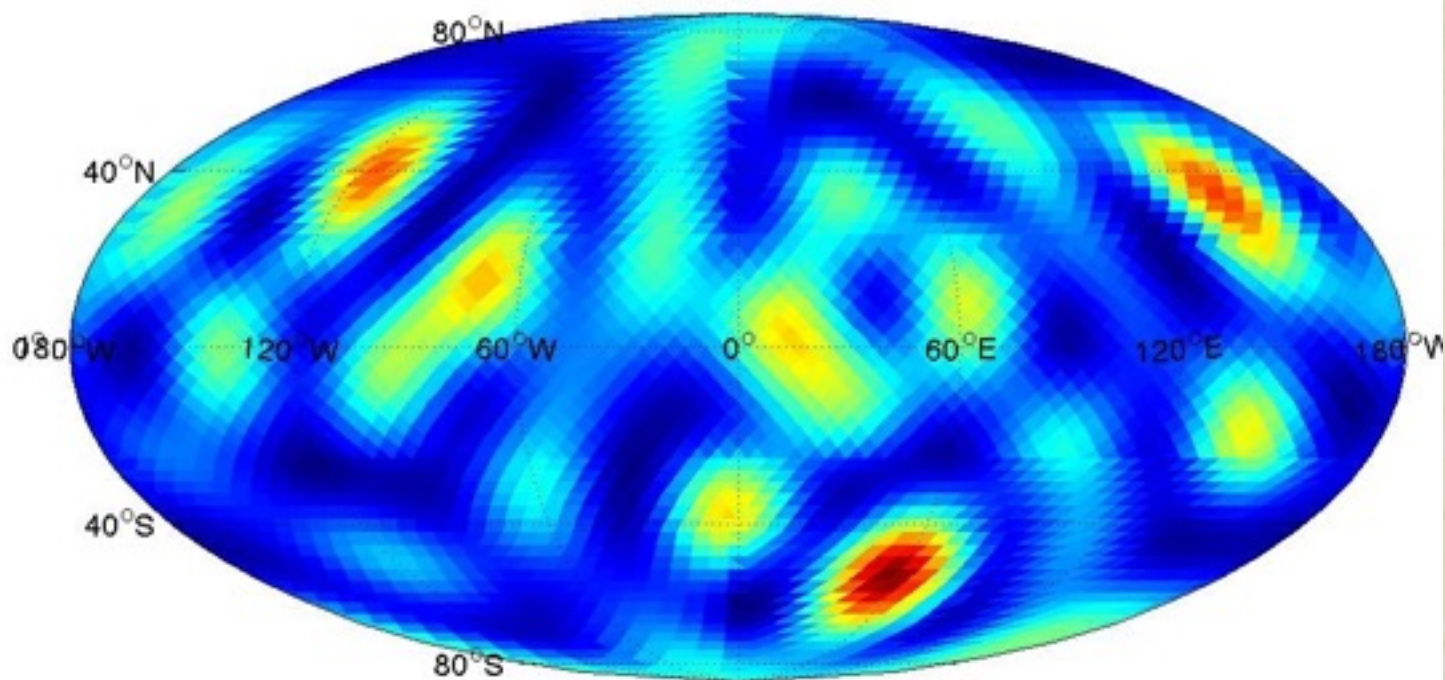


Mapping gravitational-wave backgrounds of arbitrary polarisation using pulsar timing arrays

Jonathan Gair, University of Edinburgh
IAP seminar, December 7th 2015

Phys. Rev. D **90** 082001 (2014), Phys. Rev. D **92** 102003 (2015)

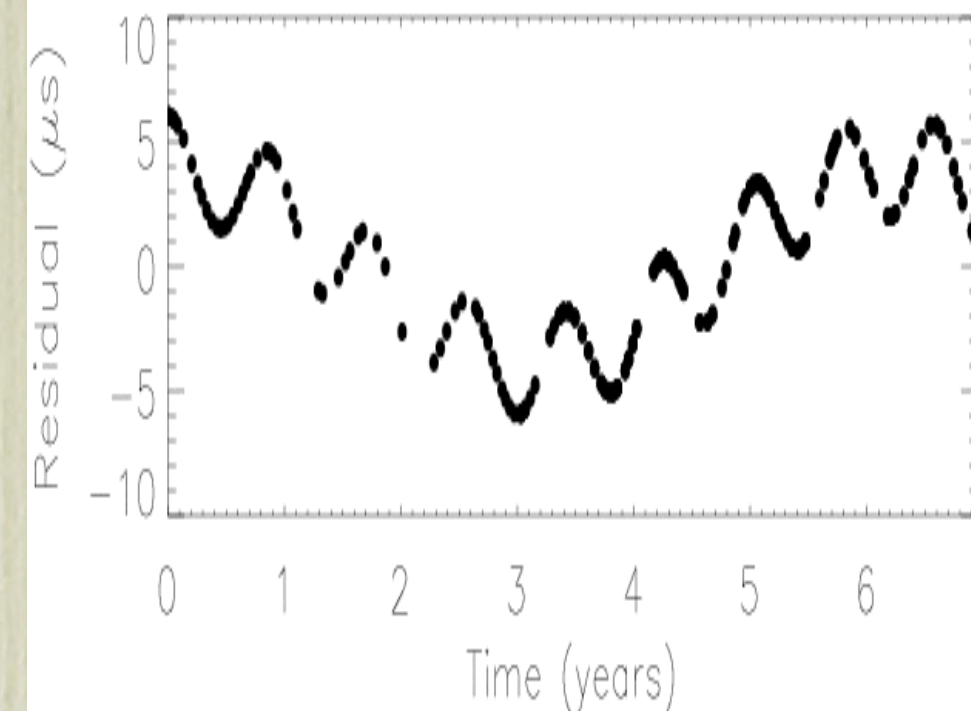
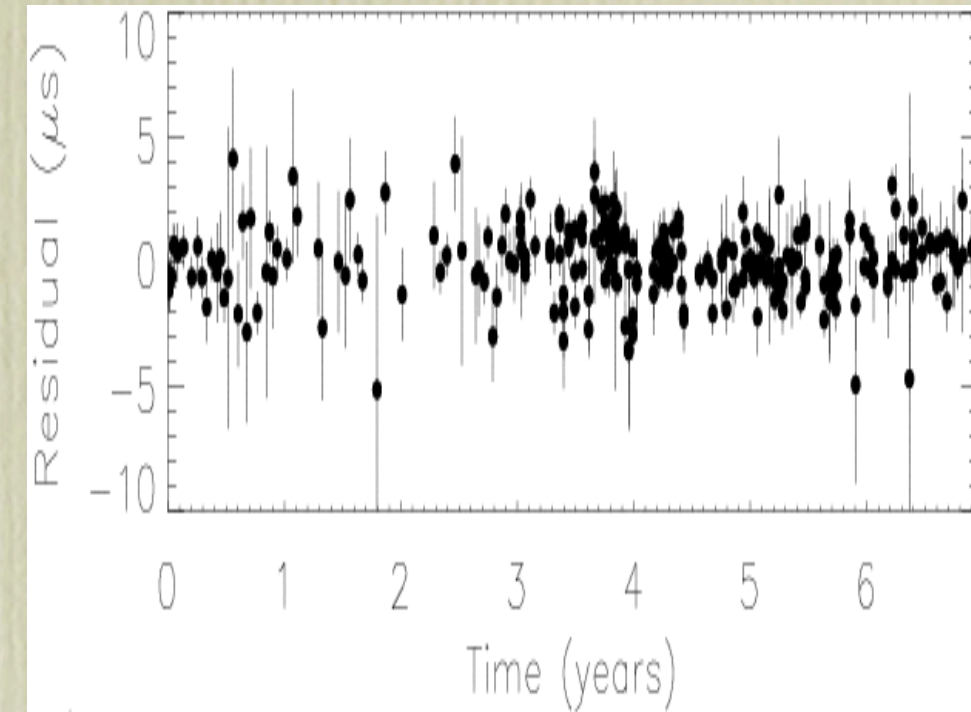
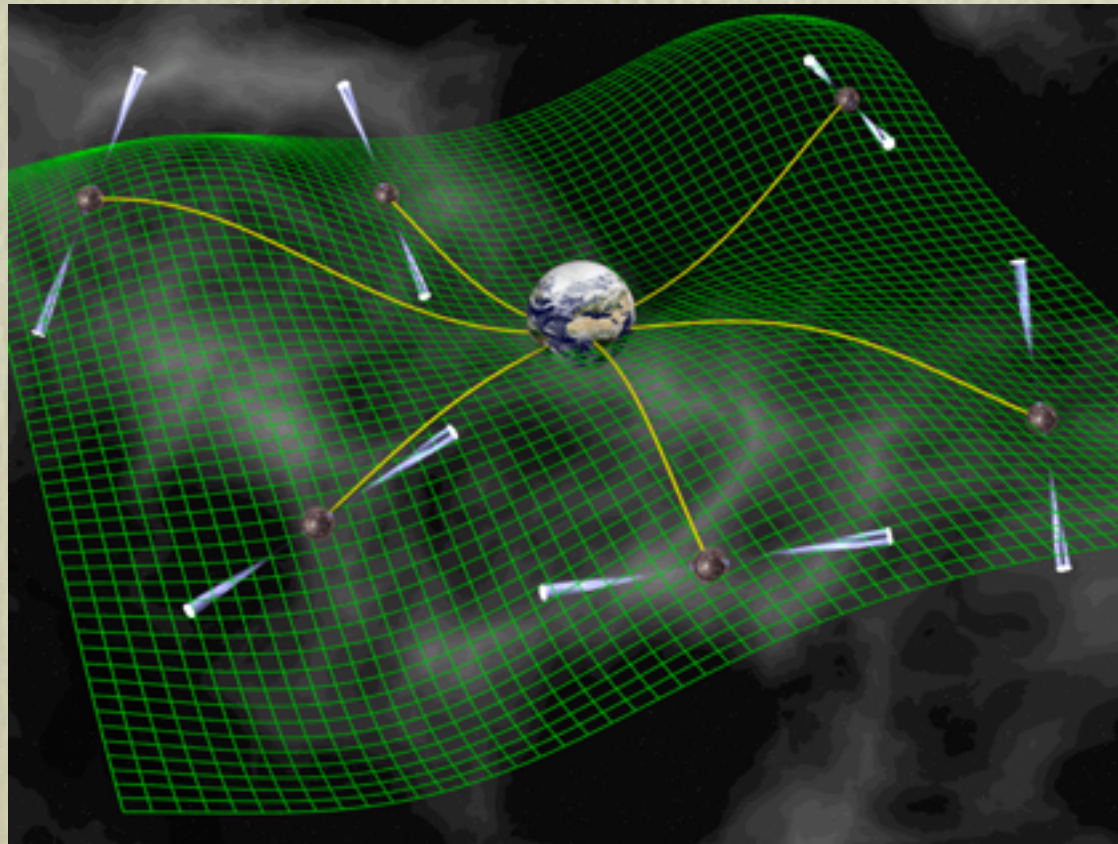
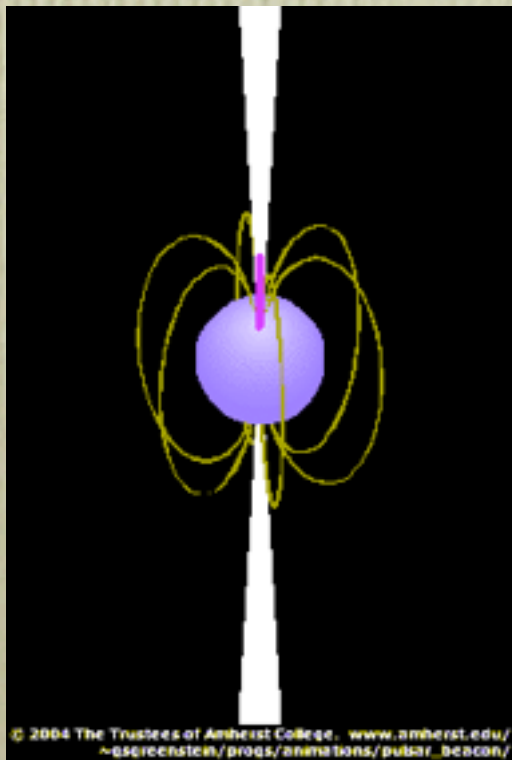


Talk Outline

- Introduction to pulsar timing arrays
- Formalism for CMB polarisation analysis
- PTA response to individual modes of the background
- Recovery of Hellings and Downs correlation curve for an isotropic uncorrelated background
- Characterising and measuring general backgrounds
- Implications of a measurement of the coefficients inconsistent with expectations
- Extension to ground-based interferometers

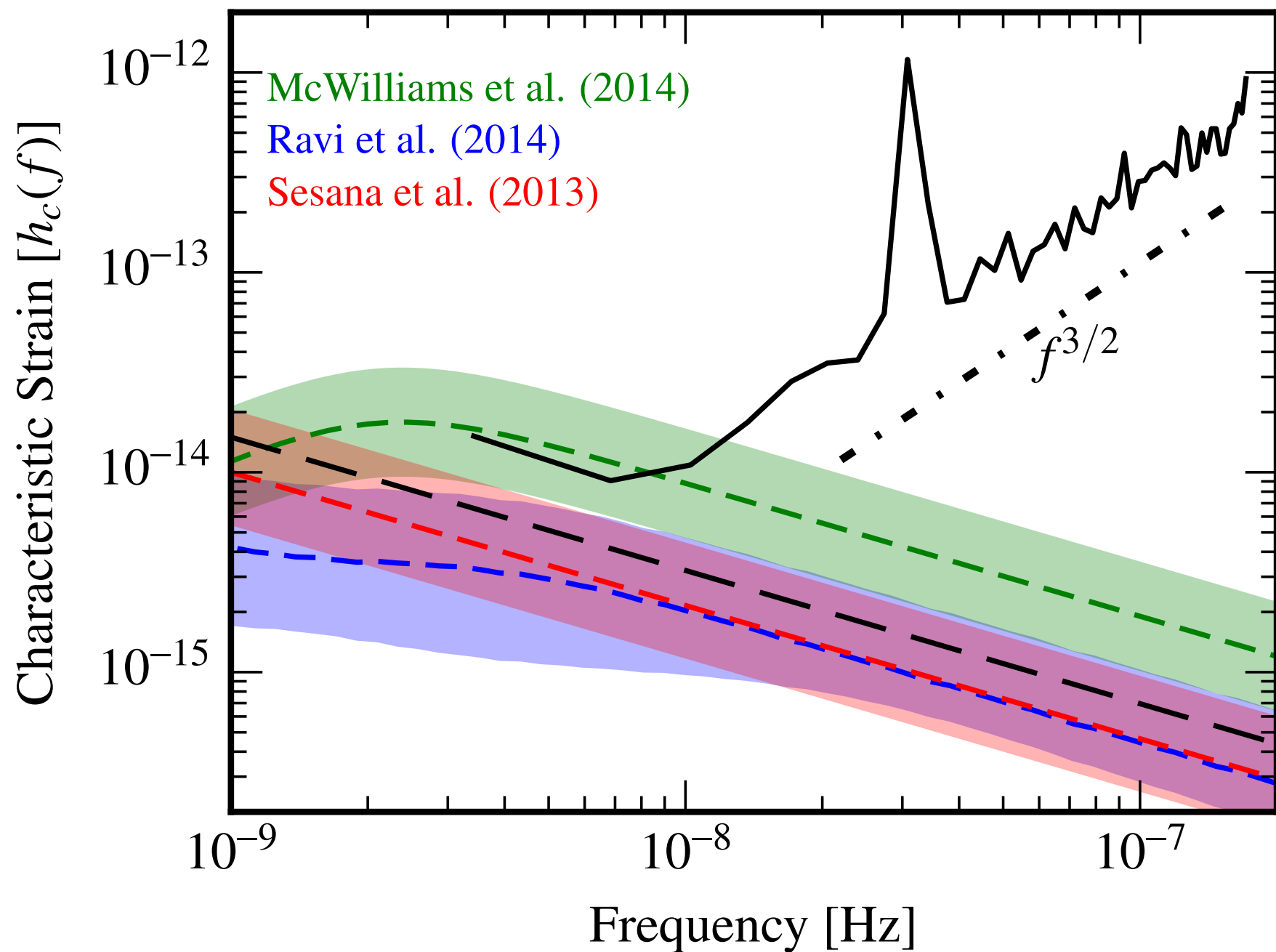
Pulsar timing arrays

- Pulsars are very accurate clocks.
 - GW passing between source and observer induces periodic change in pulse time of arrival.
 - Use a network (array) of pulsars to increase signal to noise.
 - Ongoing international effort using various radio telescopes - EPTA, PPTA and NANOGrav.



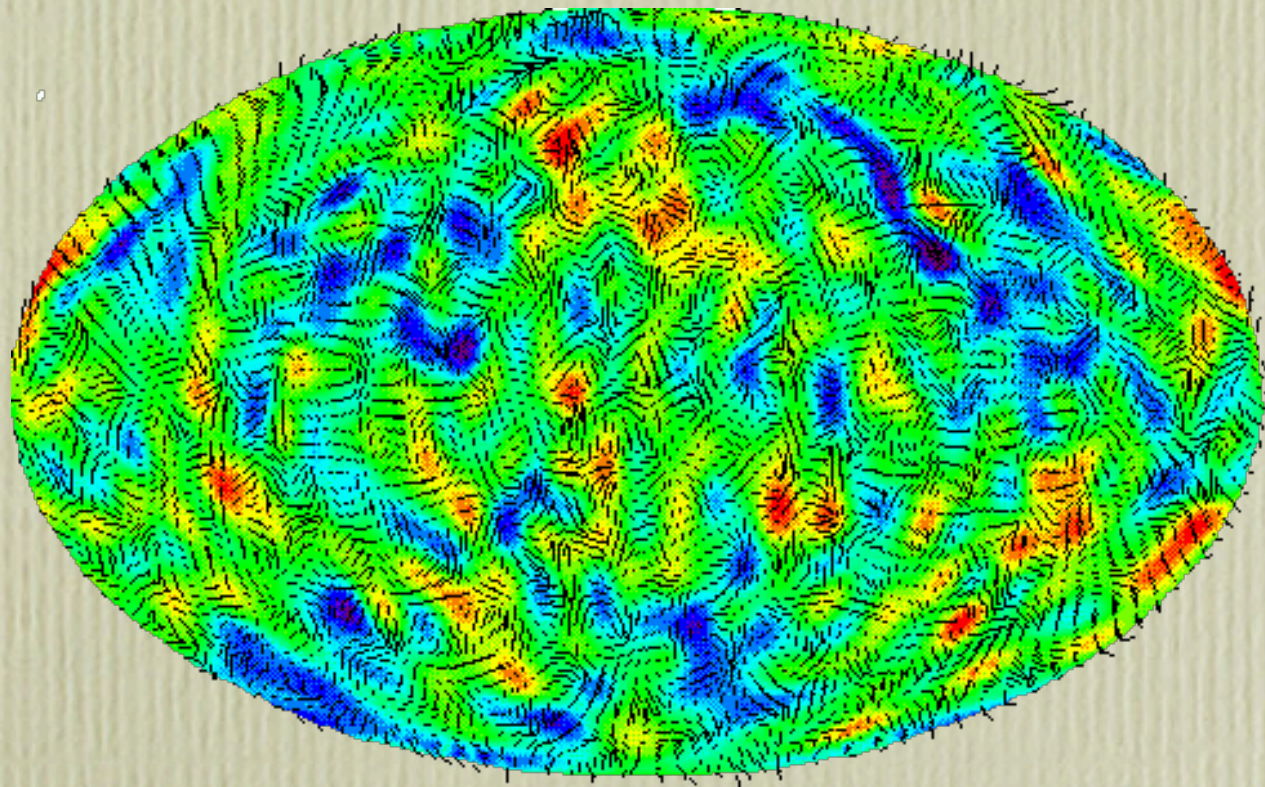
Pulsar timing arrays

- No detection yet, but recent limits are starting to become astrophysical interesting.



NANOGrav
9-year results
[Arzoumanian
et al. (2015)]

Lessons from the CMB



- CMB community measure temperature and polarisation maps
- Polarisation is described in terms of Stokes parameters Q and U that give the polarisation tensor

$$\mathcal{P} = \begin{pmatrix} Q & U \\ U & -Q \end{pmatrix}$$

- This is a transverse-traceless tensor on the sky, c.f. the GW field

$$h_{ab}^{\text{TT}} = \begin{pmatrix} h_{+} & h_{\times} \\ h_{\times} & -h_{+} \end{pmatrix}$$

Spin-weighted functions

- A spin-weighted function $f(\hat{k}, \hat{l}, \hat{m})$ maps a point \hat{k} and an orthonormal basis (\hat{l}, \hat{m}) on the sphere onto \mathbb{C} and has the property

$$f(\hat{k}, \cos \psi \hat{l} - \sin \psi \hat{m}, \sin \psi \hat{l} + \cos \psi \hat{m}) = e^{is\psi} f(\hat{k}, \hat{l}, \hat{m})$$

- where s is the spin weight.

- Under such a rotation

$$h_+ \rightarrow h_+ \cos 2\psi + h_\times \sin 2\psi \quad h_\times \rightarrow -h_+ \sin 2\psi + h_\times \cos 2\psi$$

- so the quantities $m_\pm^a m_\pm^b h_{ab}(\hat{k})$, where $\hat{m}_\pm^a = \hat{l}^a \pm i\hat{m}^a$ have spin-weight ± 2 . A spin-weight s function can be expanded in terms of

$${}_s Y_{lm}(\theta, \phi) = \sqrt{\frac{(l-s)!}{(l+s)!}} \check{\partial}^s Y_{lm}(\theta, \phi)$$

$$\check{\partial}^s \eta = -(\sin \theta)^s \left[\frac{\partial}{\partial \theta} + i \csc \theta \frac{\partial}{\partial \phi} \right] (\sin \theta)^{-s} \eta$$

Grad and curl spherical harmonics

- Can decompose any transverse-traceless tensor field on the sky as a superposition of gradients and curls of spherical harmonics

$$Y_{(lm)ab}^G = N_l \left(Y_{(lm);ab} - \frac{1}{2} g_{ab} Y_{(lm);c}{}^c \right)$$

$$Y_{(lm)ab}^C = \frac{N_l}{2} \left(Y_{(lm);ac} \epsilon^c{}_b + Y_{(lm);bc} \epsilon^c{}_a \right)$$

$$N_l = \sqrt{\frac{2(l-2)!}{(l+2)!}}$$

- NB we have modes with $l \geq 2$ only. Using standard polarisation tensors on the sky

$$e_{ab}^+(\hat{k}) = \hat{\theta}_a \hat{\theta}_b - \hat{\phi}_a \hat{\phi}_b \quad e_{ab}^\times(\hat{k}) = \hat{\theta}_a \hat{\phi}_b + \hat{\phi}_a \hat{\theta}_b$$

- we have

$$Y_{(lm)ab}^G(\hat{k}) = \frac{N_l}{2} \left[W_{(lm)}(\hat{k}) e_{ab}^+(\hat{k}) + X_{(lm)}(\hat{k}) e_{ab}^\times(\hat{k}) \right]$$

$$Y_{(lm)ab}^C(\hat{k}) = \frac{N_l}{2} \left[W_{(lm)}(\hat{k}) e_{ab}^\times(\hat{k}) - X_{(lm)}(\hat{k}) e_{ab}^+(\hat{k}) \right]$$

Grad and curl spherical harmonics

- The W and X functions are related to spin-2 spherical harmonics

$$\pm_2 Y_{(lm)}(\hat{k}) = \frac{N_l}{\sqrt{2}} \left[W_{(lm)}(\hat{k}) \pm i X_{(lm)}(\hat{k}) \right]$$

- and can be written in terms of associated Legendre polynomials

$$W_{(lm)}(\hat{k}) = e^{im\phi} \times \{\text{combinations of } P_l^m \text{'s}\}$$

$$iX_{(lm)}(\hat{k}) = m e^{im\phi} \times \{\text{combinations of } P_l^m \text{'s}\}$$

- In terms of these grad and curl harmonics, a general GW background with GR polarisation can be written

$$h_{ab}(t, \vec{x}) = \int_{-\infty}^{\infty} df \int_{S^2} d^2\Omega_{\hat{k}} \left\{ \sum_{l=2}^{\infty} \sum_{m=-l}^l \left[a_{(lm)}^G(f) Y_{(lm)ab}^G(\hat{k}) + a_{(lm)}^C(f) Y_{(lm)ab}^C(\hat{k}) \right] \right\} e^{i2\pi f(t - \hat{k} \cdot \vec{x}/c)}$$

PTA response

- A plane gravitational wave induces a redshift in a pulsar signal

$$z(t, \hat{k}) \equiv \frac{\Delta v(t)}{\nu_0} = \frac{1}{2} \frac{\hat{u}^a \hat{u}^b}{1 + \hat{k} \cdot \hat{u}} \Delta h_{ab}(t, \hat{k})$$

- The redshift induced by a GW background can be written as

$$\begin{aligned} z(t) &= \int_{-\infty}^{\infty} df \int_{S^2} d^2\Omega_{\hat{k}} \frac{1}{2} \frac{\hat{u}^a \hat{u}^b}{1 + \hat{k} \cdot \hat{u}} h_{ab}(f, \hat{k}) \left[1 - e^{-i2\pi f L(1 + \hat{k} \cdot \hat{u})/c} \right] e^{i2\pi f(t - \hat{k} \cdot \vec{x}/c)} \\ &= \int_{-\infty}^{\infty} df \sum_{(lm)} \sum_P R_{(lm)}^P(f) a_{(lm)}^P(f) e^{i2\pi f t} \end{aligned}$$

- where the response functions for individual modes are given by

$$R_{(lm)}^P(f) = \int_{S^2} d^2\Omega_{\hat{k}} \frac{1}{2} \frac{\hat{u}^a \hat{u}^b}{1 + \hat{k} \cdot \hat{u}} Y_{(lm)ab}^P(\hat{k}) e^{-i2\pi f \hat{k} \cdot \vec{x}/c} \left[1 - e^{-i2\pi f L(1 + \hat{k} \cdot \hat{u})/c} \right]$$

- We make the simplifying assumption that $\vec{x} \approx 0$. We will use the notation $y \equiv 2\pi f L/c$ and often assume $y \gg 0$.

Alternative polarisation states

- GR admits two transverse and traceless (TT) polarisations

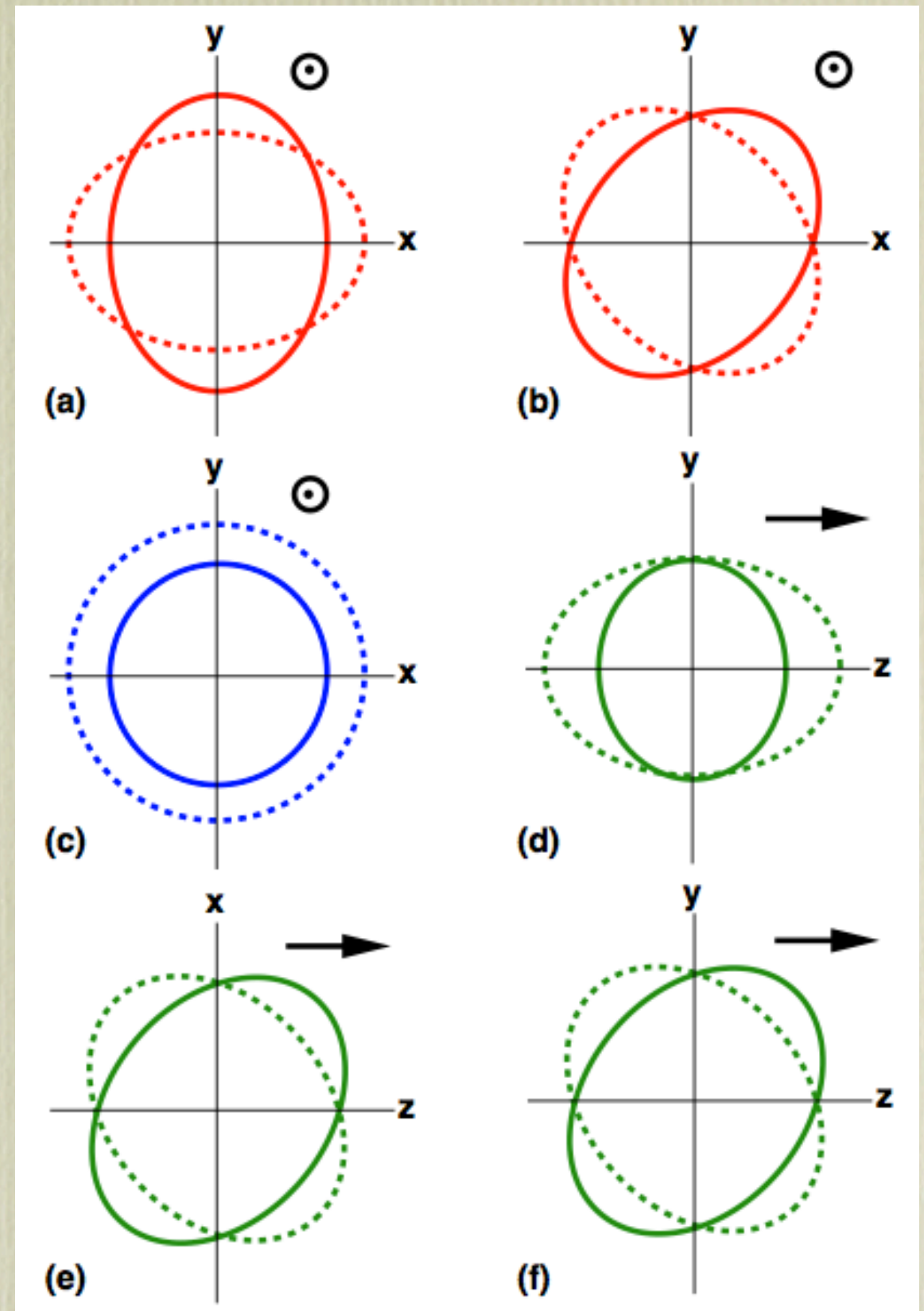
$$e_{ij}^+ = \begin{pmatrix} 1 & 0 & 0 \\ 0 & -1 & 0 \\ 0 & 0 & 0 \end{pmatrix} \quad e_{ij}^\times = \begin{pmatrix} 0 & 1 & 0 \\ 1 & 0 & 0 \\ 0 & 0 & 0 \end{pmatrix}$$

- In other metric theories of gravity, can have up to four additional states

$$e_{ij}^B = \begin{pmatrix} 1 & 0 & 0 \\ 0 & 1 & 0 \\ 0 & 0 & 0 \end{pmatrix} \quad e_{ij}^L = \begin{pmatrix} 0 & 0 & 0 \\ 0 & 0 & 0 \\ 0 & 0 & 1 \end{pmatrix}$$

$$e_{ij}^X = \begin{pmatrix} 0 & 0 & 1 \\ 0 & 0 & 0 \\ 1 & 0 & 0 \end{pmatrix} \quad e_{ij}^Y = \begin{pmatrix} 0 & 0 & 0 \\ 0 & 0 & 1 \\ 0 & 1 & 0 \end{pmatrix}$$

- Can use a similar approach to map non-GR polarisation backgrounds.



Extensions - alternative polarisations

- For the scalar modes (B, L) the quantities

$$\hat{m}_{\pm}^a \hat{m}_{\pm}^b h_{ab}^B(\hat{k}) \qquad \hat{m}_{\pm}^a \hat{m}_{\pm}^b h_{ab}^L(\hat{k})$$

- where $\hat{m}_{\pm}^a = \hat{l}^a \pm i\hat{m}^a$ as before, are invariant under rotations, i.e., they are spin-weight zero.
- Expand in terms of **standard spherical harmonics**, e.g.,

$$h_{ab}(t, \vec{x}) = \int_{-\infty}^{\infty} df \int_{S^2} d^2\hat{\Omega}_{\hat{k}} h_B(f, \hat{k}) e_{ab}^B(\hat{k}) e^{i2\pi f(t - \hat{k} \cdot \vec{x}/c)}$$

$$h_B(f, \hat{k}) = \frac{1}{\sqrt{2}} \sum_{l=0}^{\infty} \sum_{m=-l}^l a_{(lm)}^B(f) Y_{lm}(\hat{k})$$

$$R_{(lm)}^B(f) = \int_{S^2} d^2\Omega_{\hat{k}} \left[\frac{1}{2\sqrt{2}} \frac{\hat{u}^a \hat{u}^b}{1 + \hat{k} \cdot \hat{u}} e_{ab}^B(\hat{k}) Y_{lm}(\hat{k}) \left(1 - e^{-iy(1 + \hat{k} \cdot \hat{u})} \right) \right]$$

Extensions - alternative polarisations

- For the vector modes (X, Y) the quantities

$$\hat{m}_{\pm}^a \hat{m}_{\pm}^b h_{ab}^X(\hat{k}) \qquad \hat{m}_{\pm}^a \hat{m}_{\pm}^b h_{ab}^Y(\hat{k})$$

- transform like spin-weight ± 1 objects under rotations. **Expand in terms of spin-weight ± 1 spherical harmonics**

$$h_{ab}(t, \vec{x}) = \int_{-\infty}^{\infty} df \int_{S^2} d^2\Omega_{\hat{k}} \left[h_X(f, \hat{k}) e_{ab}^X(\hat{k}) + h_Y(f, \hat{k}) e_{ab}^Y(\hat{k}) \right] e^{i2\pi f(t - \hat{k} \cdot \vec{x}/c)}$$

$$h_X(f, \hat{k}) = \frac{1}{2\sqrt{2}} \sum_{lm} \left[v_{(lm)}^G(f) \left(-{}_1Y_{lm}(\hat{k}) - {}_1Y_{lm}(\hat{k}) \right) - iv_{(lm)}^C(f) \left(-{}_1Y_{lm}(\hat{k}) + {}_1Y_{lm}(\hat{k}) \right) \right],$$

$$h_Y(f, \hat{k}) = \frac{1}{2\sqrt{2}} \sum_{lm} \left[v_{(lm)}^C(f) \left(-{}_1Y_{lm}(\hat{k}) - {}_1Y_{lm}(\hat{k}) \right) + iv_{(lm)}^G(f) \left(-{}_1Y_{lm}(\hat{k}) + {}_1Y_{lm}(\hat{k}) \right) \right]$$

- Can write

$$Y_{(lm)_a}^{VG}(\hat{k}) = \frac{1}{2\sqrt{2}} \left[\left(-{}_1Y_{lm}(\hat{k}) - {}_1Y_{lm}(\hat{k}) \right) \hat{l}_a + i \left(-{}_1Y_{lm}(\hat{k}) + {}_1Y_{lm}(\hat{k}) \right) \hat{m}_a \right],$$

$$Y_{(lm)_a}^{VC}(\hat{k}) = \frac{1}{2\sqrt{2}} \left[\left(-{}_1Y_{lm}(\hat{k}) - {}_1Y_{lm}(\hat{k}) \right) \hat{m}_a - i \left(-{}_1Y_{lm}(\hat{k}) + {}_1Y_{lm}(\hat{k}) \right) \hat{l}_a \right]$$

Extensions - alternative polarisations

- Then we define

$$Y_{(lm)ab}^{VG} = Y_{(lm)a}^{VG} \hat{k}_b + Y_{(lm)b}^{VG} \hat{k}_a ,$$

$$Y_{(lm)ab}^{VC} = Y_{(lm)a}^{VC} \hat{k}_b + Y_{(lm)b}^{VC} \hat{k}_a ,$$

- so that

$$h_{ab}(t, \vec{x}) = \int_{-\infty}^{\infty} df \int_{S^2} d^2\Omega_{\hat{k}} \left\{ \sum_{(lm)} \left[a_{(lm)}^{VG}(f) Y_{(lm)ab}^{VG}(\hat{k}) + a_{(lm)}^{VC}(f) Y_{(lm)ab}^{VC}(\hat{k}) \right] \right\} e^{i2\pi f(t - \hat{k} \cdot \vec{x}/c)}$$

- and work with the responses

$$R_{(lm)}^{VG}(f) = \int_{S^2} d^2\Omega_{\hat{k}} \left[\frac{1}{2} \frac{\hat{u}^a \hat{u}^b}{1 + \hat{k} \cdot \hat{u}} \left(1 - e^{-iy(1 + \hat{k} \cdot \hat{u})} \right) Y_{(lm)ab}^{VG}(\hat{k}) \right] ,$$

$$R_{(lm)}^{VC}(f) = \int_{S^2} d^2\Omega_{\hat{k}} \left[\frac{1}{2} \frac{\hat{u}^a \hat{u}^b}{1 + \hat{k} \cdot \hat{u}} \left(1 - e^{-iy(1 + \hat{k} \cdot \hat{u})} \right) Y_{(lm)ab}^{VC}(\hat{k}) \right]$$

Pulsar response functions

- Compute response in *computational frame*, in which pulsar is in the z -direction. Expansion coefficients transform under a rotation in a similar way to spherical harmonic coefficients.

$$Y_{(lm)ab}^P(\theta, \phi) = \sum_{m'=-l}^l [D^l_{mm'}(\chi_I, \zeta_I, 0)]^* Y_{(lm')\bar{a}\bar{b}}^P(\bar{\theta}, \bar{\phi}) \mathbf{R}(\chi_I, \zeta_I, 0)^{\bar{a}}_a \mathbf{R}(\chi_I, \zeta_I, 0)^{\bar{b}}_b$$

- Deduce that the response functions in the cosmic frame for a pulsar in direction $\hat{u}_I^a = (\sin \zeta_I \cos \chi_I, \sin \zeta_I \sin \chi_I, \cos \zeta_I)$ take the form

$$R_{I(lm)}^P(f) = Y_{lm}(\hat{u}_I) \mathcal{R}_l^P(y_I)$$

- for all polarisation states.

Response to tensor modes

- In the computational frame we have

$$\frac{1}{2} \frac{\hat{u}^a \hat{u}^b}{1 + \hat{k} \cdot \hat{u}} e_{ab}^+(\hat{k}) = \frac{1}{2} (1 - \cos \theta), \quad \frac{1}{2} \frac{\hat{u}^a \hat{u}^b}{1 + \hat{k} \cdot \hat{u}} e_{ab}^\times(\hat{k}) = 0$$

- Recall

$$Y_{(lm)ab}^G(\hat{k}) = \frac{N_l}{2} \left[W_{(lm)}(\hat{k}) e_{ab}^+(\hat{k}) + X_{(lm)}(\hat{k}) e_{ab}^\times(\hat{k}) \right]$$

$$Y_{(lm)ab}^C(\hat{k}) = \frac{N_l}{2} \left[W_{(lm)}(\hat{k}) e_{ab}^\times(\hat{k}) - X_{(lm)}(\hat{k}) e_{ab}^+(\hat{k}) \right]$$

- We deduce that, in this frame

$$R_{(lm)}^C = - \int_0^{2\pi} d\bar{\phi} \int_{-1}^1 d \cos \bar{\theta} \frac{N_l}{2} F^+(\bar{\theta}, \bar{\phi}) X_{(l0)}(\bar{\theta}, \bar{\phi}) \left[1 - e^{-iy(1+\cos \bar{\theta})} \right] = 0$$

- We have **zero sensitivity to curl modes** in any frame.

Response to tensor modes

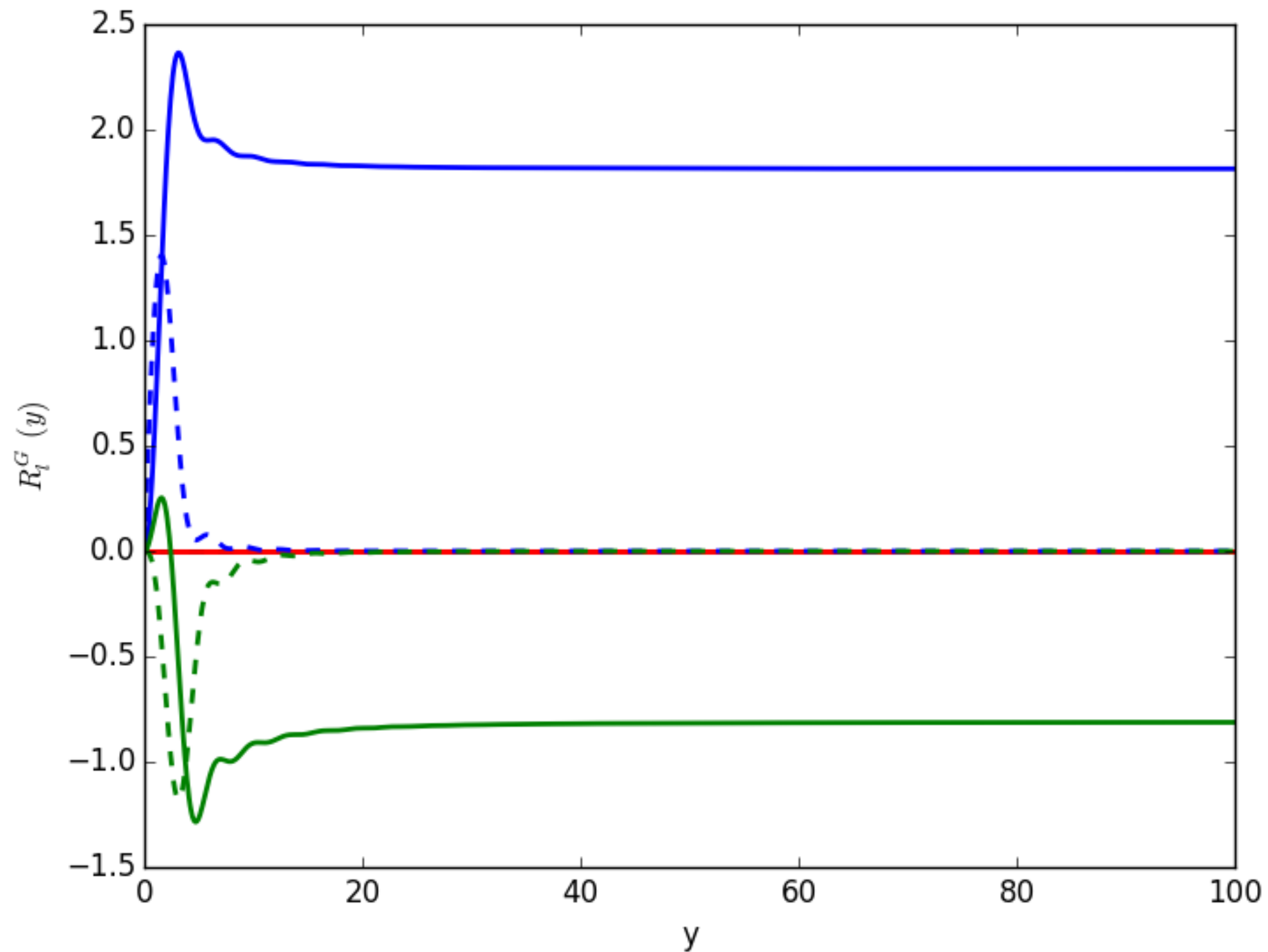
- For the grad modes we have

$$\begin{aligned}
 R_{(lm)}^G &= \int_0^{2\pi} d\bar{\phi} \int_{-1}^1 d\cos\bar{\theta} \frac{N_l}{4} (1 - \cos\bar{\theta}) W_{(l0)}(\bar{\theta}, \bar{\phi}) \left[1 - e^{-iy(1+\cos\bar{\theta})} \right] \\
 &= \frac{\sqrt{(2l+1)\pi}}{2} N_l (-i)^l e^{-iy} \left[(2 - 2iy + y^2) j_l(y) - i(6 + 4iy + y^2) \frac{dj_l}{dy} \right. \\
 &\quad \left. - (6iy - y^2) \frac{d^2 j_l}{dy^2} - iy^2 \frac{d^3 j_l}{dy^3} \right]
 \end{aligned}$$

- The y -dependent terms are the contributions from the pulsar term and are negligible for $y \gtrsim 10$, the regime in which PTAs operate.
- Deduce that the response functions in the cosmic frame for a pulsar in direction $\hat{u}_I^a = (\sin \zeta_I \cos \chi_I, \sin \zeta_I \sin \chi_I, \cos \zeta_I)$ are

$$R_{I(lm)}^G = 2\pi (-1)^l N_l Y_{(lm)}(\hat{u}_I) \qquad R_{(lm)}^C = 0$$

Response to tensor modes



Response to scalar modes

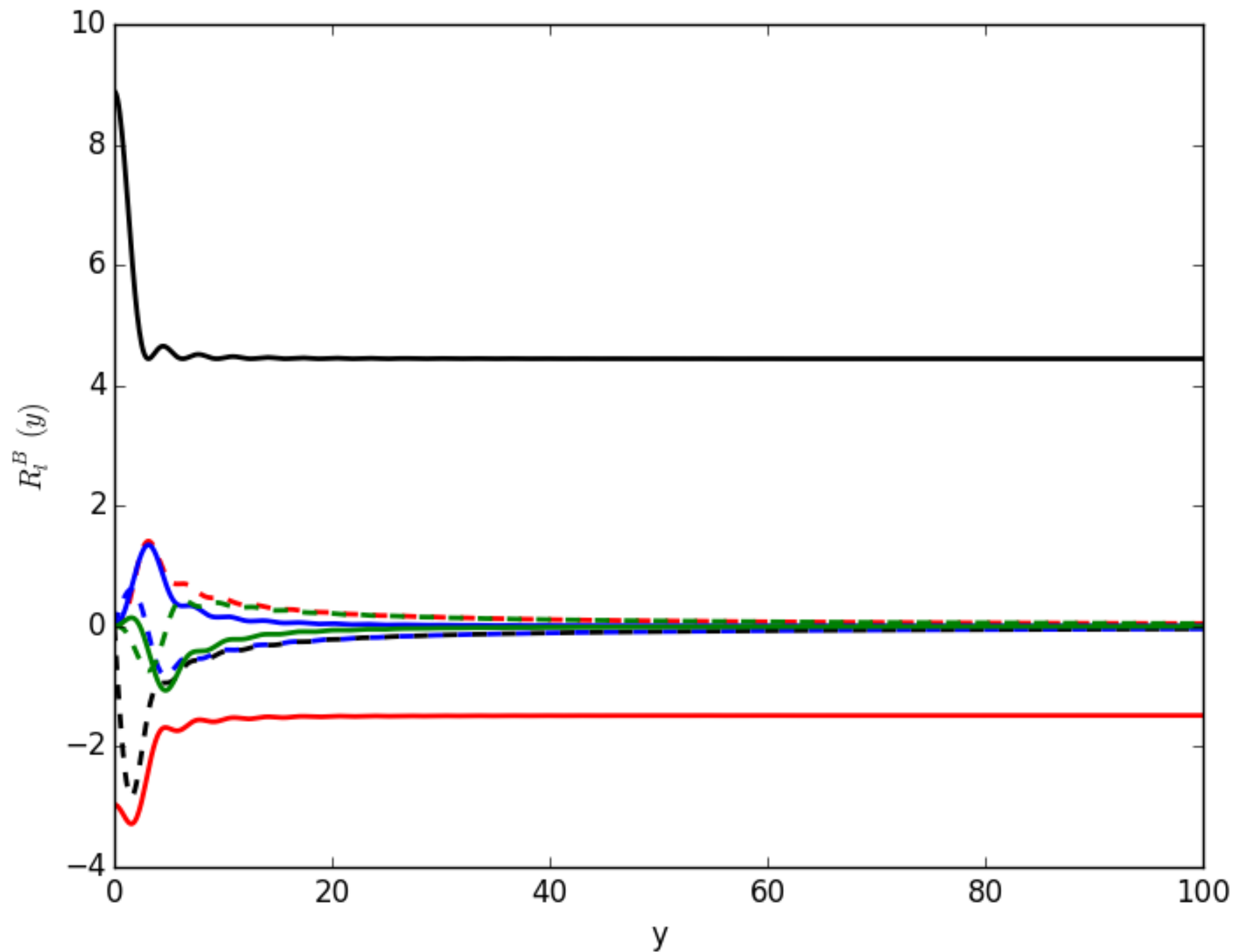
- For the breathing mode, we find

$$\begin{aligned}\mathcal{R}_l^B(y) &= 2\pi \frac{1}{\sqrt{2}} \int_{-1}^1 dx \frac{1}{2} (1-x) P_l(x) \left(1 - e^{-i(1+x)y}\right) \\ &= 2\pi \frac{1}{\sqrt{2}} \left\{ \delta_{l0} - \frac{1}{3} \delta_{l1} - (-i)^l e^{-iy} \left[\left(1 - i \frac{l}{y}\right) j_l(y) + i j_{l+1}(y) \right] \right\}\end{aligned}$$

- and in the limit in which we can ignore the pulsar term, this becomes

$$R_{I(lm)}^B = 4\pi N_l^0 \sqrt{\frac{\pi}{2l+1}} Y_{lm}(\hat{u}_I) \left[\delta_{l0} - \frac{1}{3} \delta_{l1} \right]$$

Response to breathing modes



Response to scalar modes

- For the scalar longitudinal modes $R_{I(lm)}^L(f) = Y_{lm}(\hat{u}_I) \mathcal{R}_l^L(y_I)$

$$\begin{aligned} \mathcal{R}_l^L(y) &\equiv 2\pi \int_{-1}^1 dx \frac{1}{2} \frac{x^2}{1+x} P_l(x) \left(1 - e^{-iy(1+x)}\right) \\ &= 2\pi \int_{-1}^1 dx \frac{1}{2} \left[-1 + x + \frac{1}{1+x}\right] P_l(x) \left(1 - e^{-iy(1+x)}\right) \\ &= 2\pi \left\{ -\delta_{l0} + \frac{1}{3}\delta_{l1} + (-i)^l e^{-iy} \left[\left(1 - i\frac{l}{y}\right) j_l(y) + i j_{l+1}(y) \right] + \frac{1}{2} H_l(y) \right\} \end{aligned}$$

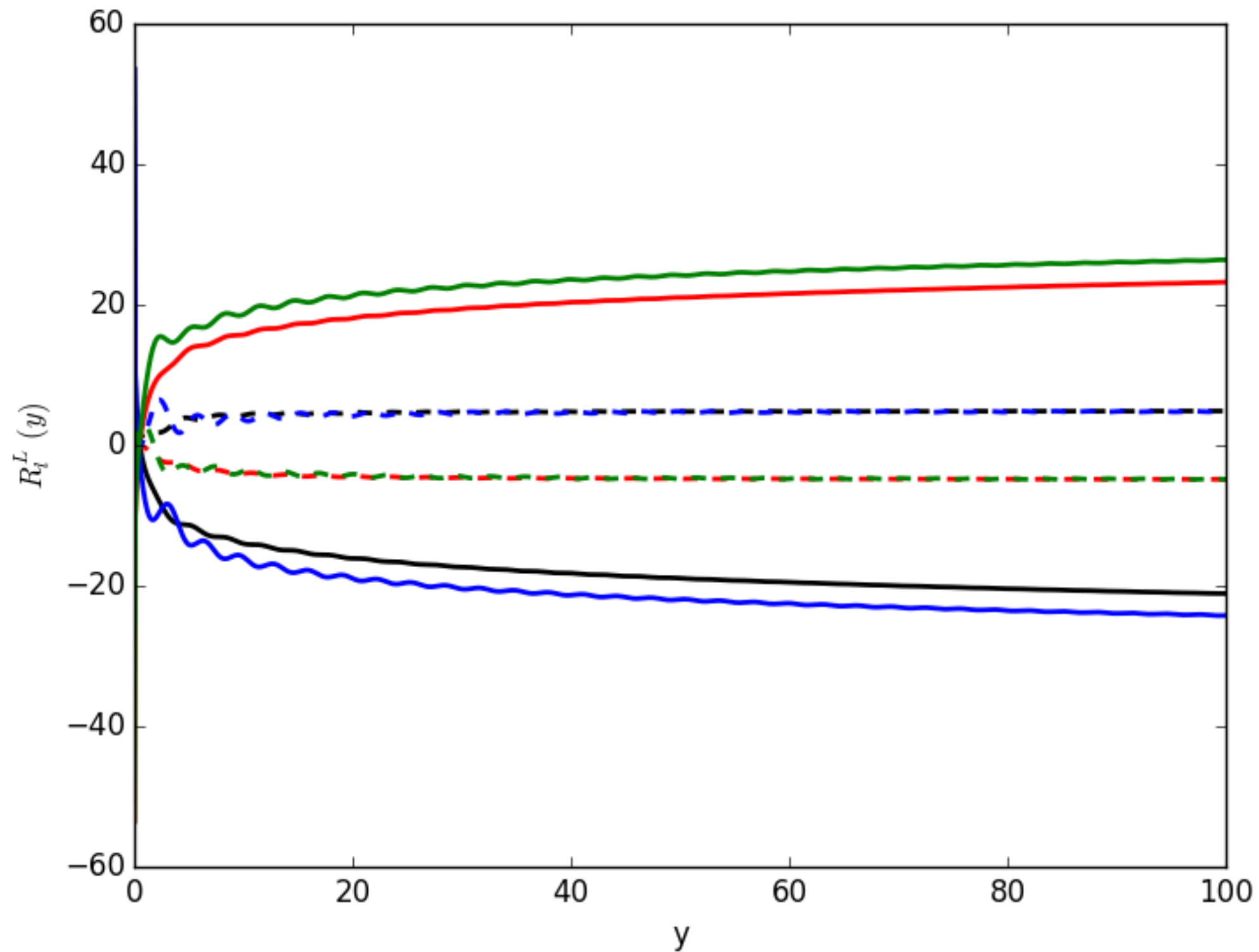
- in which

$$H_l(y) = \int_{-1}^1 dx \frac{1}{(1+x)} P_l(x) \left(1 - e^{-iy(1+x)}\right)$$

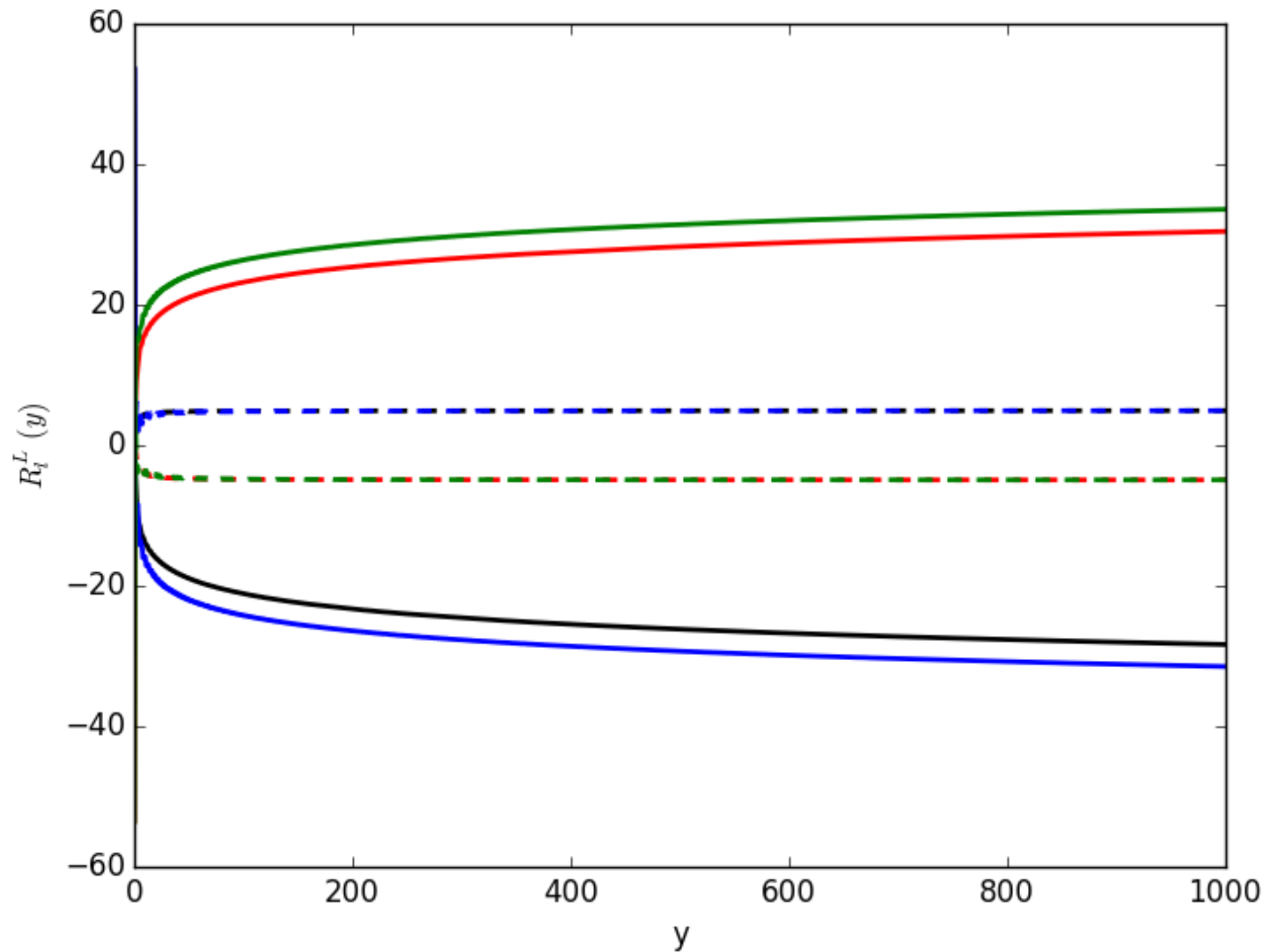
- and for large y , we have

$$R_{I(lm)}^L(f) \approx 2\pi Y_{lm}(\hat{u}_I) \left[-\delta_{l0} + \frac{1}{3}\delta_{l1} + \frac{1}{2} H_l(y_I) \right]$$

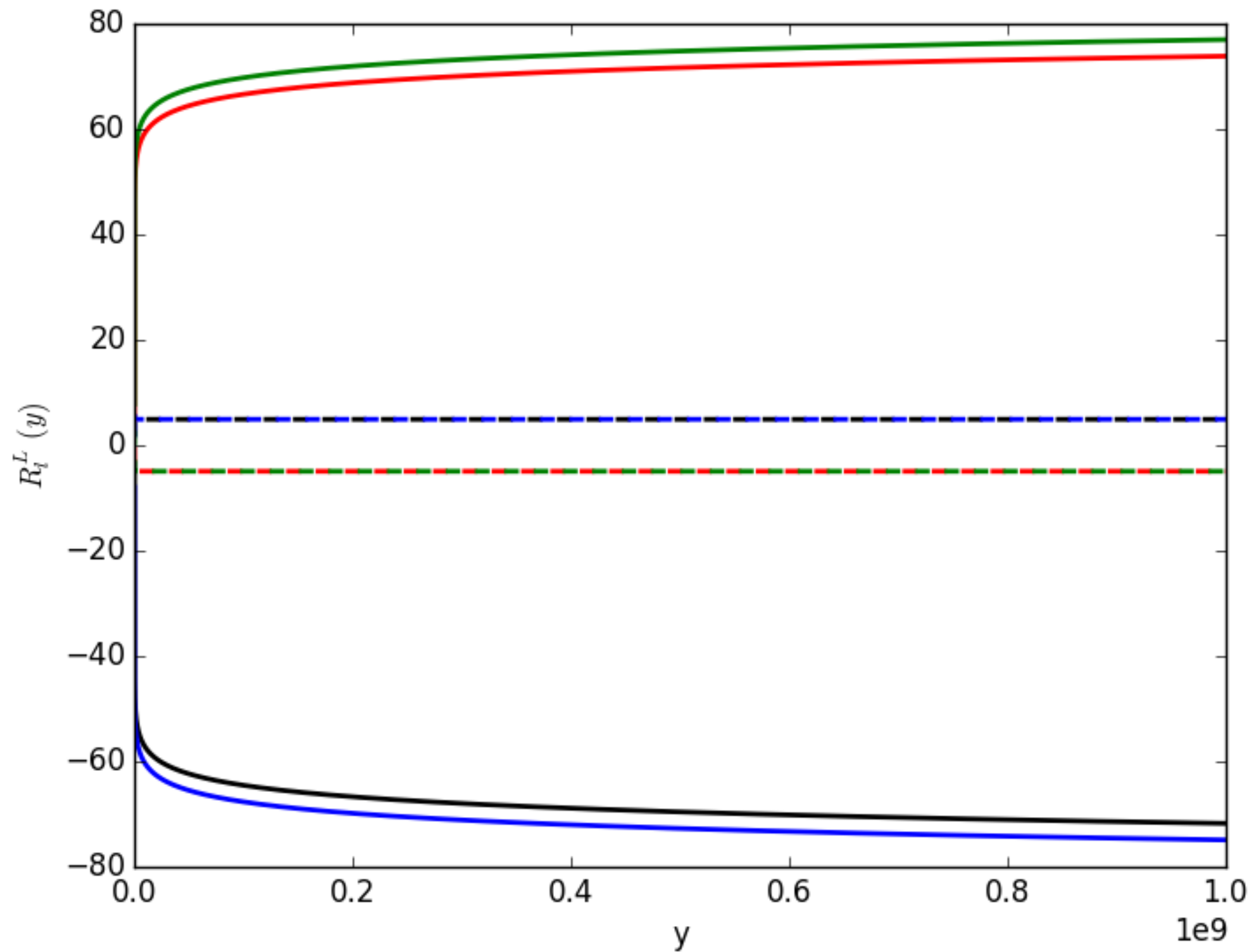
Response to scalar-longitudinal modes



Response to scalar-longitudinal modes



Response to scalar-longitudinal modes



Response to vector modes

- For the vector-longitudinal modes we have

$$R_{I(lm)}^{VG}(f) = Y_{lm}(\hat{u}_I) \mathcal{R}_l^{VG}(y_I), \quad R_{I(lm)}^{VC}(f) = 0$$

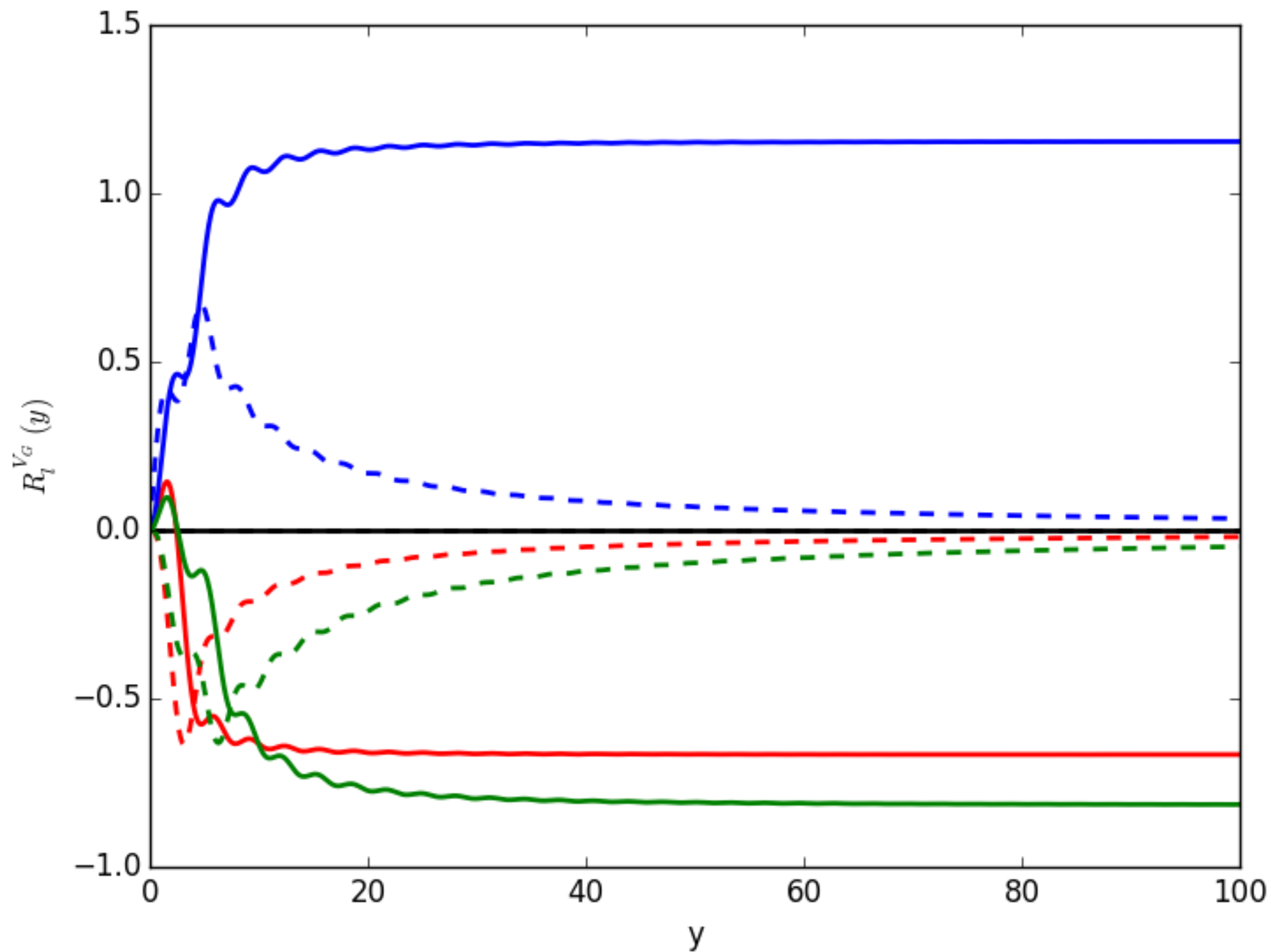
- Once again we find zero response of a PTA to the curl components of the background, but for grad modes

$$\begin{aligned} \mathcal{R}_l^{VG}(y) &= \pi^{(1)} N_l \int_{-1}^1 dx \left[x(1-x) \left(1 - e^{-iy(1+x)} \right) \frac{dP_l}{dx} \right] \\ &= \pi^{(1)} N_l \left[-2\delta_{l0} + \frac{4}{3}\delta_{l1} + (-1)^l e^{-iy} \int_{-1}^1 dx (1 + (2+iy)x + iyx^2) e^{iyx} P_l(x) \right] \\ &= \pi^{(1)} N_l \left\{ \frac{4}{3}\delta_{l1} + 2(-i)^l e^{-iy} \left[\left(1 - \frac{il}{y} \right) (l+1)j_l(y) - (y - i(2l+3))j_{l+1}(y) - iyj_{l+2}(y) \right] \right\} \end{aligned}$$

- For large y , this can be approximated by

$$R_{I(lm)}^{VG}(f) \approx 2\pi Y_{lm}(\hat{u}_I) \sqrt{\frac{2(l-1)!}{(l+1)!}} \left[\frac{2}{3}\delta_{l1} + (-1)^l \right]$$

Response to vector modes



Summary of response functions

- To summarise, the full set of response functions are

$$\mathcal{R}_l^G(y) = \pi {}^{(2)}N_l (-i)^l e^{-iy} \left[(2 - 2iy + y^2) j_l(y) - i(6 + 4iy + y^2) \frac{dj_l}{dy} - (6iy - y^2) \frac{d^2 j_l}{dy^2} - iy^2 \frac{d^3 j_l}{dy^3} \right]$$

$$\mathcal{R}_l^C(y) = 0$$

$$\mathcal{R}_l^B(y) = 2\pi \frac{1}{\sqrt{2}} \left\{ \delta_{l0} - \frac{1}{3} \delta_{l1} - (-i)^l e^{-iy} \left[\left(1 - i \frac{l}{y}\right) j_l(y) + i j_{l+1}(y) \right] \right\}$$

$$\mathcal{R}_l^L(y) = 2\pi \left\{ -\delta_{l0} + \frac{1}{3} \delta_{l1} + (-i)^l e^{-iy} \left[\left(1 - i \frac{l}{y}\right) j_l(y) + i j_{l+1}(y) \right] + \frac{1}{2} H_l(y) \right\}$$

$$H_l(y) = \int_{-1}^1 dx \frac{1}{(1+x)} P_l(x) \left(1 - e^{-iy(1+x)}\right)$$

$$R_l^{VG}(y) = \pi {}^{(1)}N_l \left\{ \frac{4}{3} \delta_{l1} + 2(-i)^l e^{-iy} \left[\left(1 - \frac{il}{y}\right) (l+1) j_l(y) - (y - i(2l+3)) j_{l+1}(y) - iy j_{l+2}(y) \right] \right\}$$

$$R_l^{VC}(y) = 0$$

- We have **zero sensitivity to tensor and vector curl modes**.
- Without the pulsar term, we have **no sensitivity to structure beyond dipole in scalar-tensor** (breathing mode) **backgrounds**.

Why zero curl response?

- PTAs have a common origin (the Solar System) for all pulsar lines of sight. Curl mode metric perturbation vanishes at the origin.
- Analogous to separation between odd and even modes, e.g., waves on a string

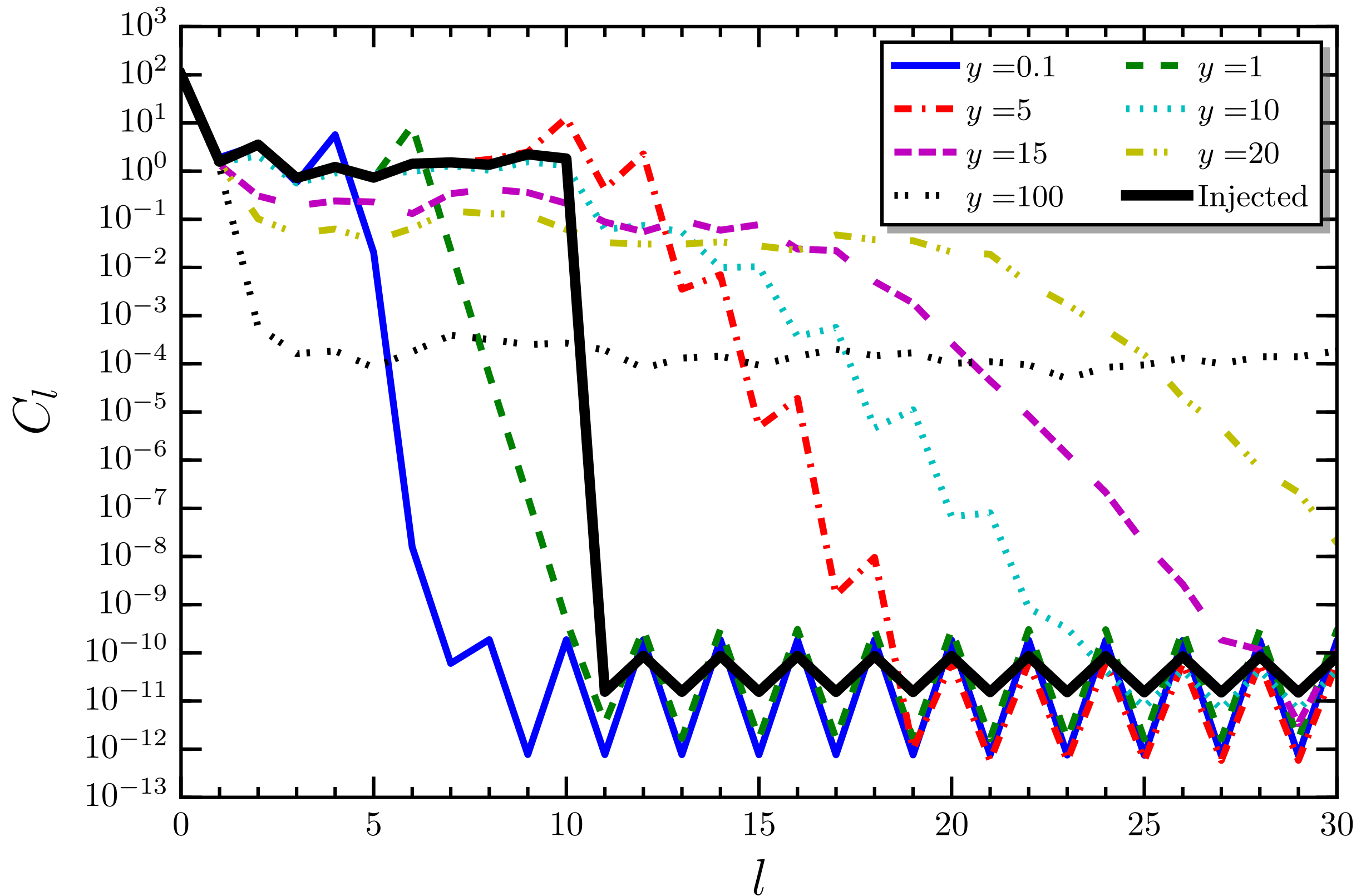
$$A \cos(x - t) + B \sin(x - t) + C \cos(x + t) + D \sin(x + t)$$

- Measurement at $x=0$ can only determine $A+C$ and $B+D$. Break degeneracy by adding a measurement at $x_1 \neq 0$ or using point-able detector that can distinguish left and right propagating modes.
- GW detectors are non-point-able and over a year

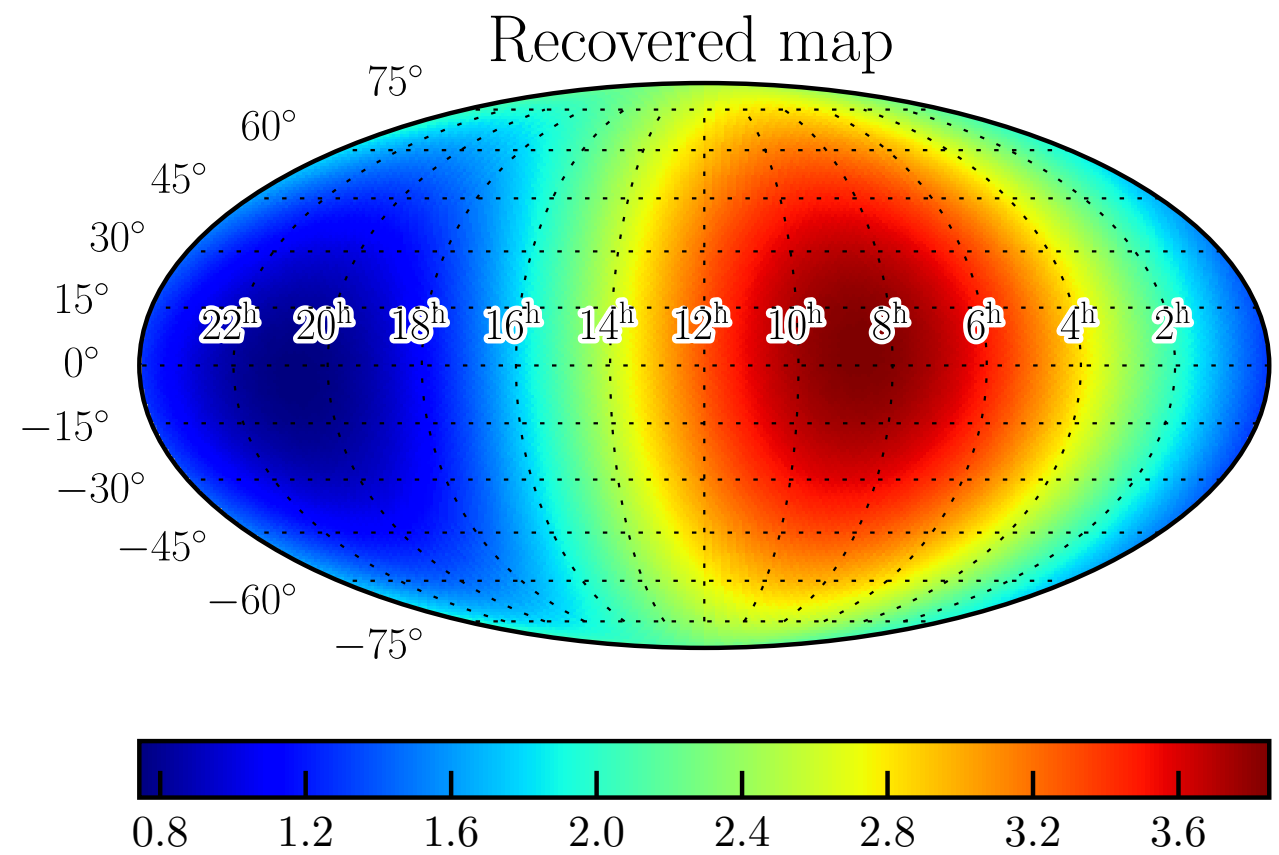
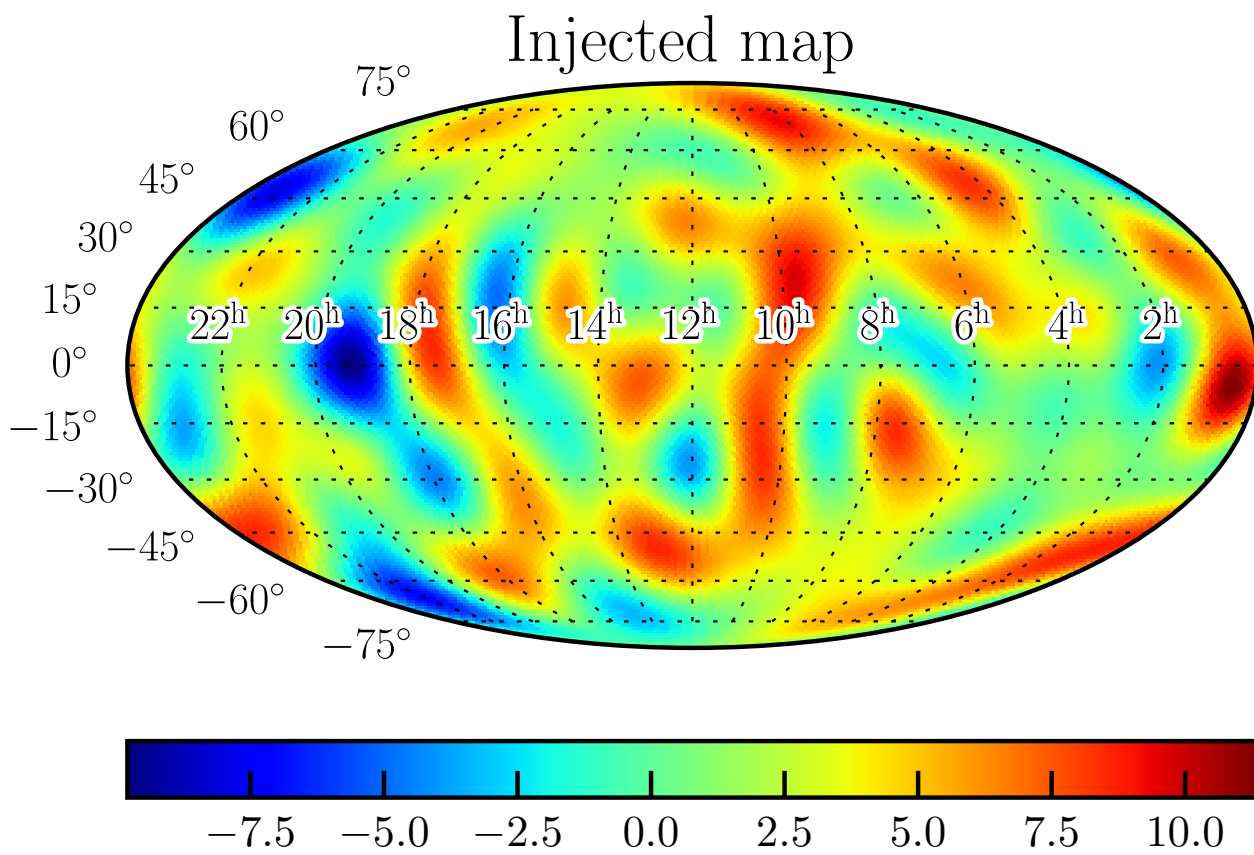
$$\Delta(f \hat{k} \cdot \vec{x}/c) \sim 0.0005$$

- for a GW frequency $f = 10^{-6}$ Hz.
- No curl sensitivity because PTA moves by much less than a GW wavelength over typical observation durations.

Scalar-tensor background recovery



Scalar-tensor background recovery



Isotropic, uncorrelated backgrounds

- An isotropic, uncorrelated and unpolarised background is described by the two-point functions

$$\langle h_+(f, \hat{k}) h_+^*(f', \hat{k}') \rangle = \langle h_\times(f, \hat{k}) h_\times^*(f', \hat{k}') \rangle = \frac{1}{2} H(f) \delta^2(\hat{k}, \hat{k}') \delta(f - f')$$

$$\langle h_+(f, \hat{k}) h_\times^*(f', \hat{k}') \rangle = \langle h_\times(f, \hat{k}) h_+^*(f', \hat{k}') \rangle = 0$$

- or in terms of the grad and curl expansion coefficients

$$\langle a_{(lm)}^G(f) a_{(l'm')}^{G*}(f') \rangle = \langle a_{(lm)}^C(f) a_{(l'm')}^{C*}(f') \rangle = \delta_{ll'} \delta_{mm'} H(f) \delta(f - f')$$

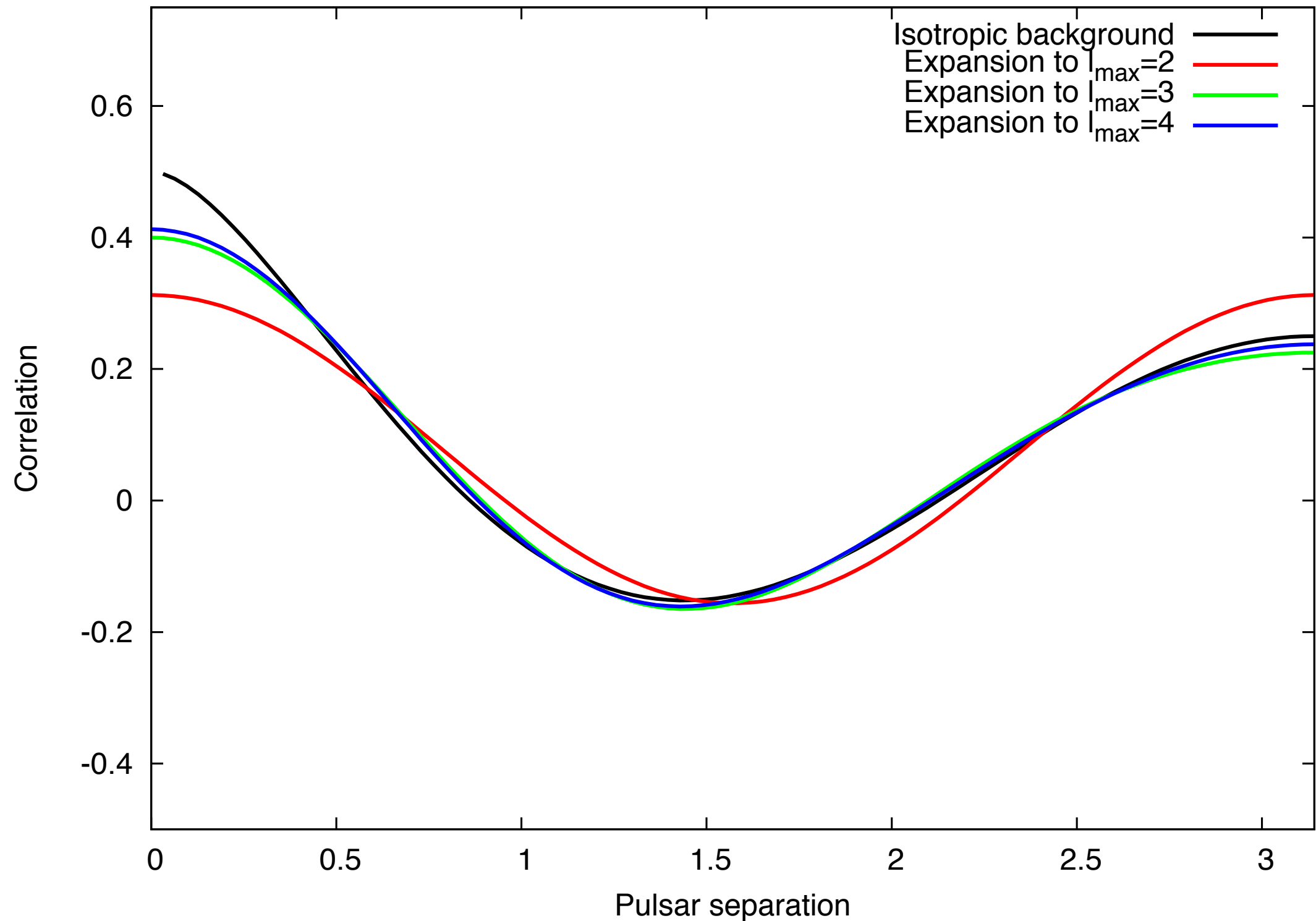
$$\langle a_{(lm)}^G(f) a_{(l'm')}^{C*}(f') \rangle = \langle a_{(lm)}^C(f) a_{(l'm')}^{G*}(f') \rangle = 0$$

- The expected correlation between the response of two pulsars for such a background is

$$\langle h_1(t) h_2(t') \rangle = \int_{-\infty}^{\infty} df e^{i2\pi f(t-t')} H(f) \Gamma_{12}(f)$$

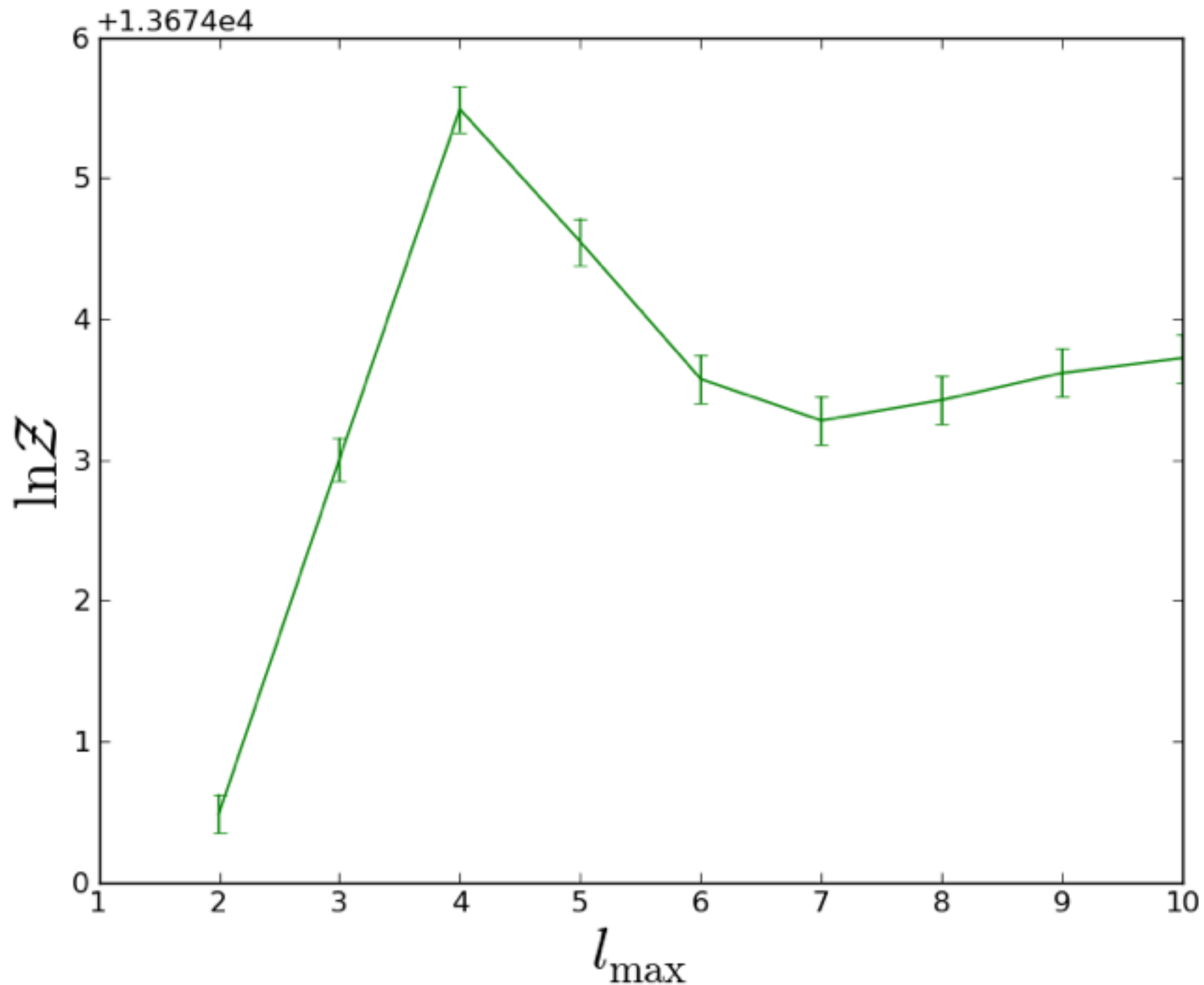
$$\Gamma_{12}(f) = \sum_{l=2}^{\infty} \sum_{m=-l}^l \sum_P R_{1(lm)}^P(f) R_{2(lm)}^{P*}(f) = \sum_{l=2}^{\infty} (N_l)^2 (2l+1) \pi P_l(\hat{u}_1 \cdot \hat{u}_2)$$

Isotropic, uncorrelated backgrounds



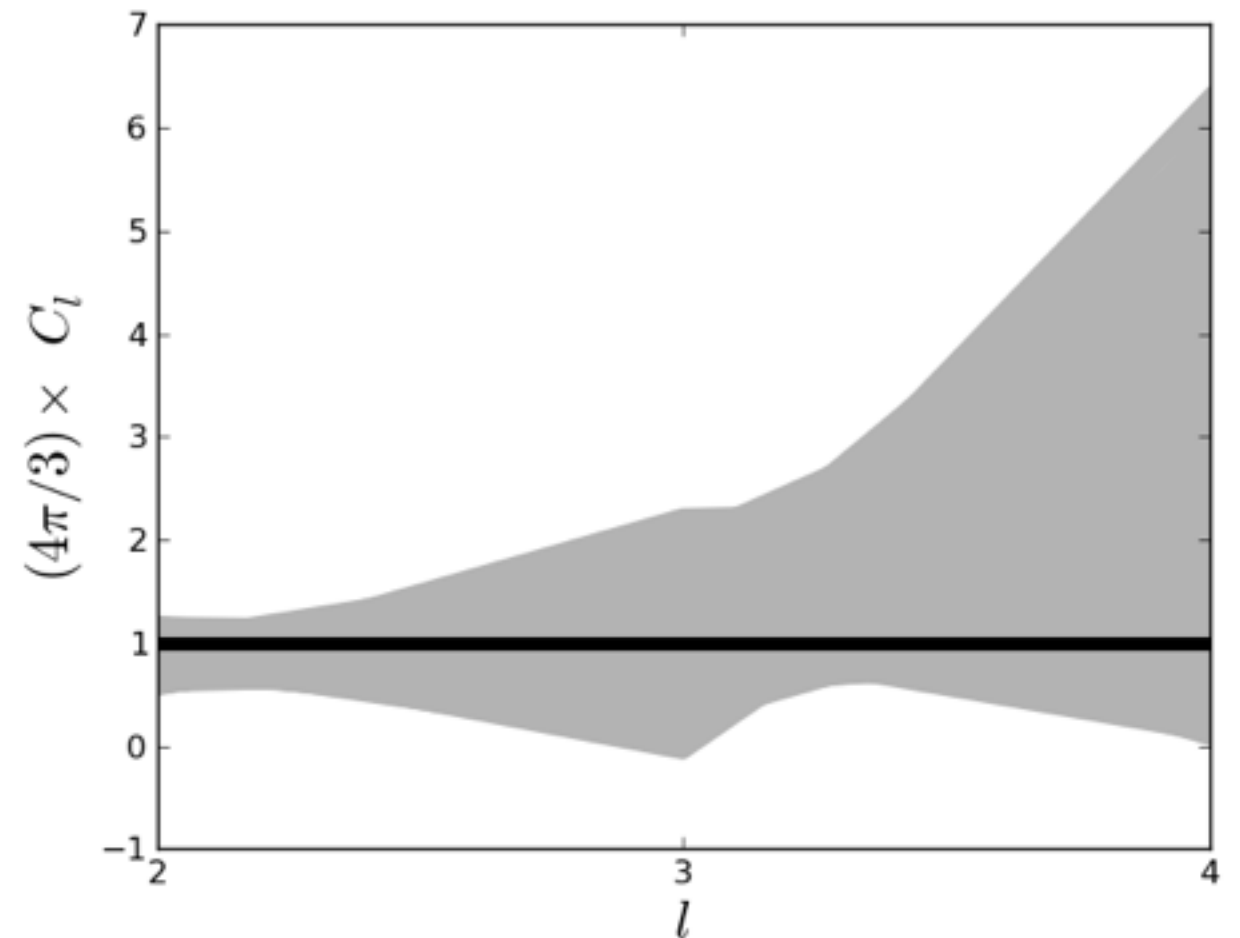
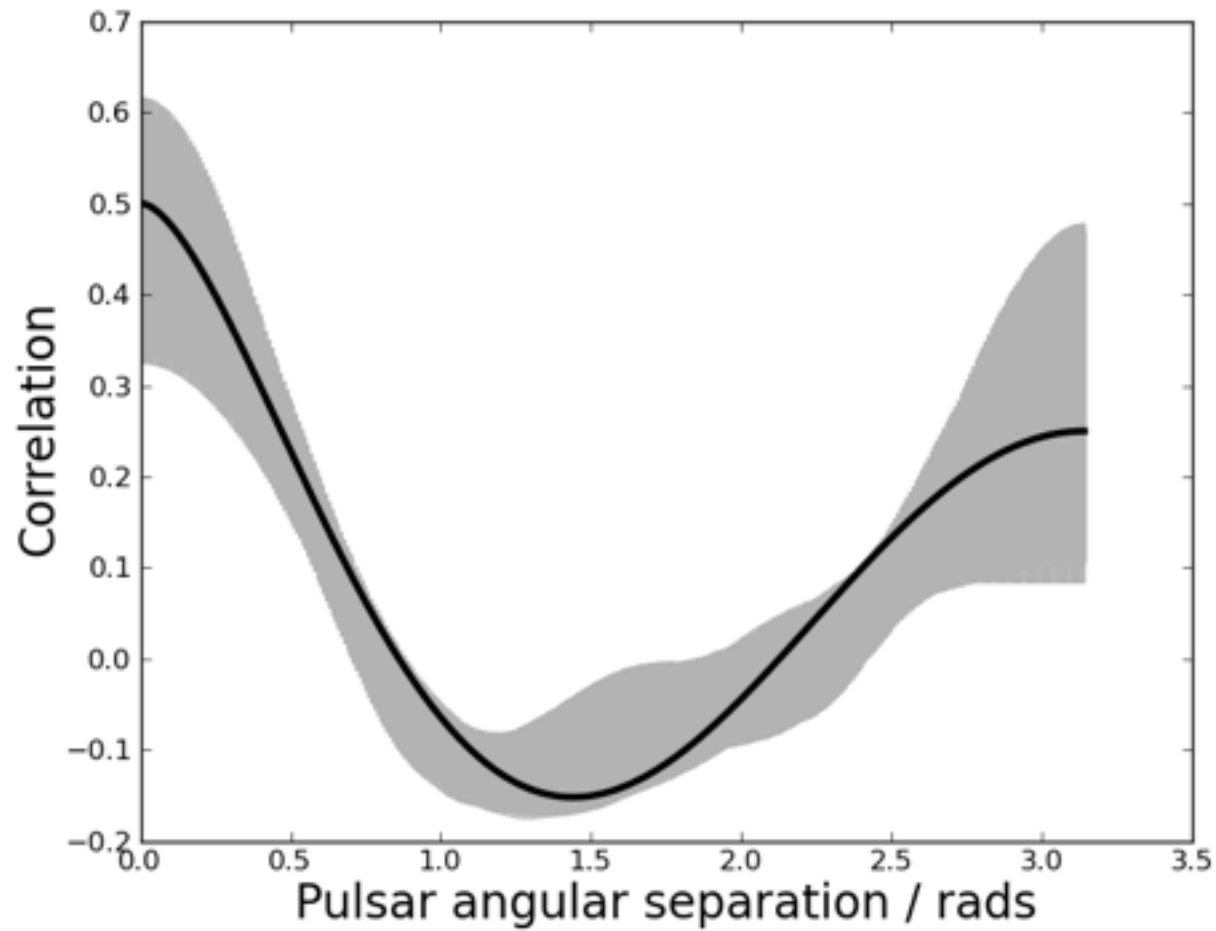
- This agrees with the standard Hellings and Downs correlation.

Isotropic, uncorrelated backgrounds



- Including three modes in the expansion is enough to characterise an isotropic background.

Isotropic, uncorrelated backgrounds



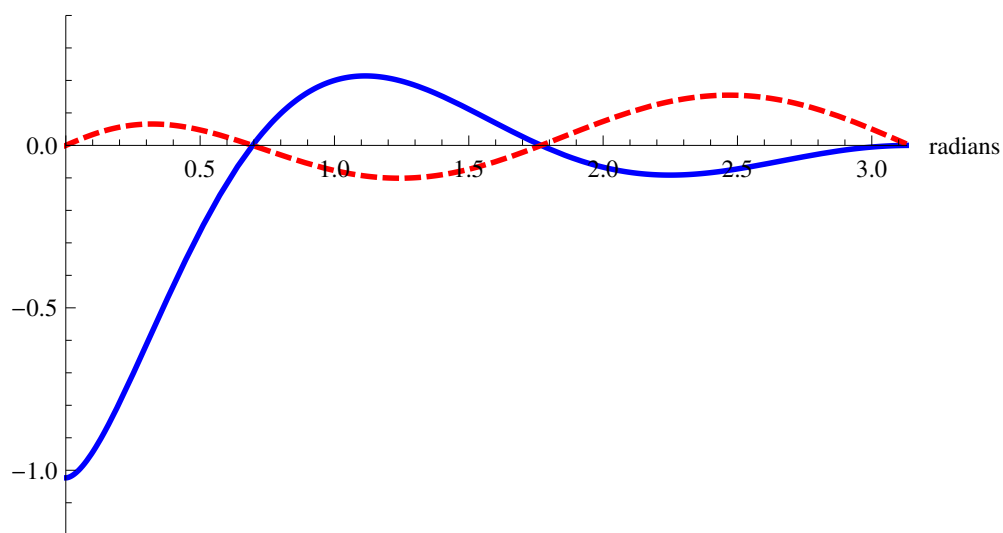
General backgrounds

- Can characterise any kind of background in this formalism

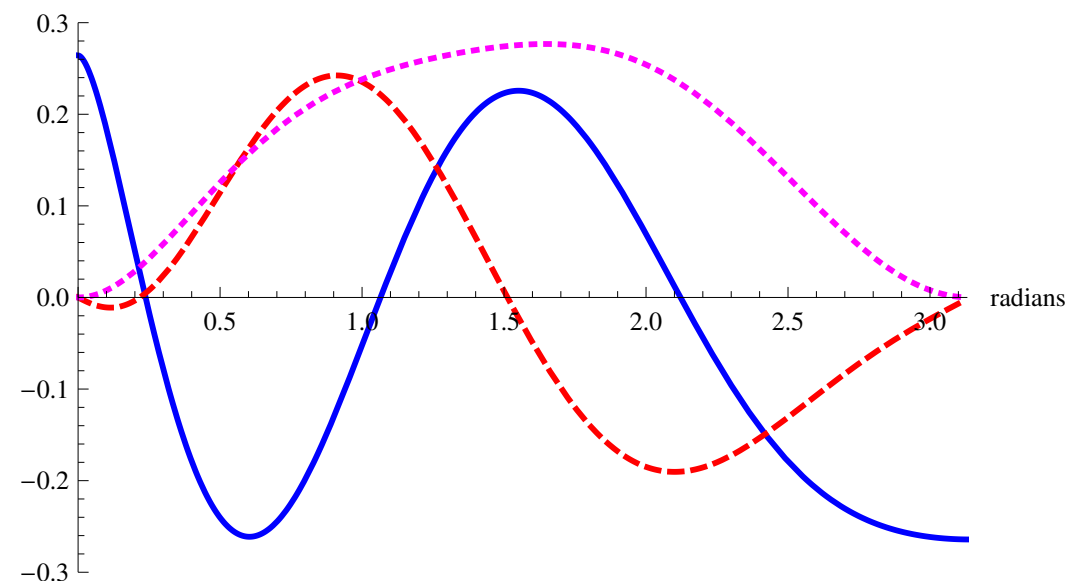
$$\langle a_{(lm)}^P(f) a_{(l'm')}^{P'*}(f') \rangle = C_{lm l'm'}^{PP'} H(f) \delta(f - f')$$

$$\Gamma_{12}(f) = 4\pi^2 \sum_{(lm)} \sum_{(l'm')} (-1)^{l+l'} N_l N_{l'} C_{lm l'm'}^{GG} Y_{(lm)}(\hat{u}_1) Y_{(l'm')}^*(\hat{u}_2)$$

- For example, recover overlap reduction functions for anisotropic, uncorrelated backgrounds (Mingarelli et al. 2013)



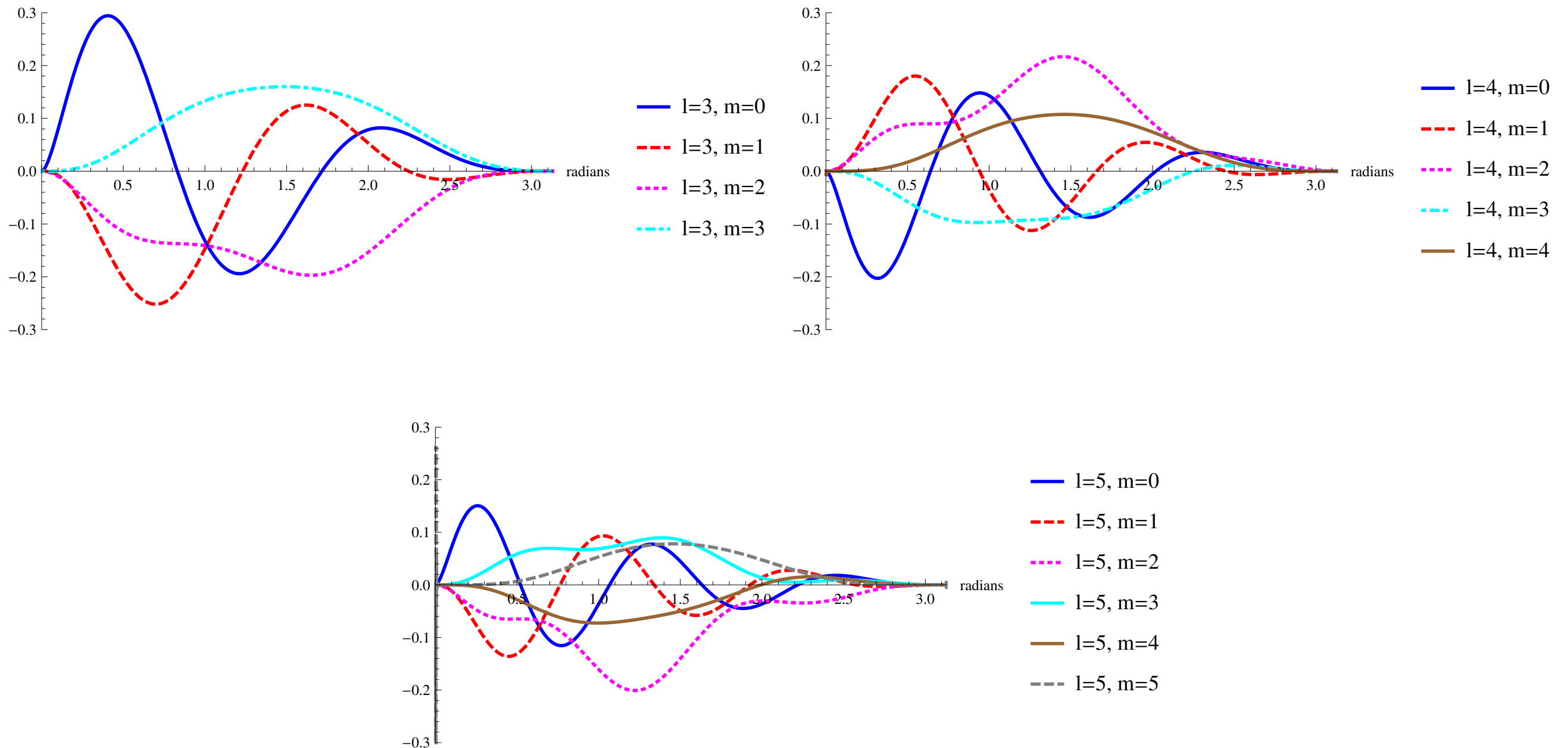
— $l=1, m=0$
 - - $l=1, m=1$



— $l=2, m=0$
 - - $l=2, m=1$
 ··· $l=2, m=2$

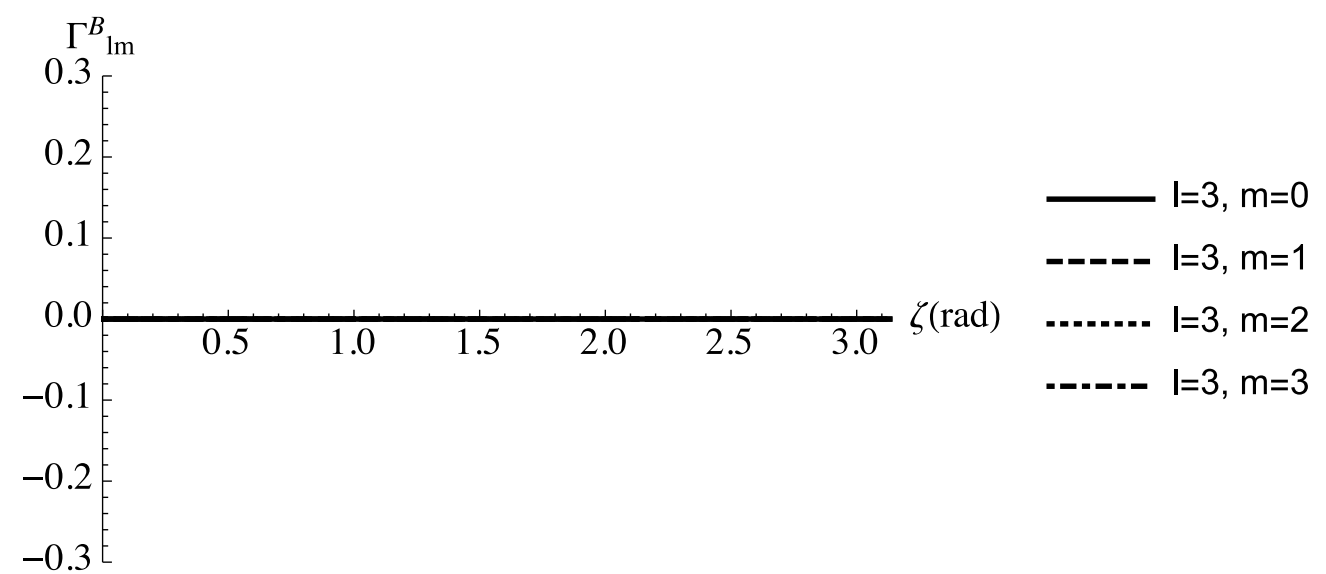
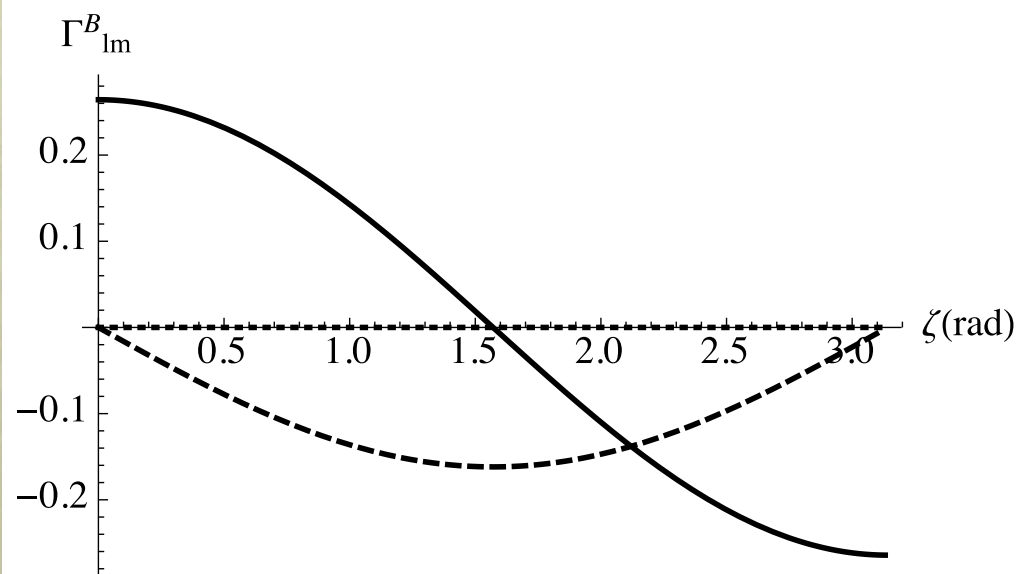
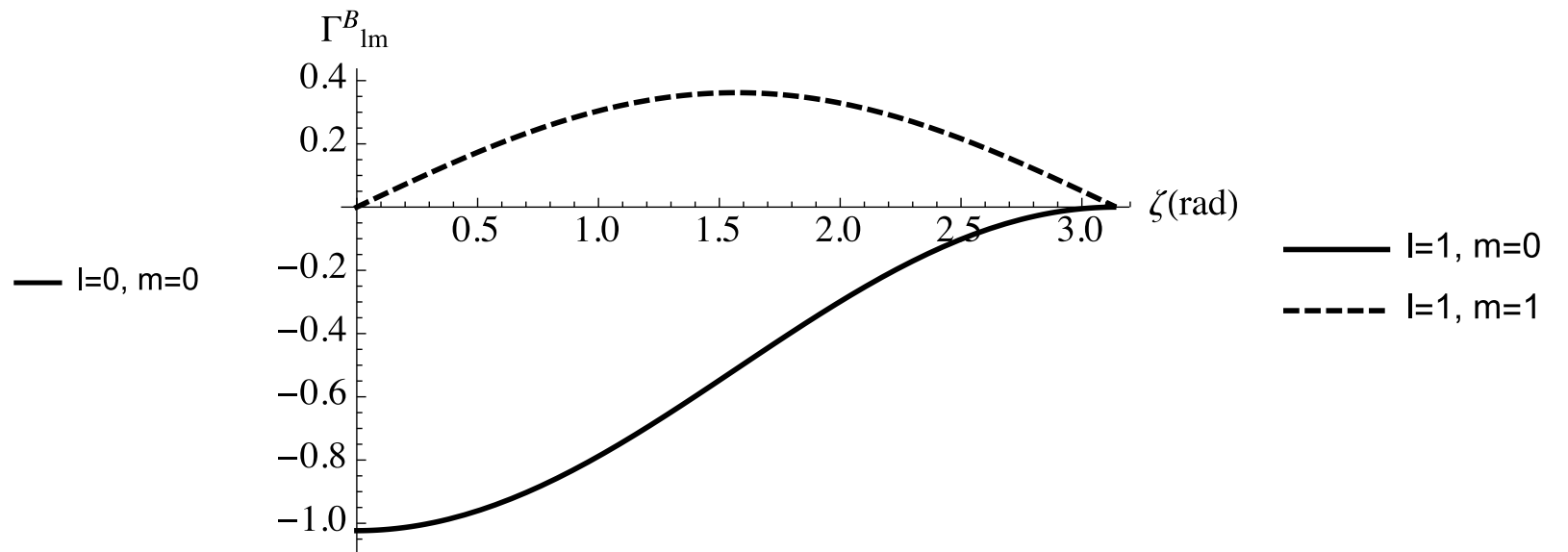
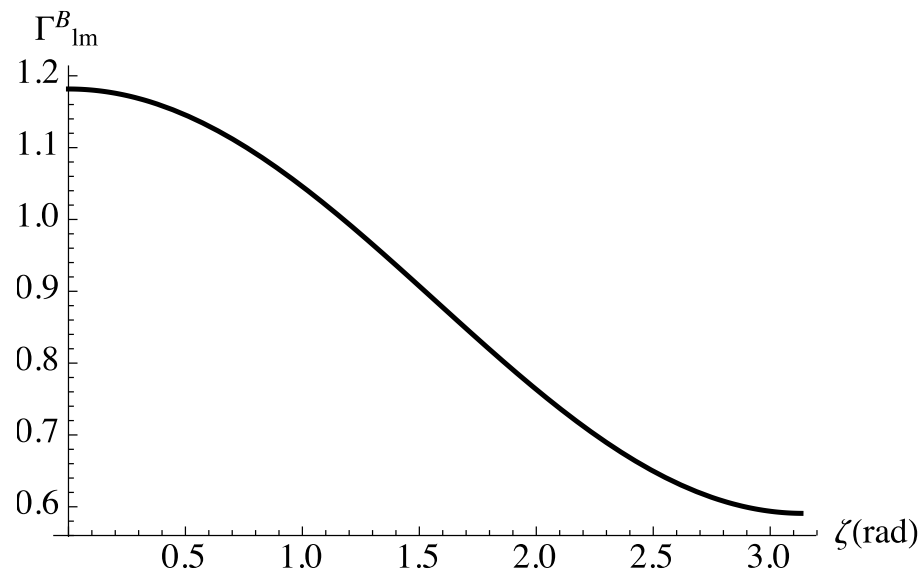
General backgrounds

- and extend these results analytically to arbitrary multipole order



General backgrounds

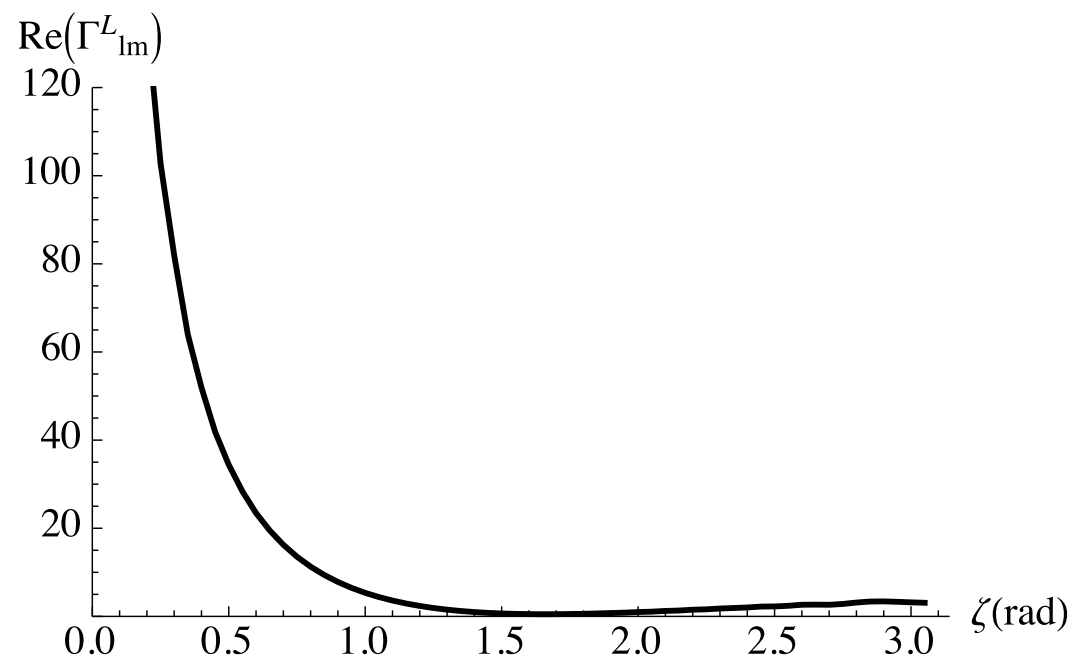
- Also obtain similar results for other polarisation states.



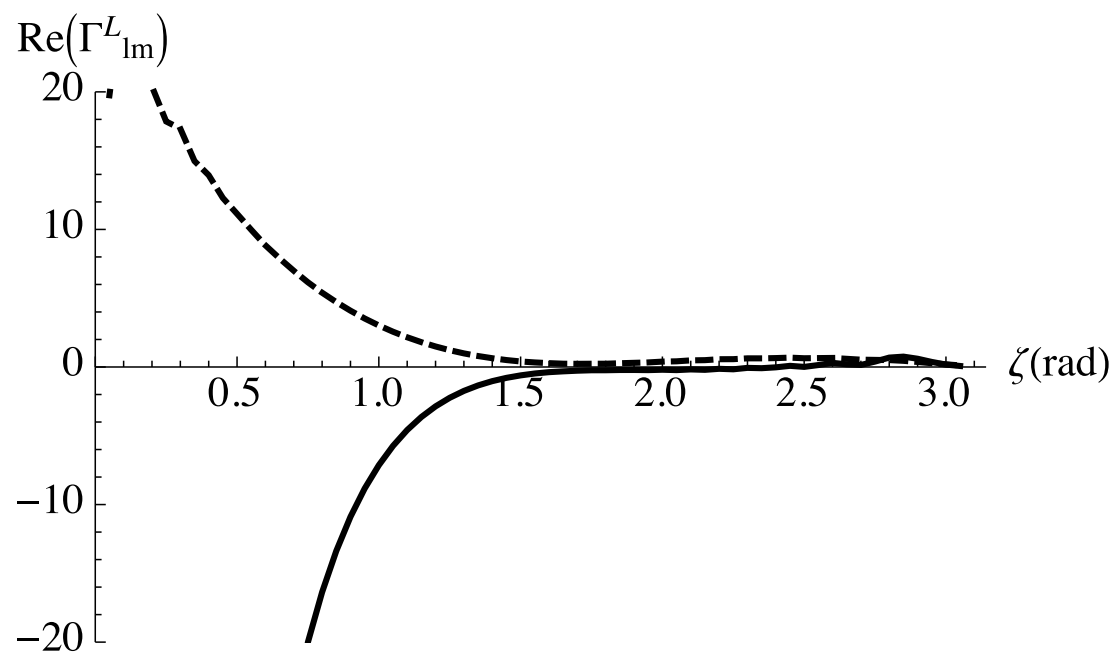
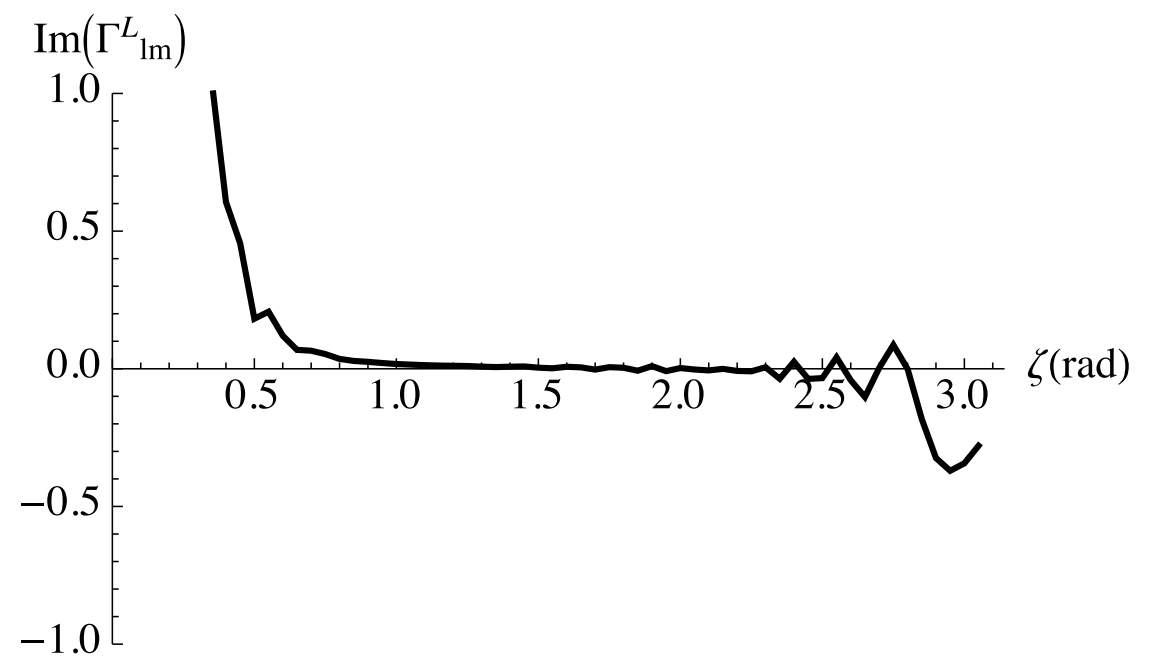
Scalar-transverse (breathing) modes

General backgrounds

Scalar-longitudinal modes

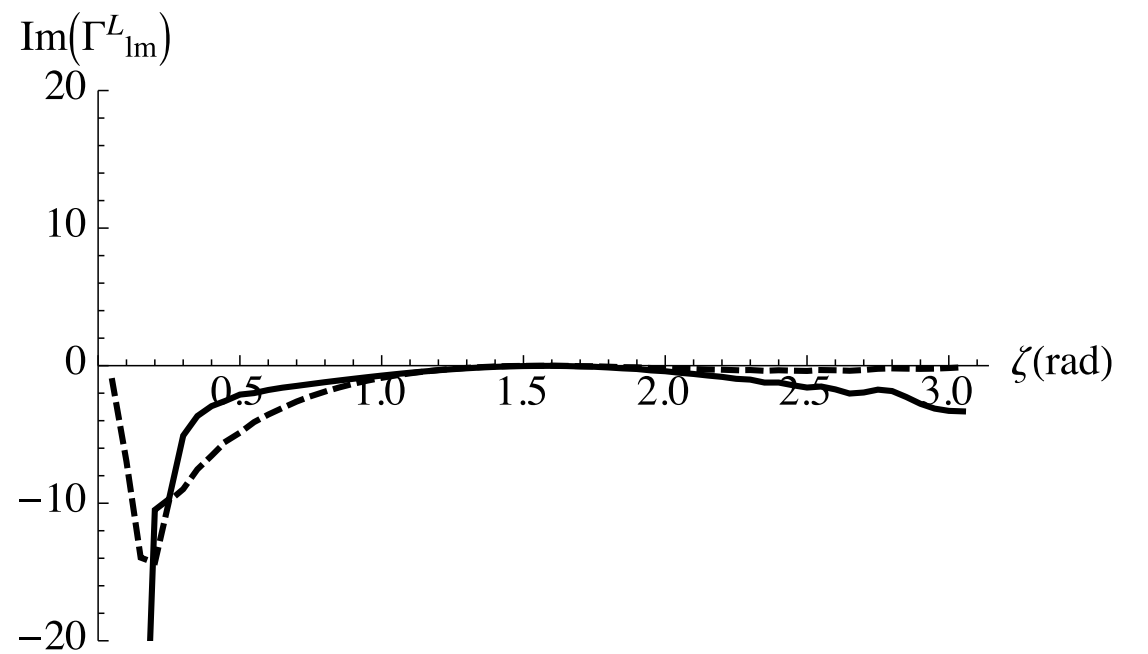


— $l=0, m=0$



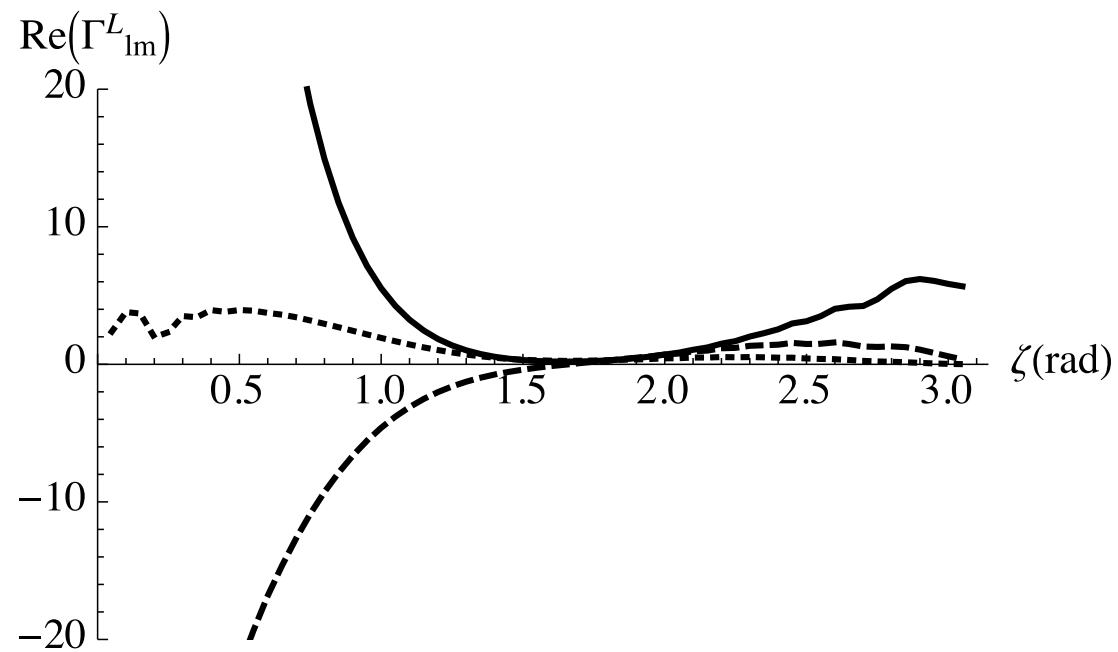
— $l=1, m=0$

- - - $l=1, m=1$

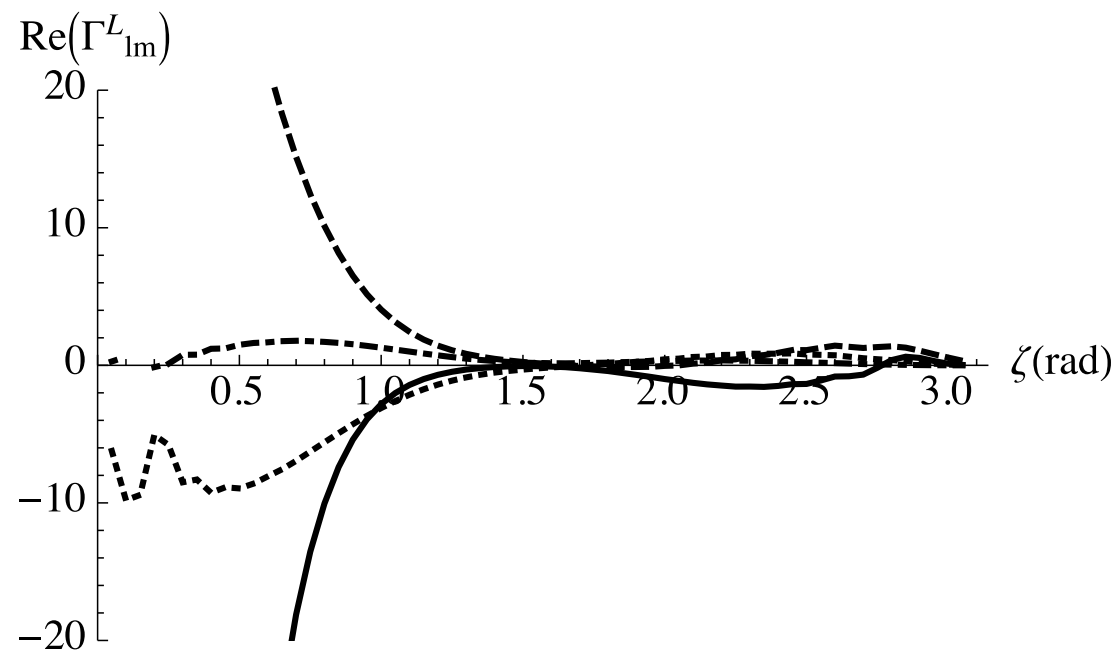
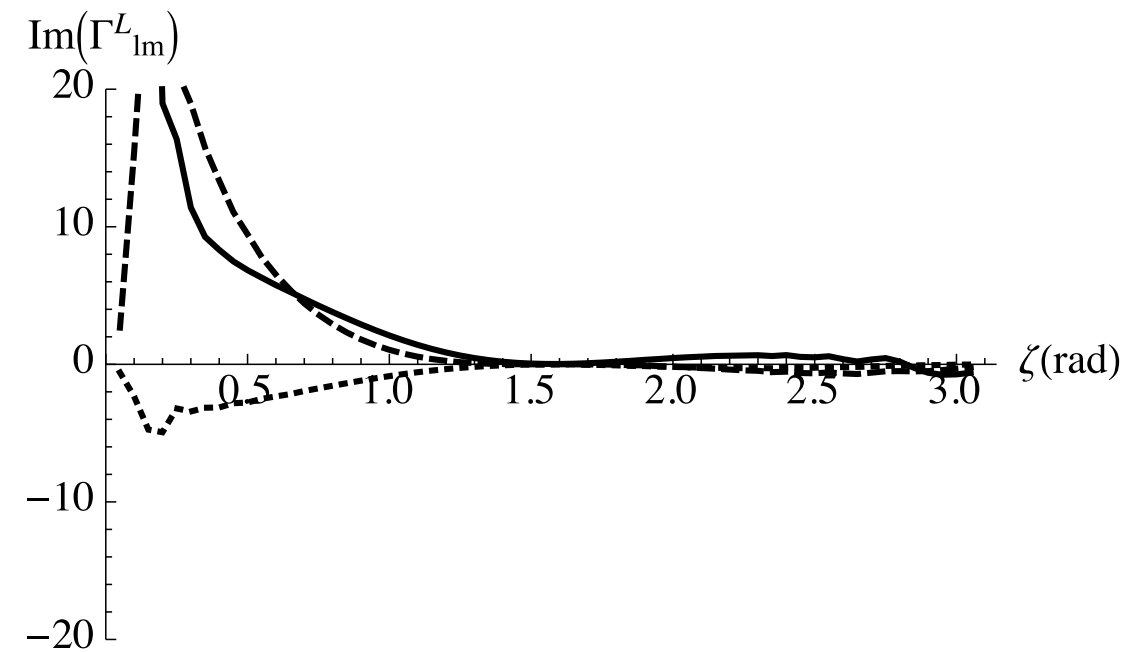


General backgrounds

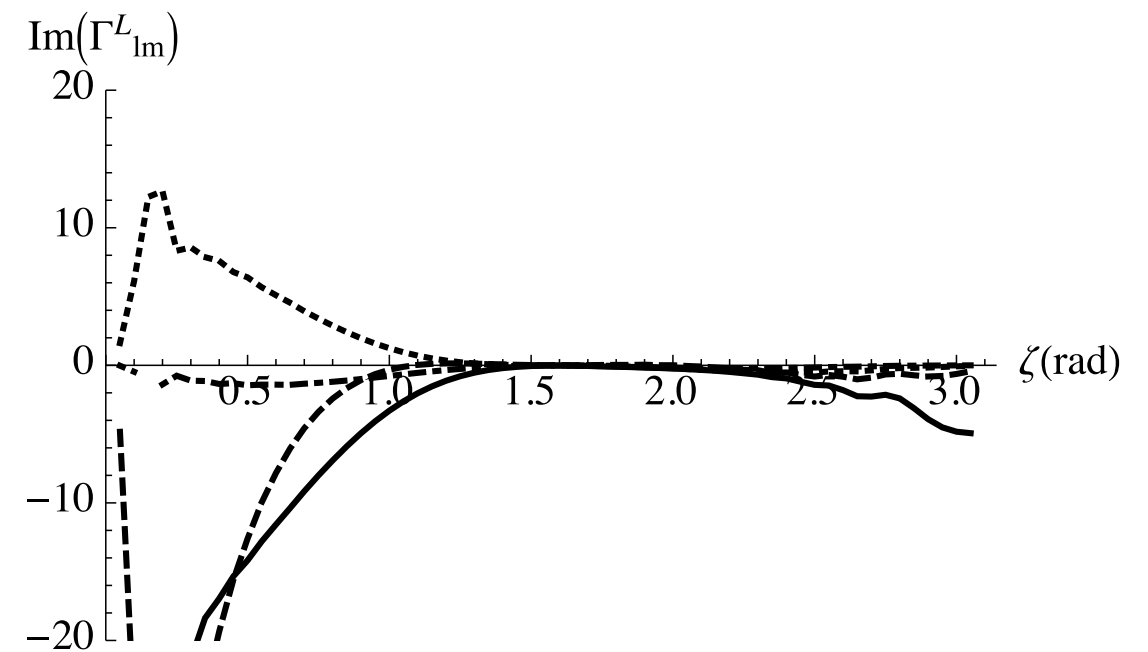
Scalar-longitudinal modes



- $l=2, m=0$
- - $l=2, m=1$
- ... $l=2, m=2$

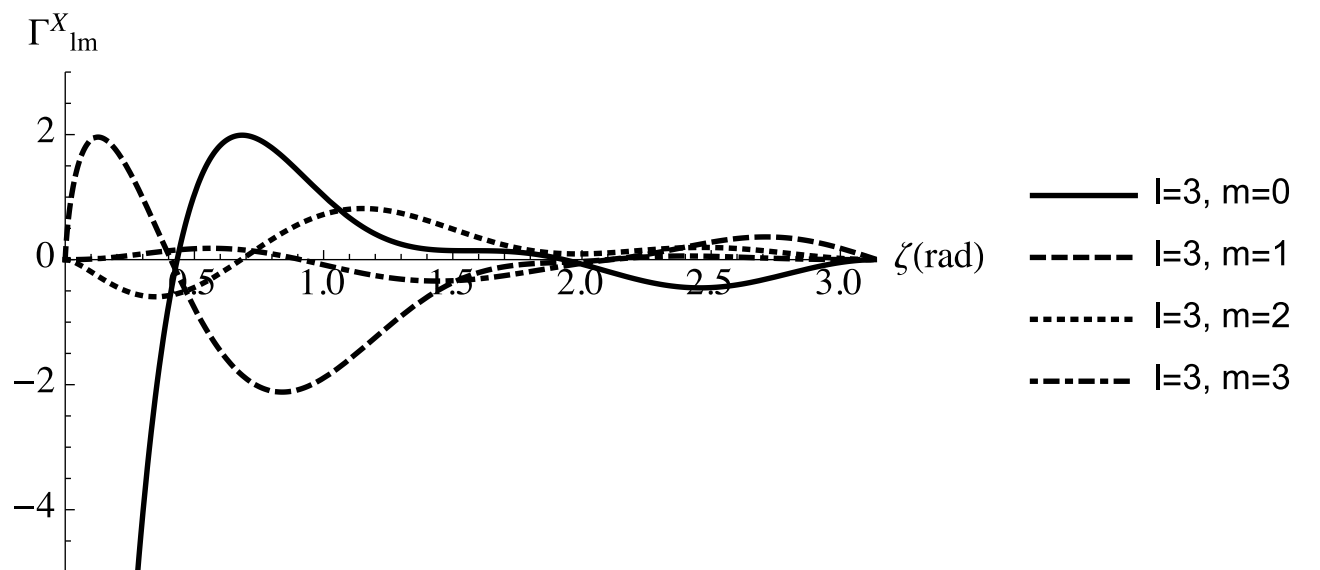
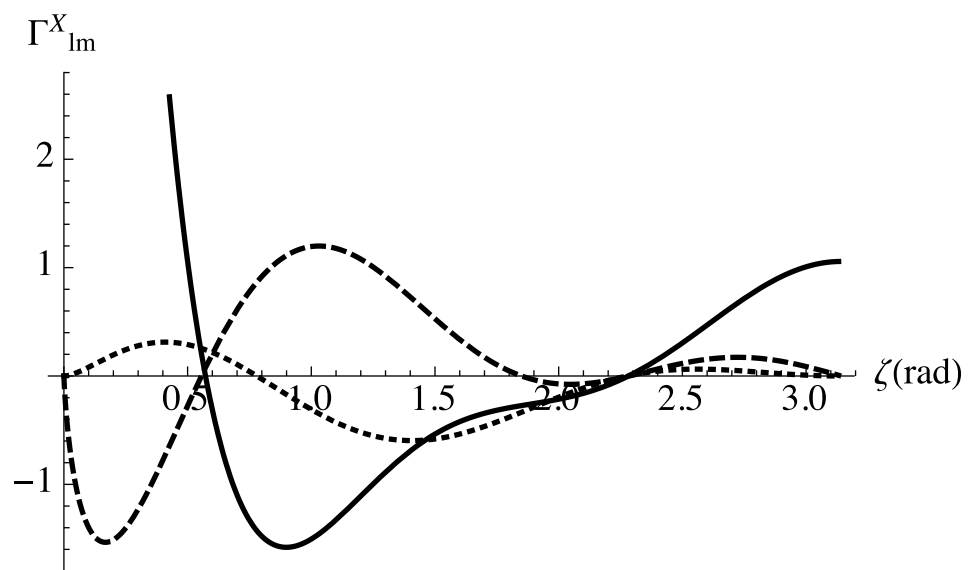
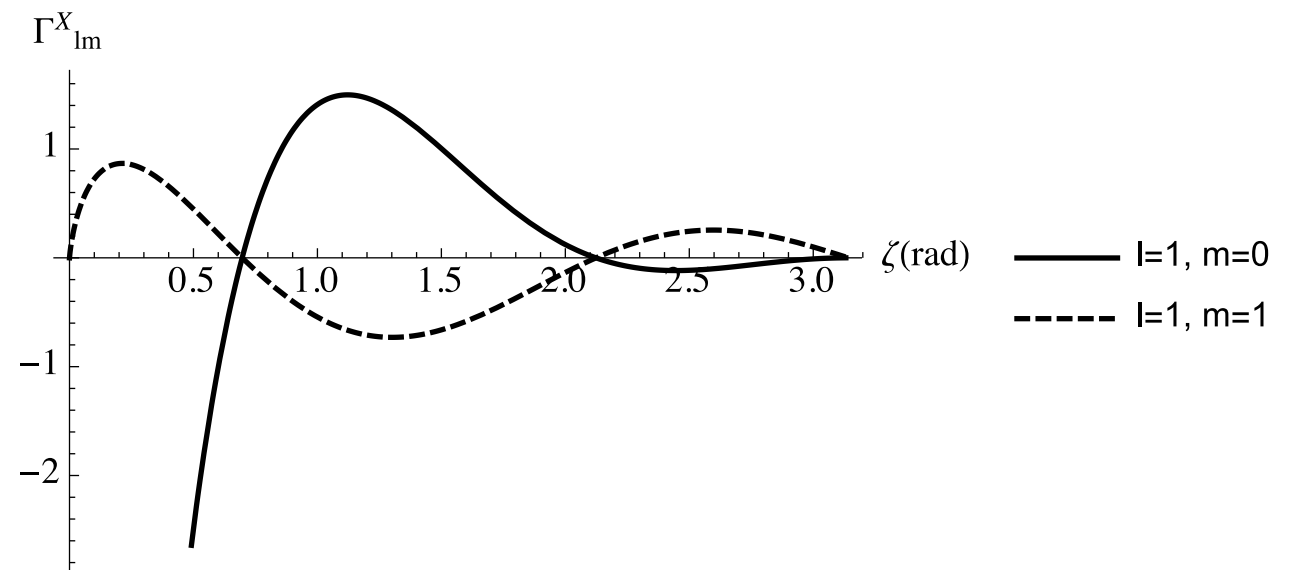
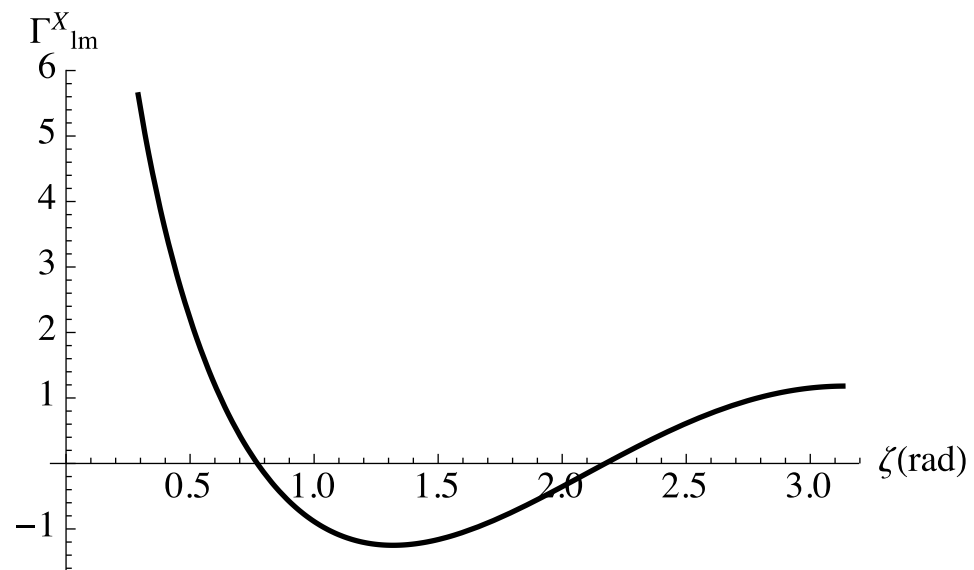


- $l=3, m=0$
- - $l=3, m=1$
- ... $l=3, m=2$
- . - $l=3, m=3$

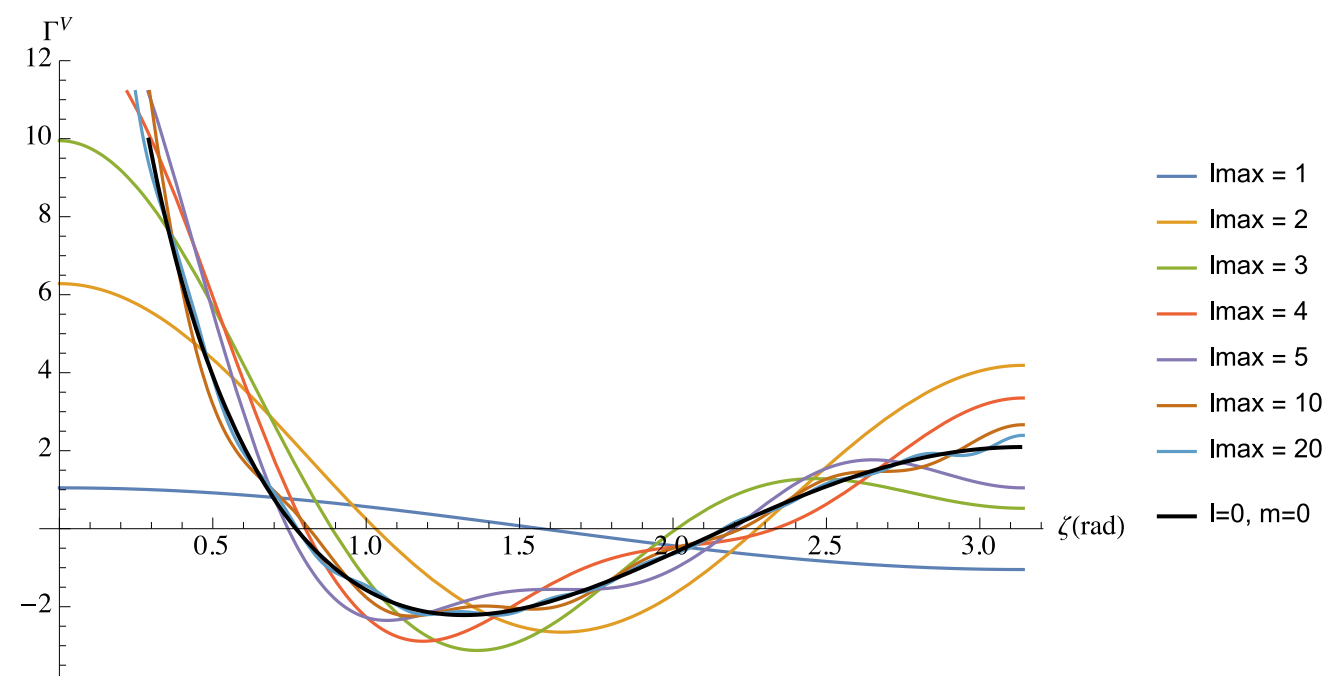
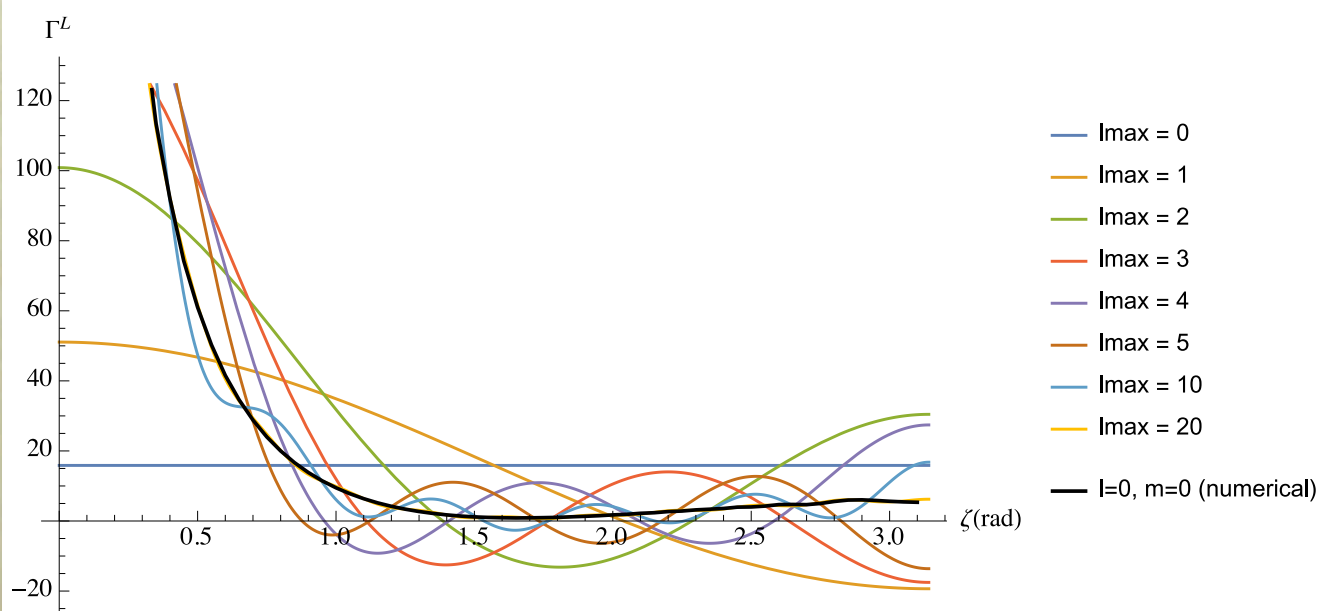
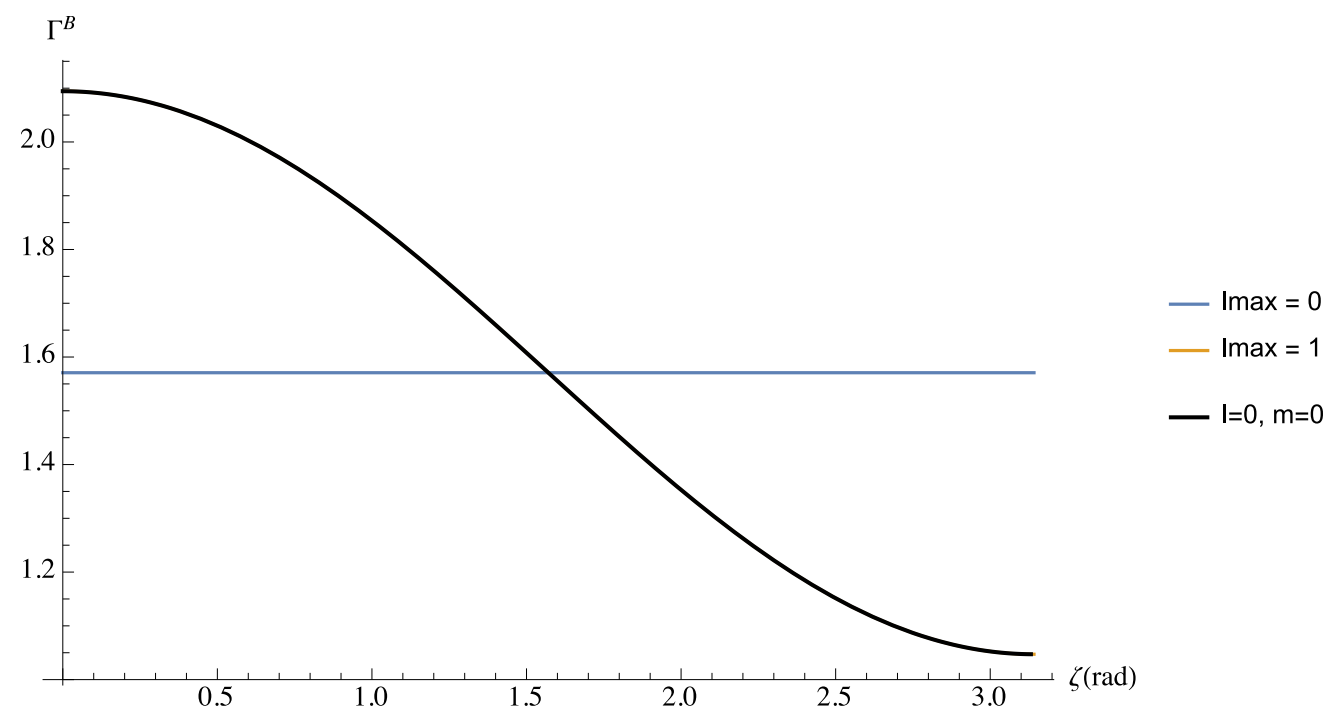
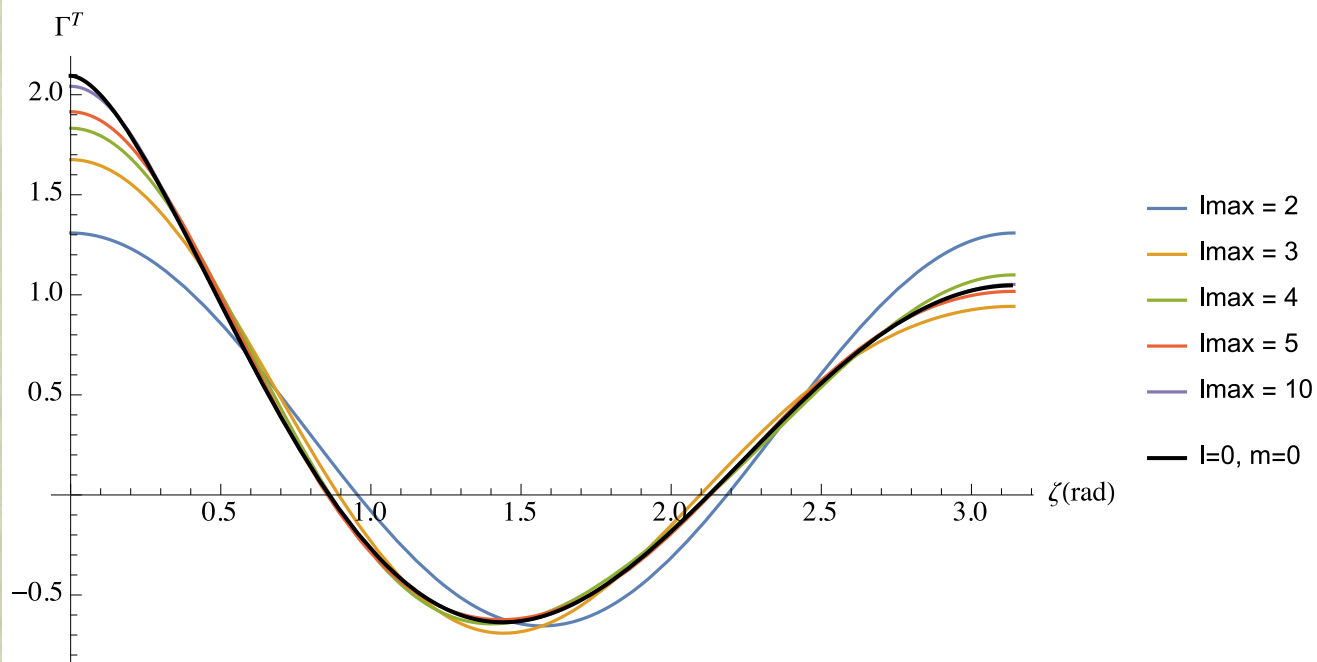


General backgrounds

Vector-longitudinal modes



Isotropic, uncorrelated backgrounds of arbitrary polarisation



Background mapping

- We can use observed timing residuals, \mathbf{s} , to infer the coefficients, \mathbf{a} , of the background. The likelihood takes the form

$$p(\mathbf{s}|F, \vec{\mathbf{a}}) \propto \exp \left[-\frac{1}{2} (\vec{\mathbf{s}} - H\vec{\mathbf{a}})^\dagger F^{-1} (\vec{\mathbf{s}} - H\vec{\mathbf{a}}) \right]$$

- At a given frequency we make only $2N_p$ measurements - an amplitude and phase for each of the N_p pulsars. Can only hope to recover N_p combinations of the (complex) $a^{G_{(lm)}}$'s.
- This shows up in a singular-value decomposition of H

$$H = U\Sigma V^\dagger$$

- The rectangular matrix Σ has at most N_p non-zero elements on the diagonal.
- We can write $U = [H_{\text{range}} H_{\text{null}}]$ where the N_p columns of H_{range} span the range of H .

Background mapping - GR modes

- In a search we can replace $H\vec{a}$ by $H_{\text{range}}\vec{b}$ in the likelihood. The value of \vec{a} corresponding to a given value of \vec{b} is given in terms of the pseudo-inverse of Σ , Σ^+ , by $\vec{a} = V\Sigma^+\vec{b}$.
- A similar analysis can be performed in a real space representation (Cornish & van Haasteren 2014).
- Which components do we expect to be able to measure? Since

$$R_{I(lm)}^G \sim \frac{1}{l^{\frac{3}{2}}} \quad \text{as } l \rightarrow \infty$$

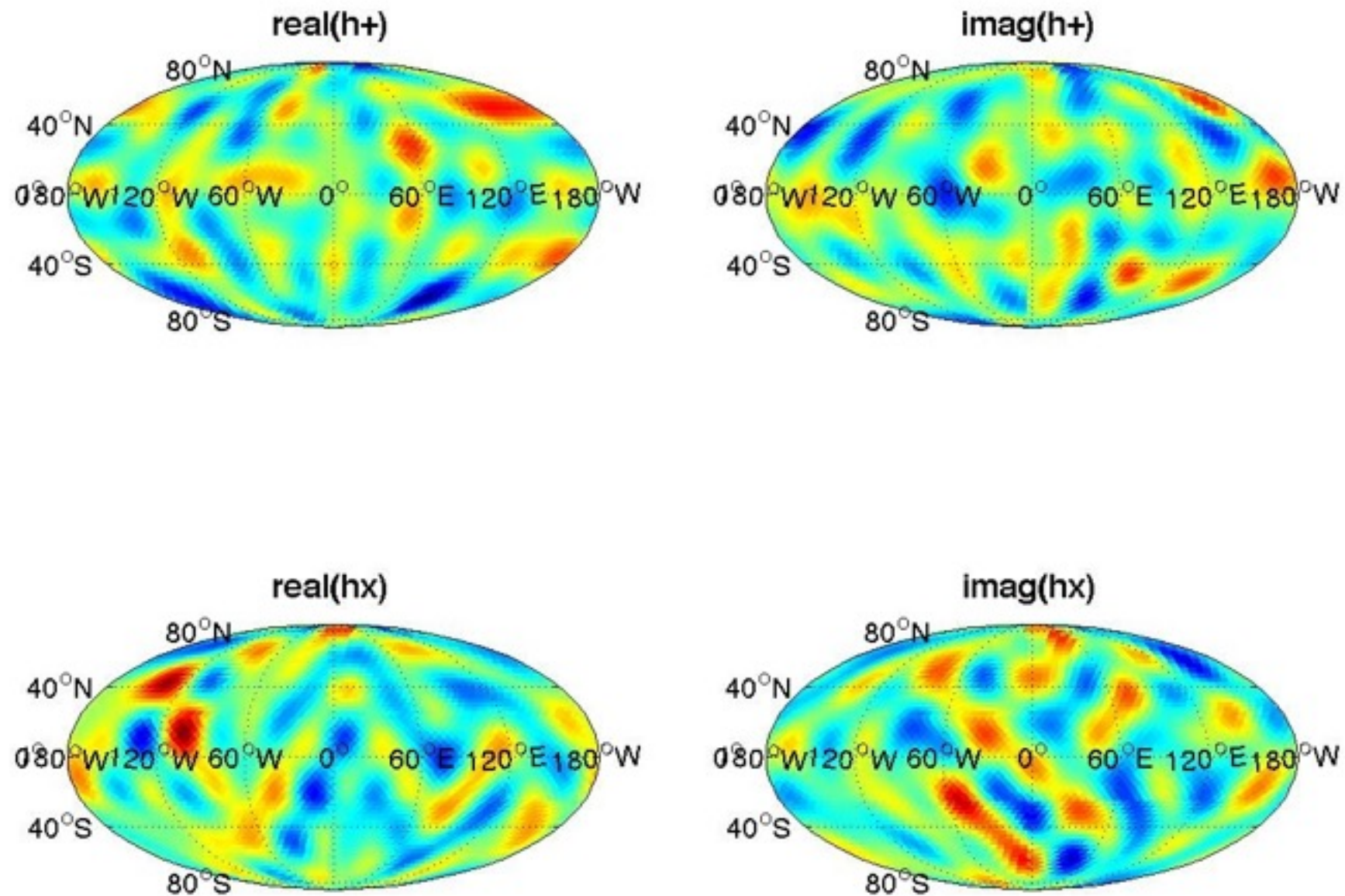
- we expect to measure the low- l modes more precisely. To reach an angular resolution of l_{max} we therefore need an array of

$$N_p \approx (l_{\text{max}} + 1)^2 - 4$$

- Need $N_p \approx 21$ pulsars to reach $l_{\text{max}}=4$ required for an isotropic background; $N_p \approx 100$ to reach single source resolution at $l_{\text{max}}=10$.

Background mapping - GR modes

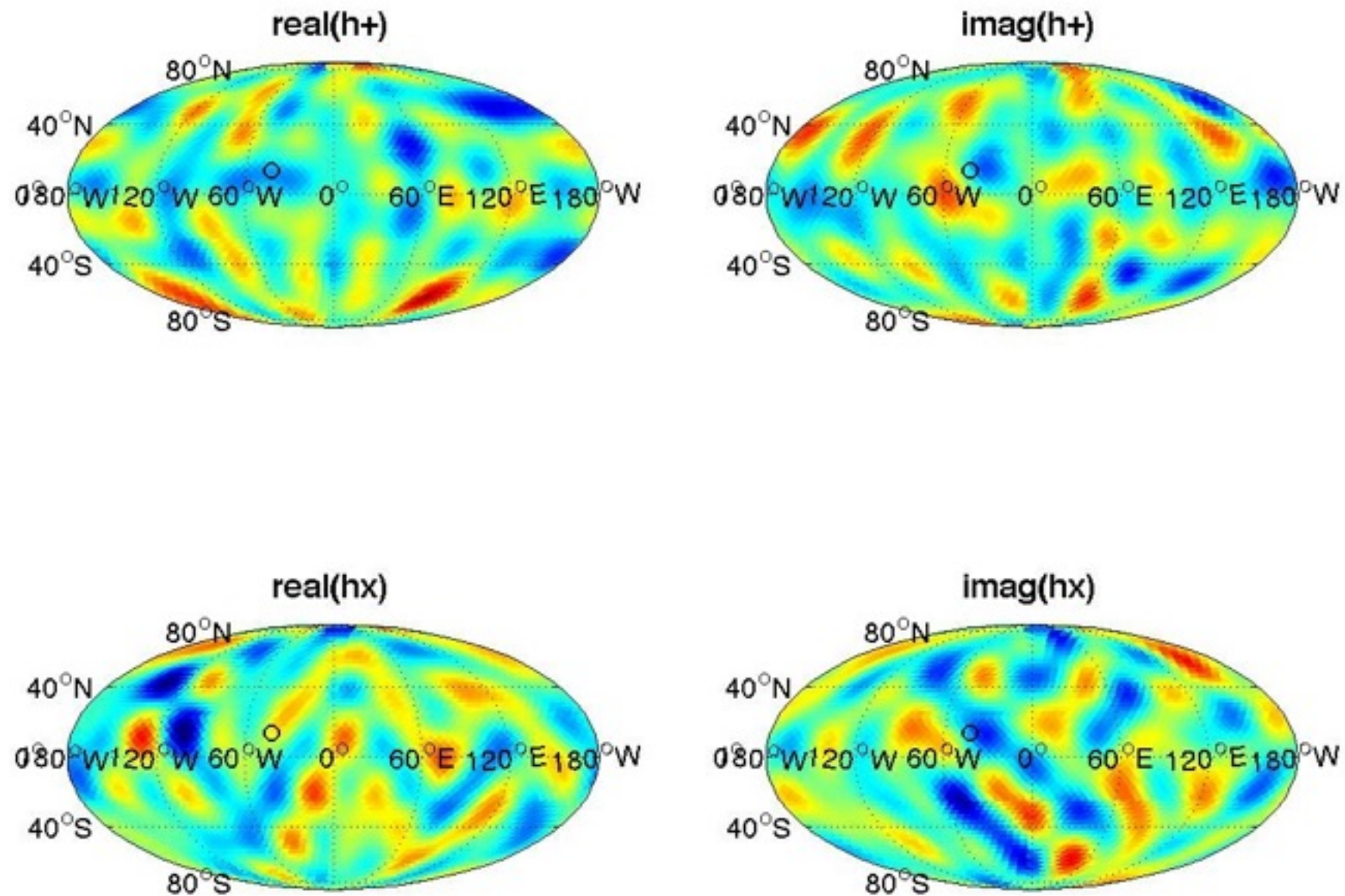
- Gradient piece of background behaves as expected. Adding more pulsars increases resolution of map and reduces residual.



Injected background

Background mapping - GR modes

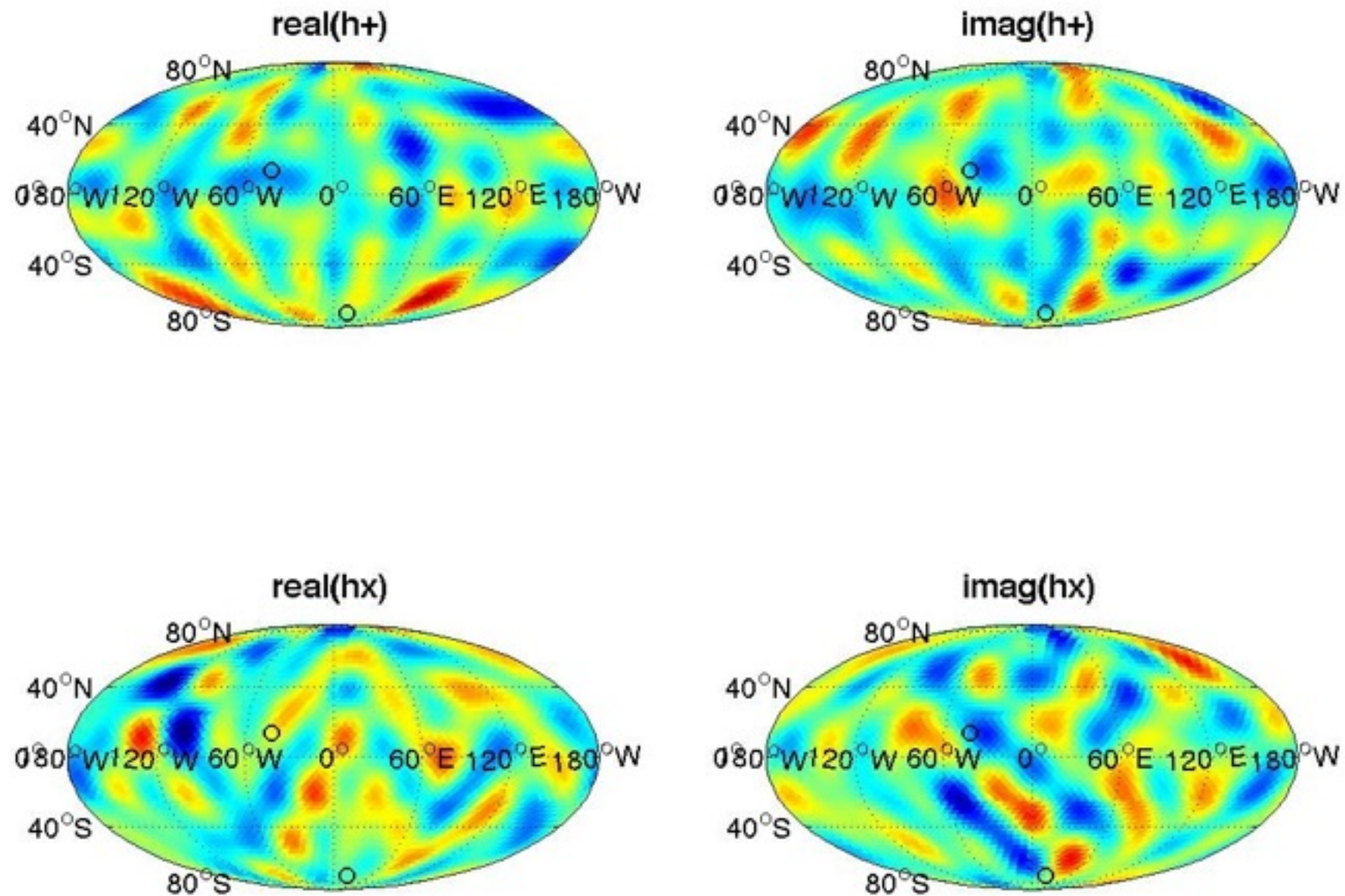
- Gradient piece of background behaves as expected. Adding more pulsars increases resolution of map and reduces residual.



Residual $N_p=1$

Background mapping - GR modes

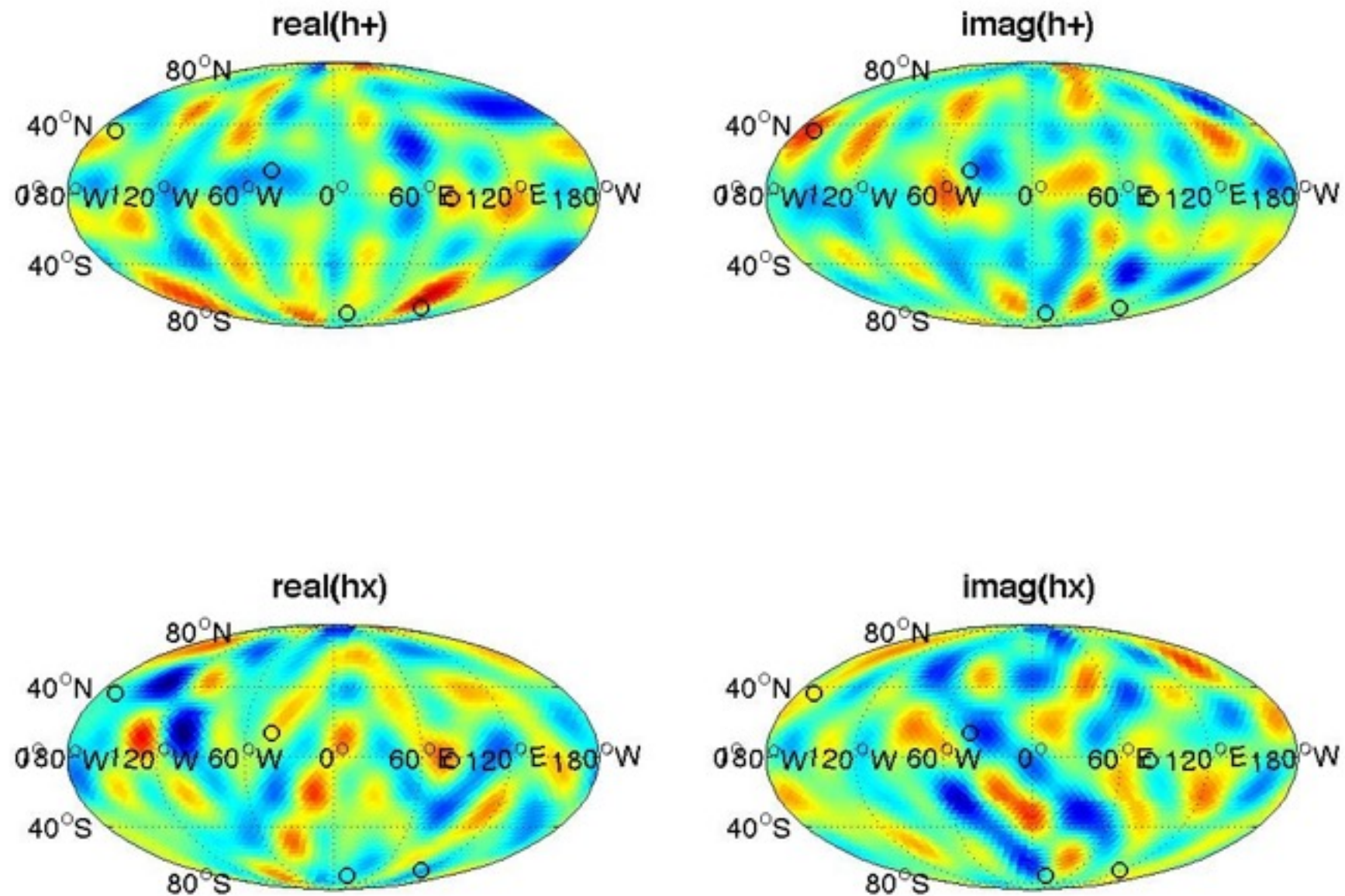
- Gradient piece of background behaves as expected. Adding more pulsars increases resolution of map and reduces residual.



Residual $N_p=2$

Background mapping - GR modes

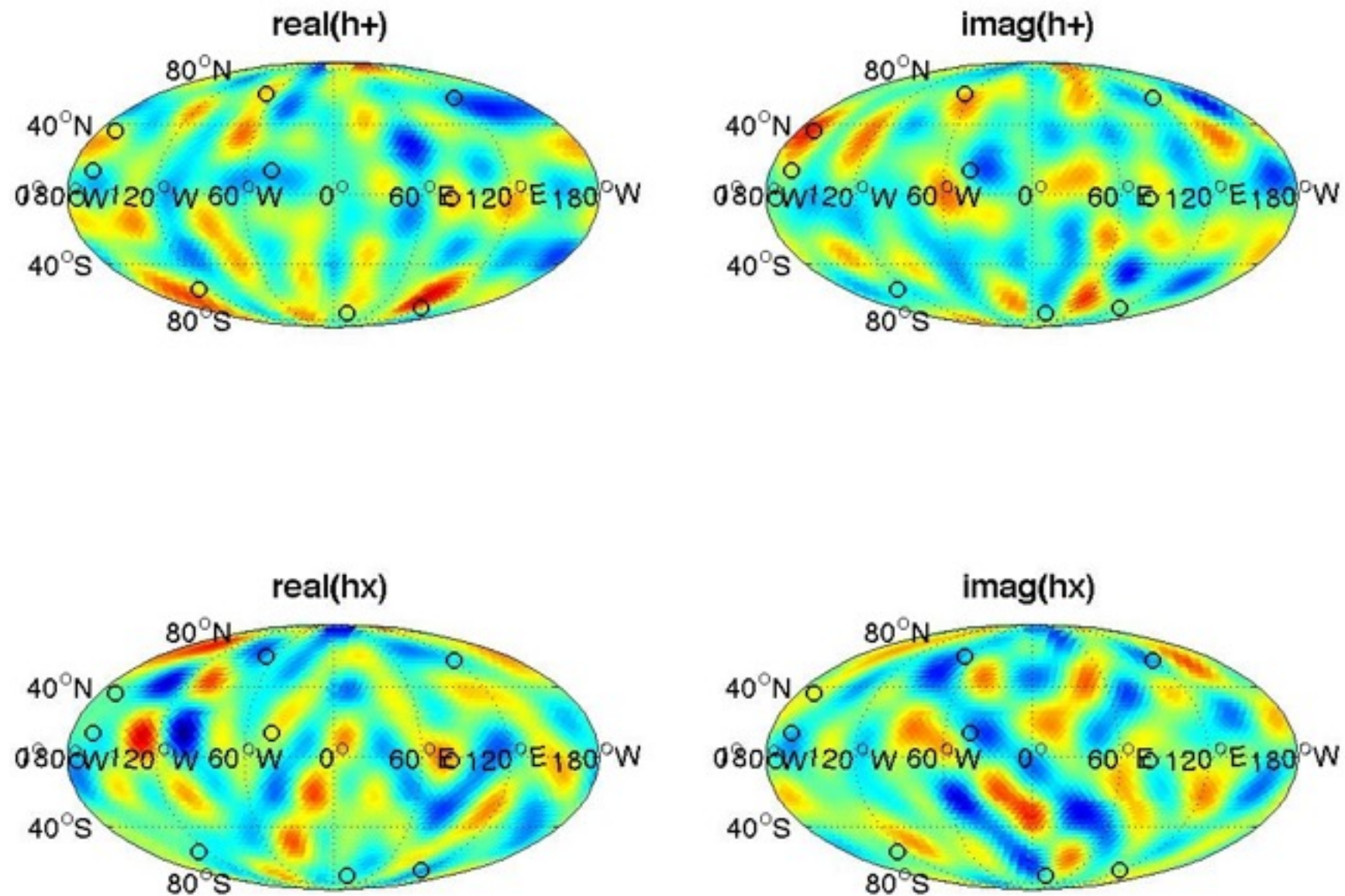
- Gradient piece of background behaves as expected. Adding more pulsars increases resolution of map and reduces residual.



Residual $N_p=5$

Background mapping - GR modes

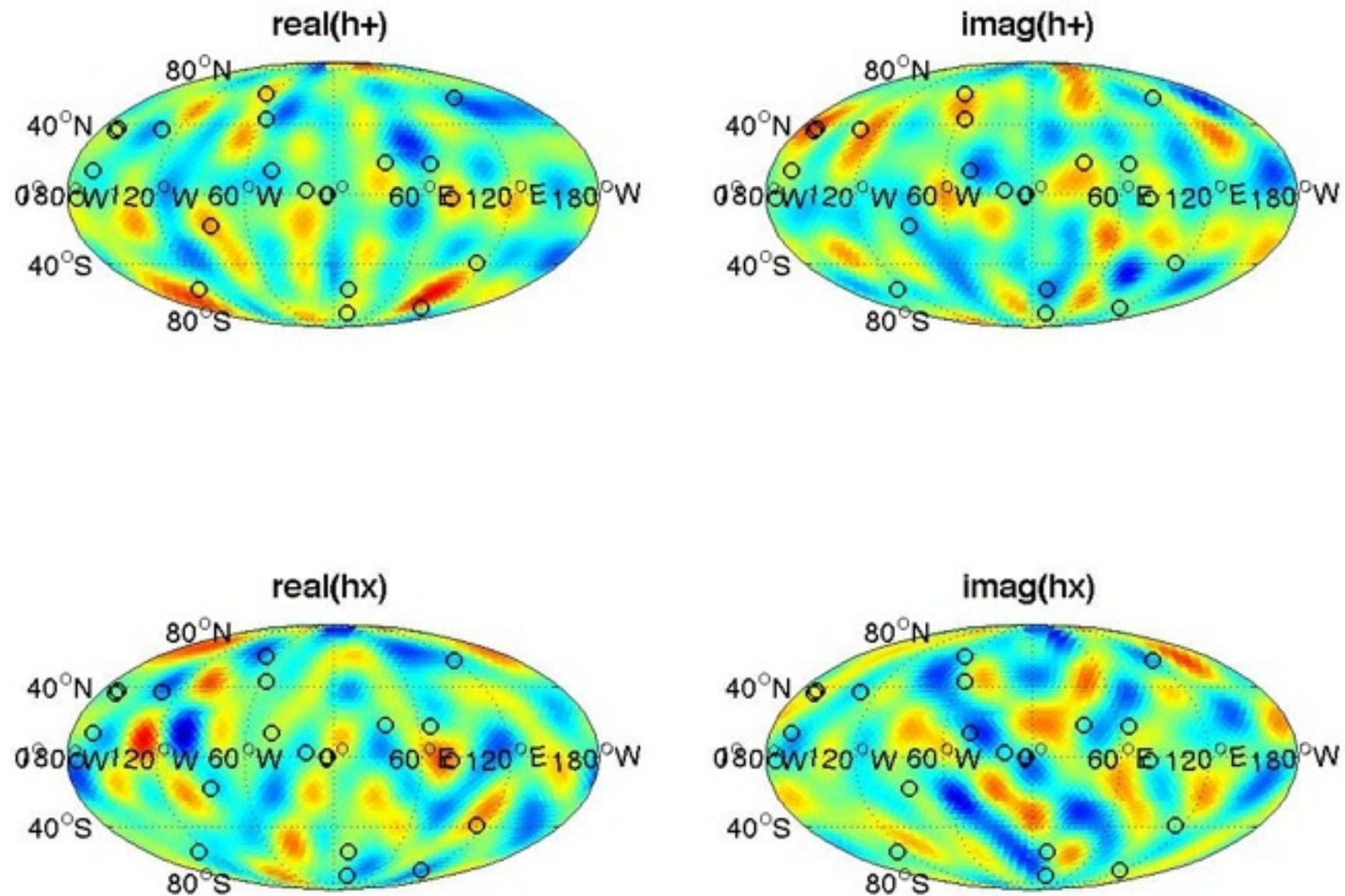
- Gradient piece of background behaves as expected. Adding more pulsars increases resolution of map and reduces residual.



Residual $N_p=10$

Background mapping - GR modes

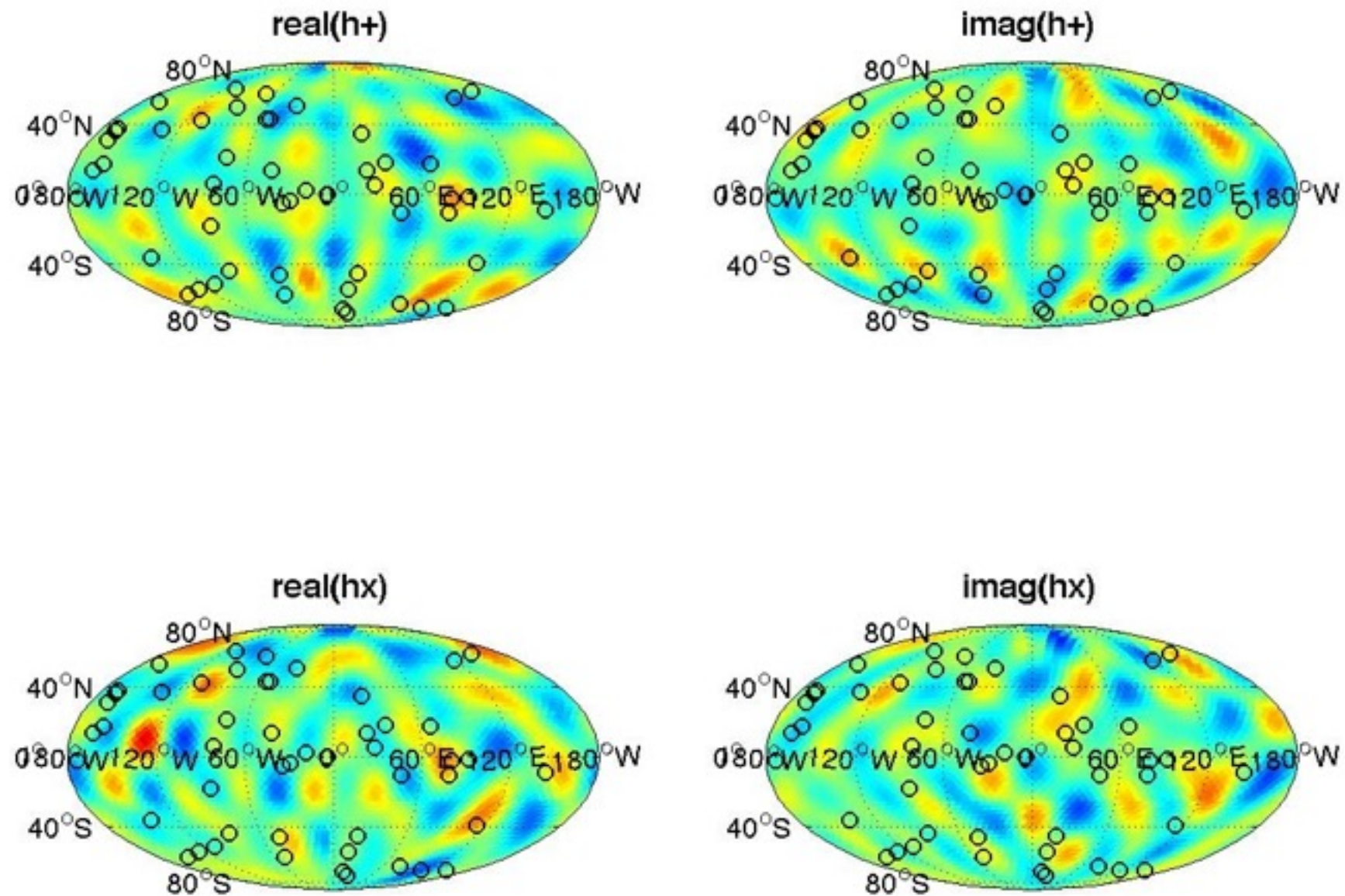
- Gradient piece of background behaves as expected. Adding more pulsars increases resolution of map and reduces residual.



Residual $N_p=20$

Background mapping - GR modes

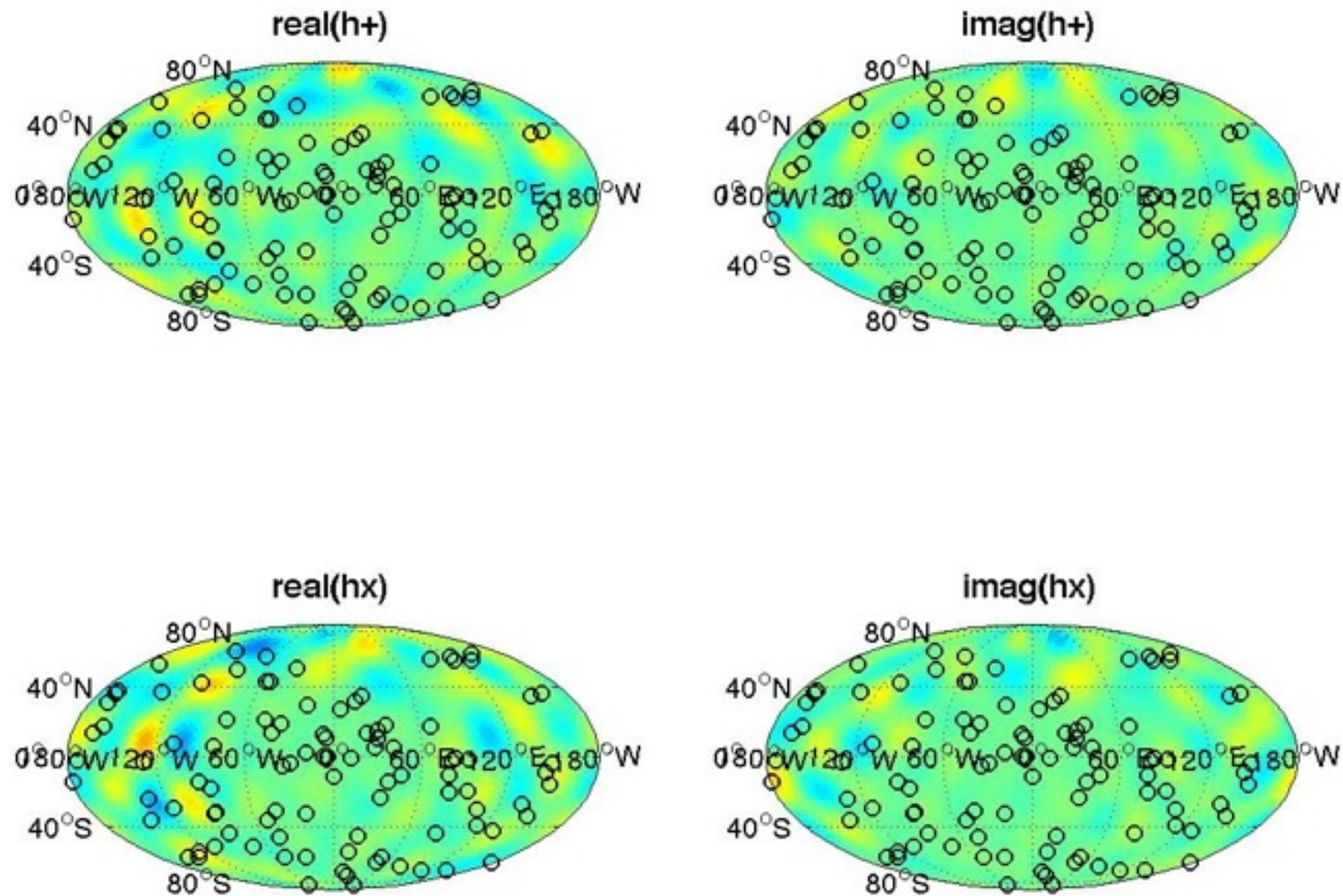
- Gradient piece of background behaves as expected. Adding more pulsars increases resolution of map and reduces residual.



Residual $N_p=50$

Background mapping - GR modes

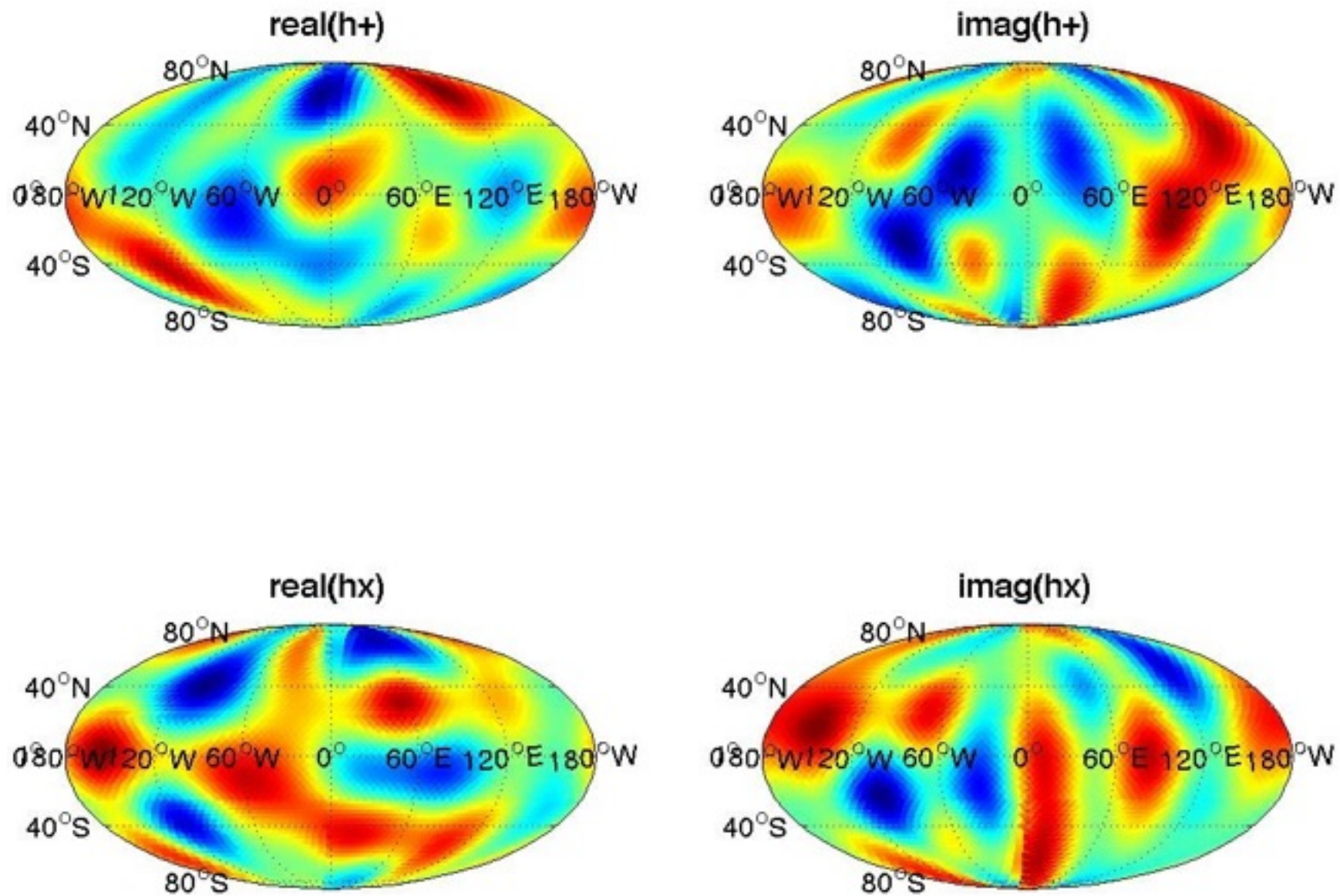
- Gradient piece of background behaves as expected. Adding more pulsars increases resolution of map and reduces residual.



Residual $N_p=100$

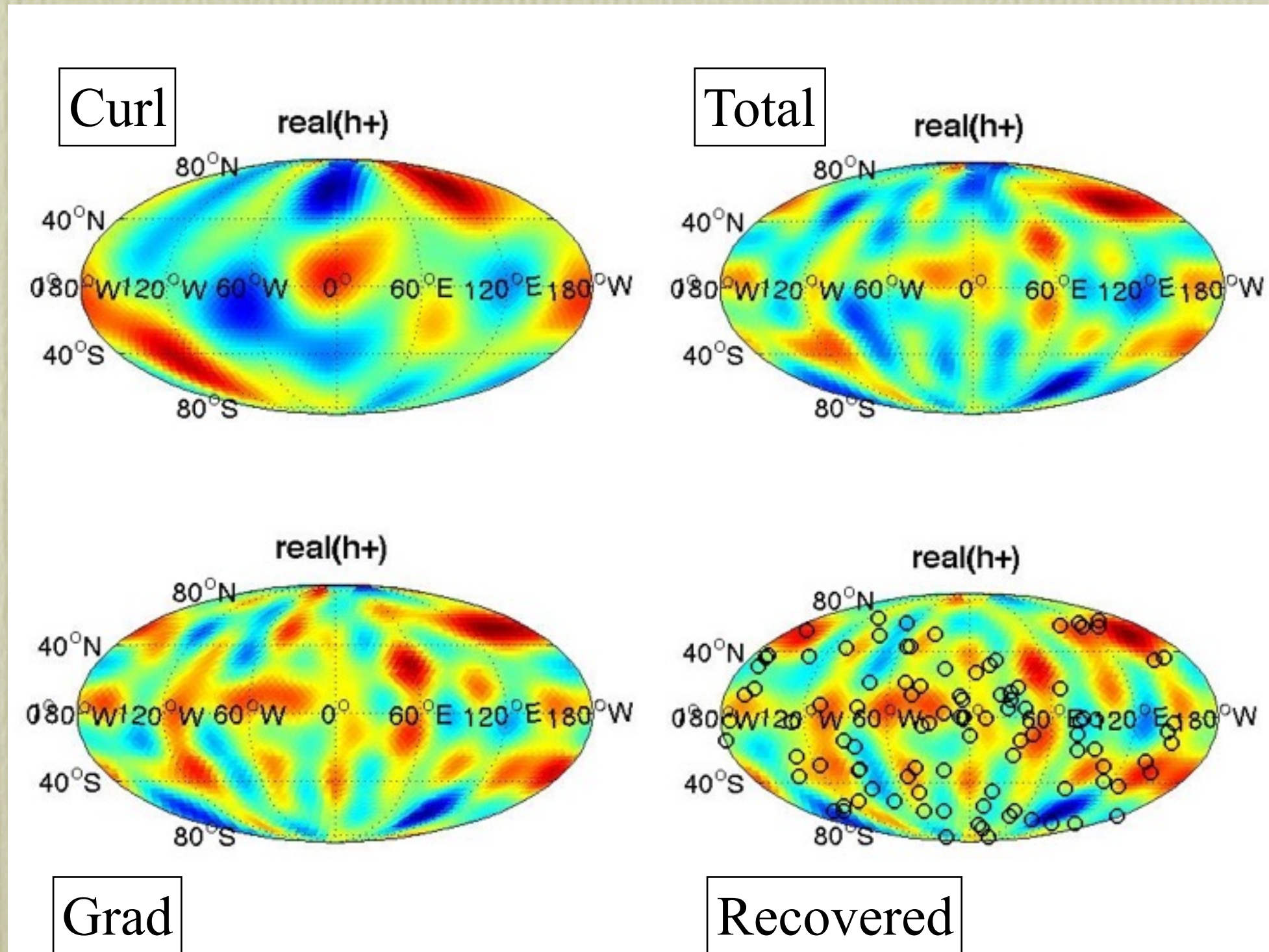
Background mapping - GR modes

- Curl part of background can never be observed.



Background mapping - GR modes

- Total GW background map could still be missing a significant component.

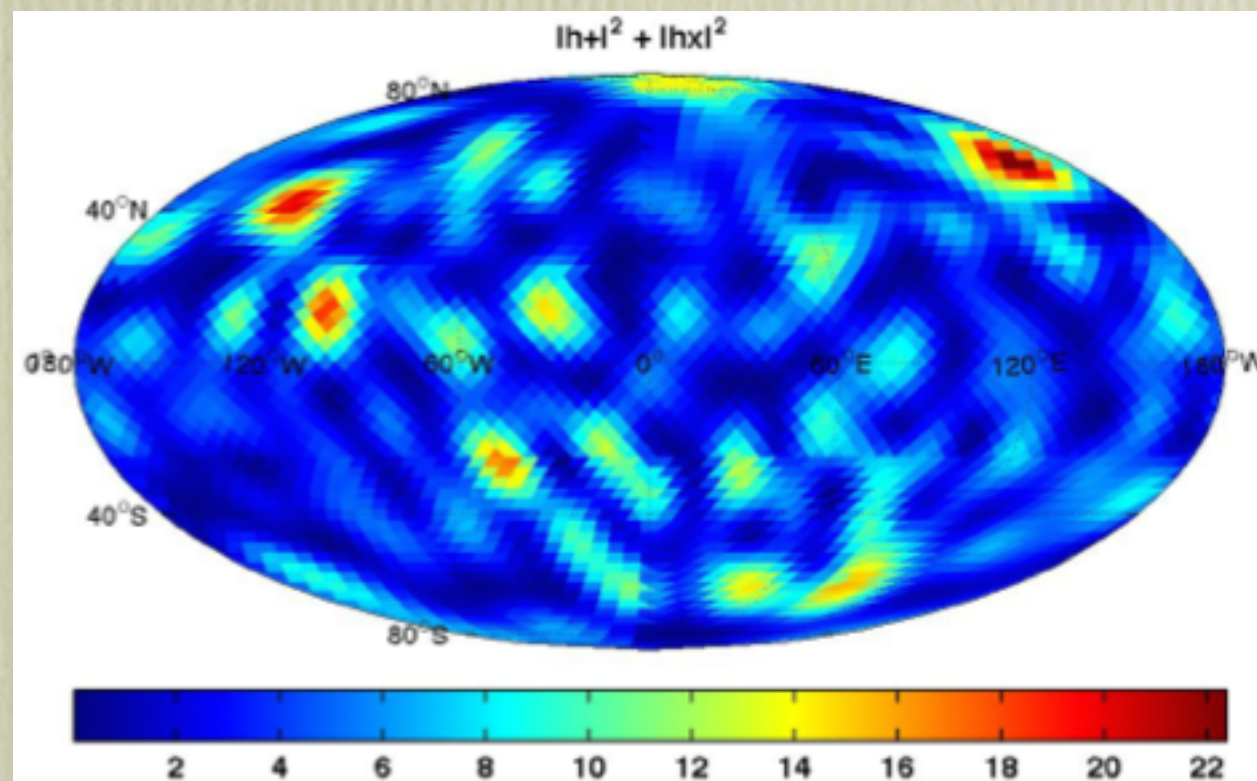


Implications

- Individual modes of the background represent GW emission that is correlated between different points on the sky.

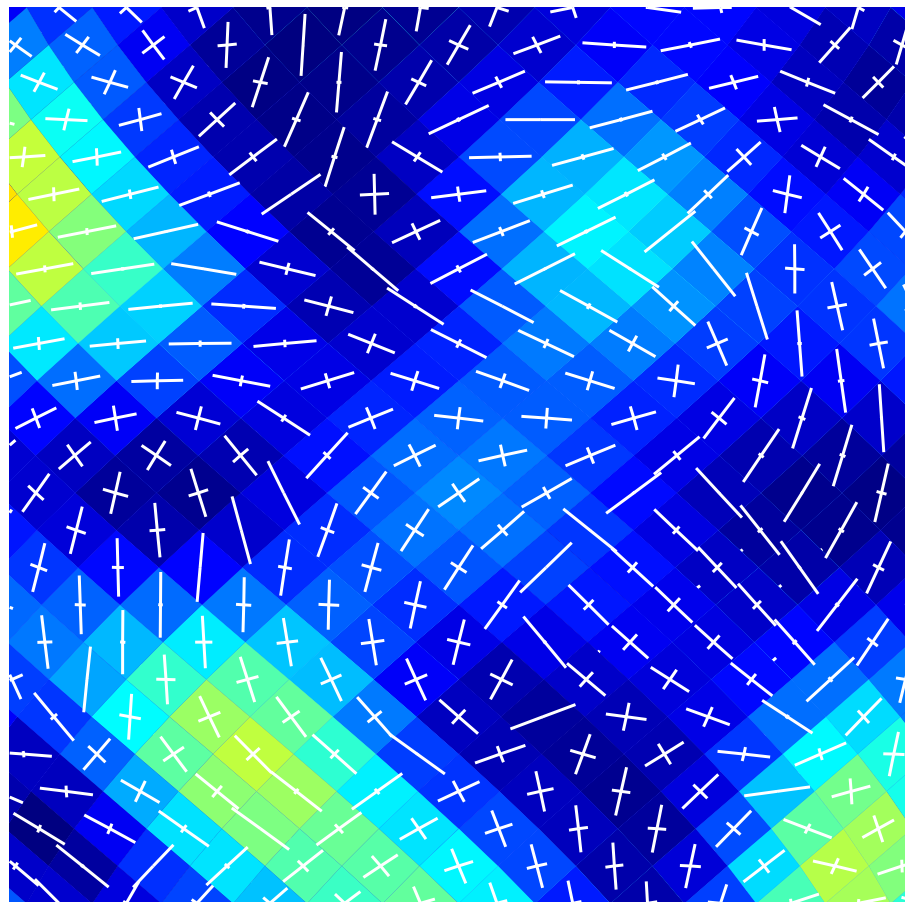
$$\langle h_+(f, \hat{k}) h_+^*(f', \hat{k}') \rangle_k = \frac{1}{2} \sum_{l=2}^{\infty} \frac{2l+1}{4\pi} (N_l)^2 [C_l^{GG}(f) G_{l2}^+(\cos\theta) + C_l^{CC}(f) G_{l2}^-(\cos\theta)] \delta(f - f')$$

- No well-established physical mechanism to create such correlations - discovery of a correlated background would be a profound result.
- Mild anisotropy expected in power of GW background - could be consistent with either uncorrelated or correlated background.



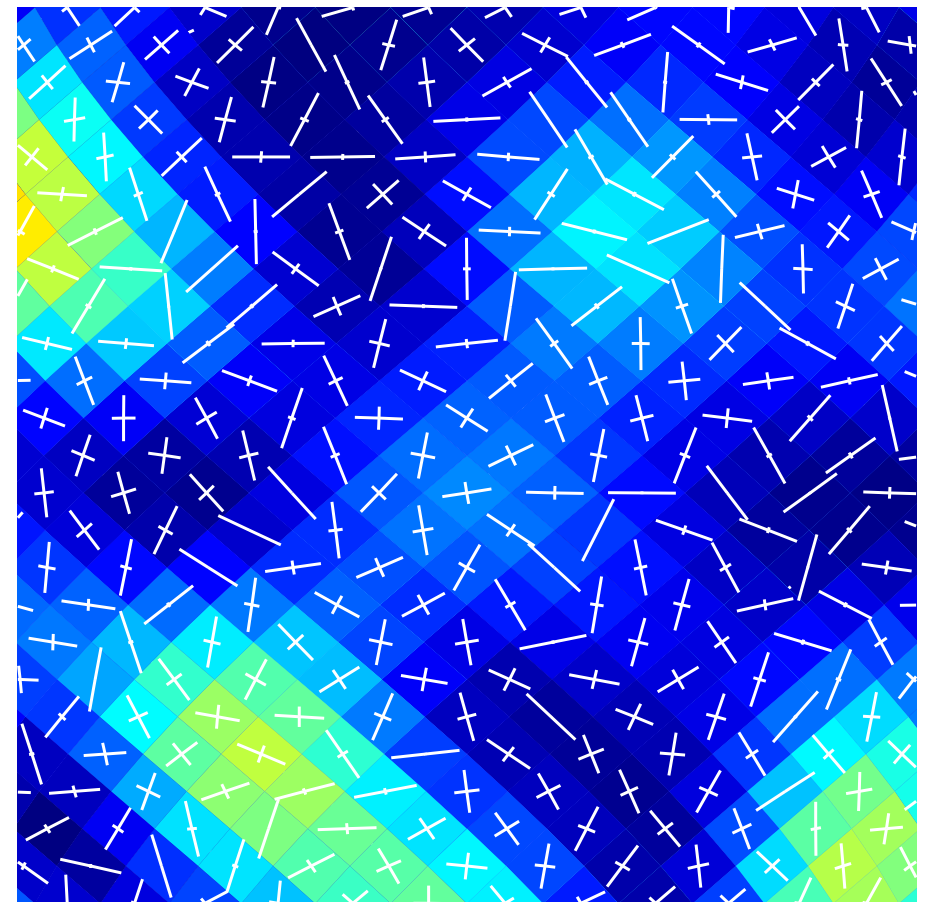
Implications

- Polarization of background can distinguish correlated and uncorrelated origin.



2 4 6 8 10 12 14 16 18 20 22

Correlated



2 4 6 8 10 12 14 16 18 20 22

Uncorrelated

Background mapping - all modes

- If we allow for alternative polarisations, the number of GR modes we can measure is reduced further.

- The total response of a pulsar in direction \hat{u}_I is

$$R_I(f) = \sum_{lm} \left(a_{(lm)}^B(f) \mathcal{R}_l^B(y_I) + a_{(lm)}^L(f) \mathcal{R}_l^L(y_I) + a_{(lm)}^{V_G}(f) \mathcal{R}_l^{V_G}(y_I) + a_{(lm)}^G(f) \mathcal{R}_l^G(y_I) \right) Y_{lm}(\hat{u}_I)$$

- If we have pulsars all over the sky, can decompose “pulsar response” map into spherical harmonic basis. Coefficients are linear combinations of different polarisations.
- No confusion between B and G modes due to range of l . Confusion with V_G and L possible unless have pulsars at several distances, i.e., several y 's.
- Even with multiple pulsar distances, we expect great confusion between V_G and other modes, due to weaker y dependence.

Background mapping - all modes

- Fisher matrix analysis predicts precision with which coefficients will be measured. E.g., analysis with $l_{\max} = 2$ and $N_p = 30$.

	(l, m) mode								
	(0, 0)	(1, -1)	(1, 0)	(1, 1)	(2, -2)	(2, -1)	(2, 0)	(2, 1)	(2, 2)
G : transverse-tensor (gradient)	—	—	—	—	0.44	0.38	0.32	0.38	0.44
G : transverse-tensor (gradient)	—	—	—	—	0.49	0.39	0.37	0.39	0.49
B : scalar-transverse (breathing)	0.16	0.53	0.46	0.53	—	—	—	—	—
G : transverse-tensor (gradient)	—	—	—	—	16.2	10.5	11.4	10.5	16.2
B : scalar-transverse (breathing)	4.36	16.1	14.1	16.1	—	—	—	—	—
L : scalar-longitudinal	0.71	0.96	0.84	0.96	1.21	0.78	0.86	0.78	1.21
G : transverse-tensor (gradient)	—	—	—	—	1.4e5	5.4e4	8.0e4	5.4e4	1.4e5
B : scalar-transverse (breathing)	18.4	9.4e4	6.2e4	9.4e4	—	—	—	—	—
L : scalar-longitudinal	3.08	11.5	8.68	11.5	20.9	7.51	11.9	7.52	20.9
V_G : vector-longitudinal (gradient)	—	6.6e4	4.4e4	6.6e4	7.0e4	2.7e4	4.0e4	2.7e4	7.0e4

- Extension to ground-based interferometers.

Extension to interferometers

- Can apply the same formalism to other GW detectors. Consider ground-based interferometers and make static approximation.
- The strain response of a static interferometer in the point detector limit may be approximated by

$$R^A(f, k) = \frac{1}{2} e_{ab}^A(\hat{k}) (u_1^a u_1^b - u_2^a u_2^b)$$

- Using separate integration frames for each arm, such that the arm is in the z -direction, and using the rotation properties of the $a_{(lm)}^P$ coefficients we find

$$R_{(lm)}^G(f) = \frac{4\pi}{5} \sqrt{\frac{1}{3}} \delta_{l,2} (Y_{2m}(\theta_1, \phi_1) - Y_{2m}(\theta_2, \phi_2))$$

$$R_{(lm)}^C(f) = 0$$

- for a detector with arms pointing in the directions (θ_i, ϕ_i) .

Extension to interferometers

- Including transfer function, still have zero curl mode response, but sensitivity to grad modes with $l > 2$ is recovered.
- A moving detector recovers curl mode sensitivity since

$$\Delta(f\hat{k} \cdot \vec{x}/c) \sim 5 \times 10^3 \rightarrow 5 \times 10^5$$

- over a year for $f = 10 \rightarrow 1000\text{Hz}$.
- Regard moving detector as superposition of static detectors at different locations.
- Under a translation to a frame with origin at \vec{x}_0

$$h_{ab}(f, \hat{k}) \rightarrow \bar{h}_{ab}(f, \hat{k}) = h_{ab}(f, \hat{k})e^{-i2\pi f\hat{k} \cdot \hat{x}_0/c}$$

Extension to interferometers

- Using the identity

$$e^{-i2\pi f \hat{k} \cdot \vec{x}_0 / c} = 4\pi \sum_{L=0}^{\infty} (-i)^L j_L(\alpha) \sum_{M=-L}^L Y_{LM}^*(\hat{x}_0) Y_{LM}(\hat{k})$$

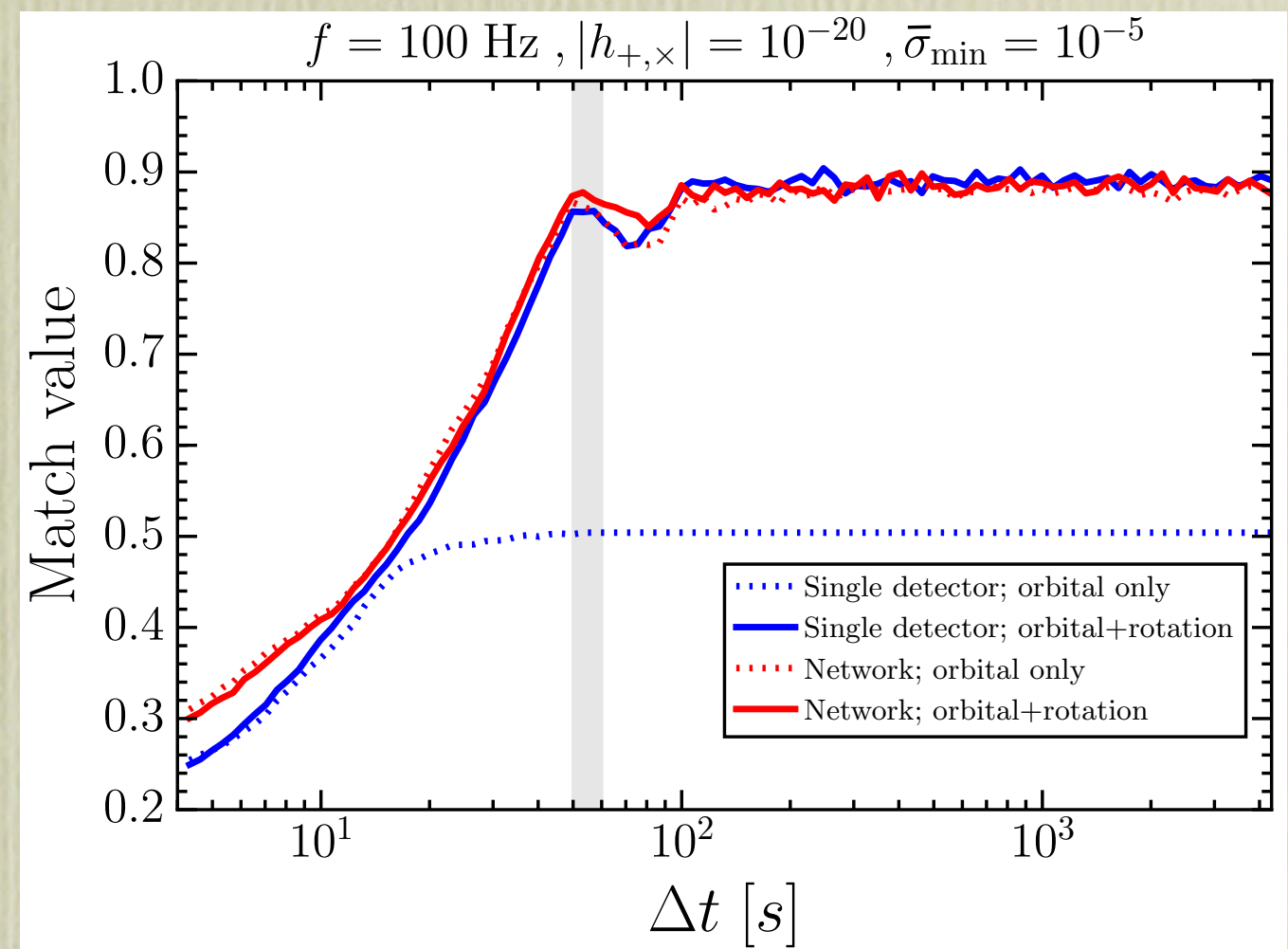
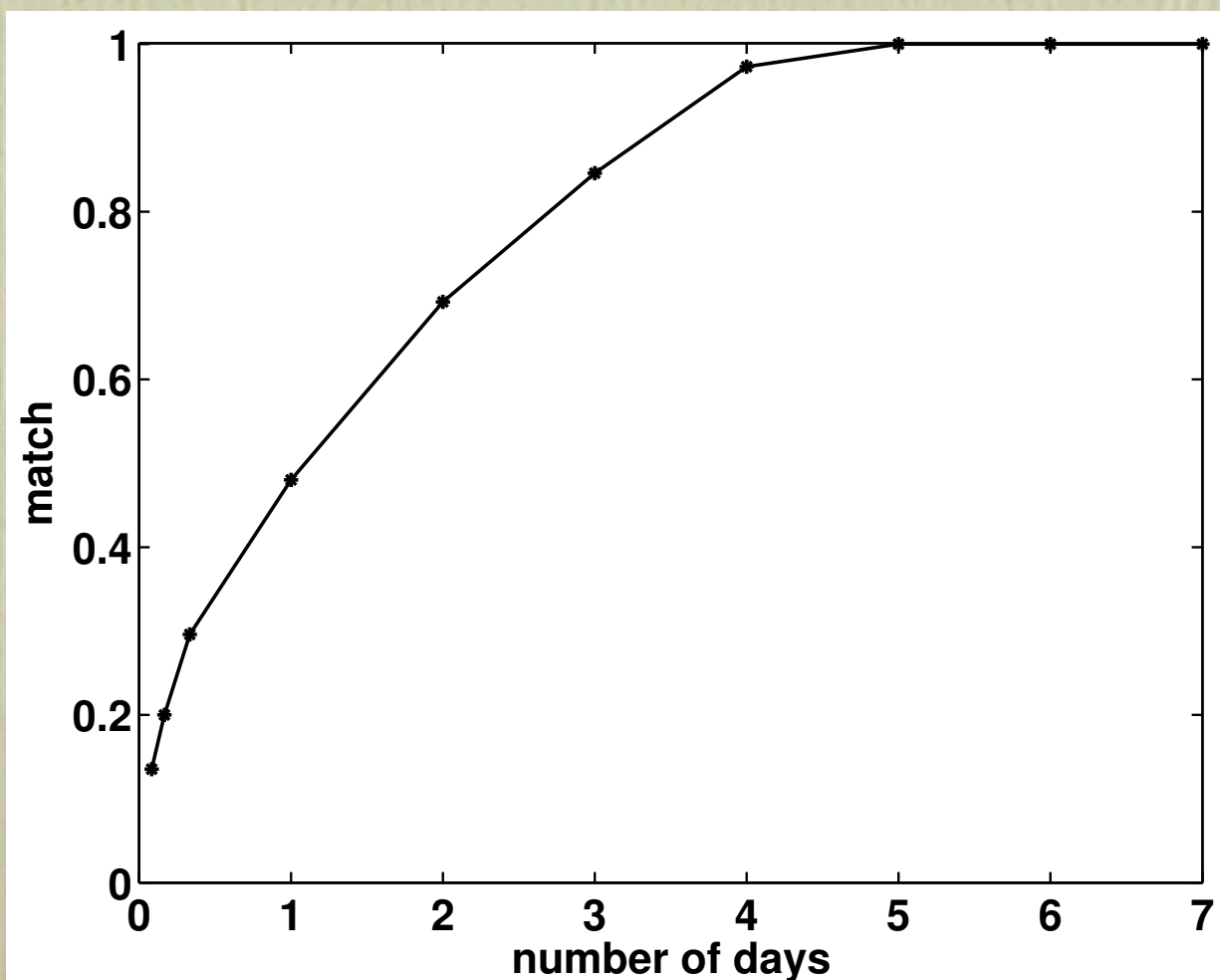
- where $\alpha \equiv 2\pi f |\vec{x}_0| / c$, we can transform the components of the background in the cosmic frame into the frame of the detector at \hat{x}_0

$$R_{(lm)}^G(f) = \sum_{m'=-2}^2 \sum_{L=l-2}^{l+2} \sum_{M=-L}^L \bar{R}_{(2m')}^G 4\pi (-i)^L j_L(\alpha) Y_{LM}^*(\hat{x}_0) \frac{(-1)^{m'}}{2} \sqrt{\frac{(2 \cdot 2 + 1)(2l + 1)(2L + 1)}{4\pi}} \begin{pmatrix} 2 & l & L \\ -m' & m & M \end{pmatrix} \begin{pmatrix} 2 & l & L \\ 2 & -2 & 0 \end{pmatrix} [(-1)^{l+L} + 1]$$

$$R_{(lm)}^C(f) = \sum_{m'=-2}^2 \sum_{L=l-2}^{l+2} \sum_{M=-L}^L \bar{R}_{(2m')}^G 4\pi (-i)^L j_L(\alpha) Y_{LM}^*(\hat{x}_0) \frac{(-1)^{m'}}{2i} \sqrt{\frac{(2 \cdot 2 + 1)(2l + 1)(2L + 1)}{4\pi}} \begin{pmatrix} 2 & l & L \\ -m' & m & M \end{pmatrix} \begin{pmatrix} 2 & l & L \\ 2 & -2 & 0 \end{pmatrix} [(-1)^{l+L} - 1]$$

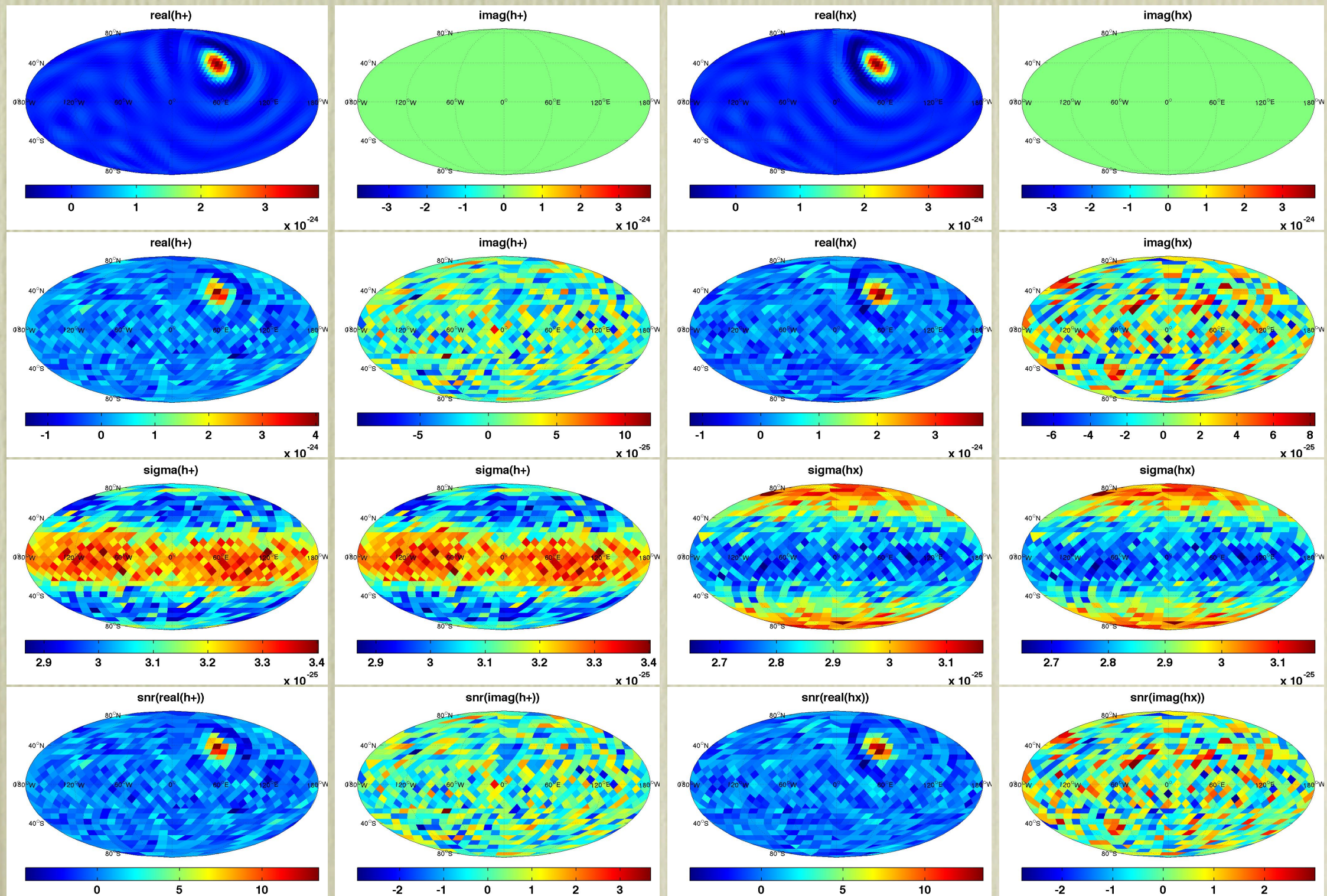
Extension to interferometers

- Recover more and more modes as number of effective independent detectors increases over time.
- Earth rotation crucial to break degeneracies for a single detector network.



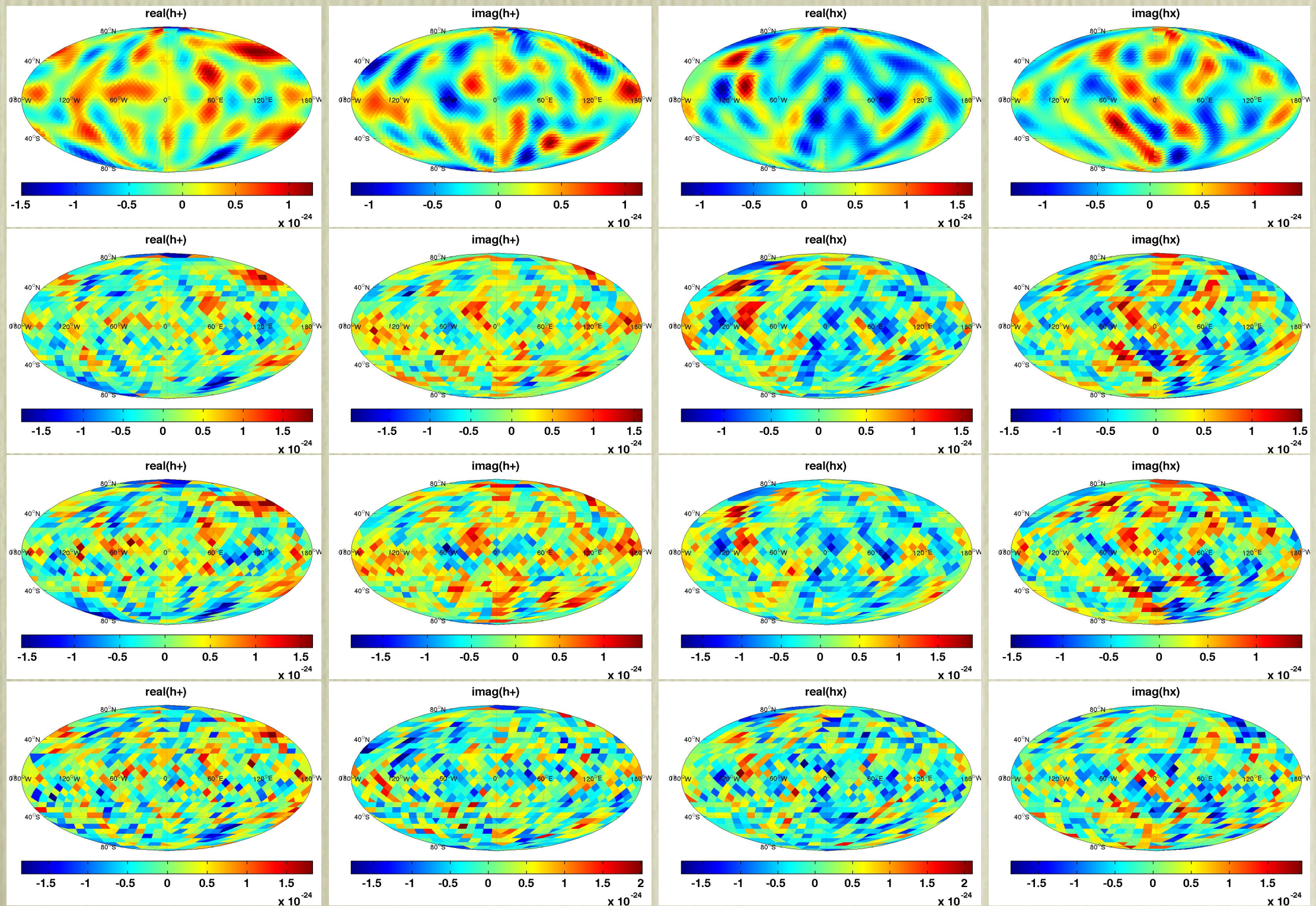
Extension to interferometers

- Recovery of point source.



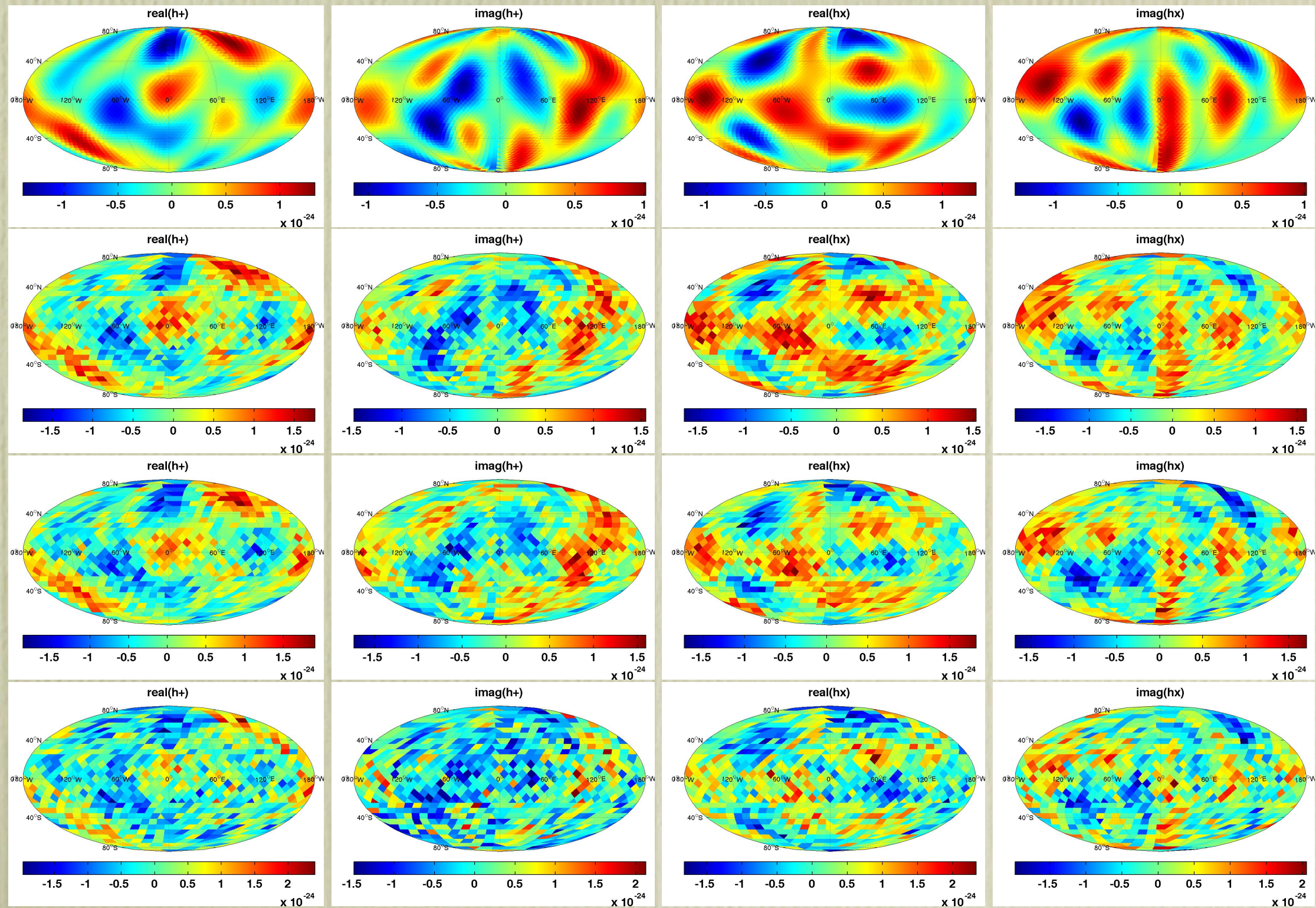
Extension to interferometers

- Recovery of grad mode GR background.



Extension to interferometers

- Recovery of curl mode GR background.



Summary

- The framework used to analyse CMB polarisation can be applied to describe arbitrary gravitational wave backgrounds.
- PTA response to modes of the background takes a simple form - spherical harmonics evaluated at pulsar locations, multiplied by distance-dependent factors.
- PTAs have no sensitivity to the curl components of the background or to modes higher than dipole in scalar-transverse backgrounds.
- Can describe an isotropic uncorrelated background with just three l -modes.
- A PTA of N_p pulsars can measure N_p combinations of the grad component of the background. PTAs are blind to the other grad components and the whole curl component.
- A measurement of unexpected values for these components would reveal correlations in the background and profound new physics.